Optimal distribution network planning in an integrated energy system

by

Sangitha Harmsen

to obtain the degree of Master of Science

at the Delft University of Technology,

to be defended publicly on Monday June 07, 2021 at 15:00 PM

Thesis committee:	Prof. dr. Peter Palensky	IEPG, TU Delft
	Dr. ir. Milos Cvetkovic	IEPG, TU Delft
	Dr. ir. Gautham Ram Chandra Mouli	DCE&S, TU Delft

TU Delft Delft University of Technology

STEDIN.NET

Abstract

The energy transition is driving extensive changes to global energy systems, including the electrification of heating and mobility, increased variable renewable electricity generation, decentralisation and a shift towards sustainable gases such as green hydrogen. These changes will need to be accompanied by major investments and modifications to energy infrastructure, especially in the following decades, considering the goals of climate-neutrality envisioned for 2050. Historically, the infrastructure and operation of different energy carriers have been planned independently. In integrated energy system planning, the system-level interactions between, for example, storage, electricity networks and gas networks are taken into account and considered as a whole.

This thesis is an investigation into the potential benefits provided by integrated energy system planning compared to only reinforcing individual networks. The focus is on the distribution grid level, and the investigation is carried out for a case study based on the Sterrenburg region in South Holland. The scope includes the electric distribution network between 13 and 150 kV, and a simplified representation of selected gas city gates. Power-gas integration by means of electrolysis and gas turbines is investigated, as well as the integration of utility-scale 4-hour electrical energy storage with batteries. Hourly demand and generation profiles are based on 2050 scenarios, specifically one scenario focusing on regional energy self-sufficiency (Regional scenario), and another focusing on international trade (International scenario). The costs and savings are analysed, as well as the spatial requirements of the infrastructure, and the sensitivity of the results to selected input parameter variations.

An expansion planning model is developed to evaluate the optimal investments for the 2050 scenarios, starting from the existing network. This mixed-integer linear programming model is based on PyPSA, an open-source energy system modelling toolbox in Python. The optimisation objective is a combination of annualised investment costs (based on 2050 cost projections) and hourly operational costs. Representative hourly time-steps are chosen from the entire year of 2050 to manage the computational complexity and solving time. Basic market signals are modelled for the exchange of energy in the case region with the rest of the grid.

The results show that power-to-gas conversion by means of electrolysis leads to system benefits which include decreased spatial use and lower infrastructure reinforcement costs in both the Regional and International scenarios. Compared to a reinforcement-only approach, the use of electrolysers decreases the annualised cost of network reinforcement investments by 18.5% in the Regional scenario and 16.7% in the International scenario. Within the scope of this analysis, gas-to-power conversion using hydrogen turbines is not chosen in any of the problem formulations, and the inclusion of 4-hour batteries has only a very limited impact. The outcomes vary substantially with changes to the electricity and hydrogen prices, and are less sensitive to the costs of electrolysis, gas turbines and storage. There are many possibilities for broadening and deepening the scope in future works. For example, different combinations of integration options such as heat networks and long-term gas storage could be considered together. The model could be extended to include a more complex market, or by modelling physical gas flows through pipelines.

Acknowledgements

This thesis is the result of many months of work, and marks the end of my Master studies at the TU Delft. I would like to express my gratitude to Milos Cvetkovic and Digvijay Gusain for their supervision, insights and feedback. From Stedin, Arjan van Voorden and Arjen Jongepier have never hesitated to engage in lively discussions and to share their expertise. With the help of my supervisors, I was able to learn much about energy system modelling, optimisation and grid operation. Additionally, I am also thankful to Peter Palensky and Gautham Ram Chandra Mouli for agreeing to be on the thesis committee, and for their involvement at moments vital to this thesis.

Various others from TU Delft and Stedin have been helpful by sharing tips, knowledge and feedback. Furthermore, the Intelligent Electrical Power Grids (IEPG) group has provided support from technical, administrative and social perspectives.

The global pandemic has added frustration and isolation to the already challenging endeavour of carrying out a thesis project. I would like to thank my family and friends for helping to lift my spirits and motivate me through this time, through their digital and in-person presence. I hope to be able to take the knowledge and skills from this thesis forward and use them to contribute to the energy transition and a more sustainable world.

Sangitha Harmsen
Delft, June 2021

Contents

List of Symbols

Optimisation formulation symbols

List of indices

b	Index of passive branches (lines, transformers)
l	Index of links
n	Index of buses
r	Index of generators
s	Index of storage units
t	Index of time-steps (snapshots)

List of variables

$E_{n,s}$	Energy storage capacity of storage unit s at bus n, in MWh
$e_{n,s,t}$	Energy state-of-charge at storage unit s at bus n and time t, in MWh
$f_{l,t}$	Flow of power into branch l at time t, in MW
F_l	Power capacity at the input bus of link l, in MW
$g_{n,r,t}$	Dispatch of generator r at bus n and time t, in MW t
$H_{n,s}$	Power capacity of storage unit s at bus n, in MW
$h_{n,s,t}$	Dispatch of storage unit s at bus n and time t, in MW
M_b	Big-M value for a constraint of branch b
u_b	Passive branch binary investment variable
$\theta_{n,t}$	Voltage angle at bus n and time t, in radians

List of parameters

c_b	Capital cost of branch b, per MW
c_l	Capital cost of link l, per MW
$c_{n,s}$	Capital cost of storage unit s at bus n, per MW
$d_{n,t}$	Demand at bus n and time t, in MW
F_b	Capacity of branch b, in MW
$G_{n,r}$	Nominal power of generator r at branch n, in MW
$o_{n,r}$	Marginal cost of dispatch of generator r at bus b, per MW
$o_{n,s}$	Marginal cost of dispatch of storage unit s at bus b, per MW
o_l	Marginal cost of operating link l, per MW
w_t	Weighting of time-step t
x_b	Reactance of branch b in ohms
$\alpha_{l,n}$	Factor indicating direction of flow at link l and bus n
η_l	Efficiency of link l

Remaining symbols

A_c	Annuity factor
B_{ik}	Susceptance between buses i and k in siemens
$C(\boldsymbol{x})$	Optimisation objective function with variables $\boldsymbol{x}$
G_{ik}	Conductance between buses i and k in siemens
L_c	Lifetime, in years, of component c
P_i	Real power injected at bus i, in W
Q_i	Reactive power injected at bus i, in W
R_{ik}	Resistance between buses i and k in ohms
r	Discount rate, per year
S_i	Apparent power injected at bus i, in W
V_i	Voltage at bus i in volts
X_{ik}	Reactance between buses i and k in ohms
Y_{ik}	Admittance between buses i and k in siemens
Z_{ik}	Impedance between buses i and k in ohms

Abbreviations

AC	Alternating current
CAPEX	Capital expenditure
CHP	Combined heat and power
DC	Direct current
DG	Distributed generation
DSM	Demand-side management
DSO	Distribution system operator
GTS	Gasunie Transport Services
HHV/LHV	Higher heating value/lower heating value
HV/MV	High voltage/medium voltage
LCOE	Levelised cost of energy
(MI)LP	(Mixed-integer) Linear programming
NPV	Net present value
OPEX	Operational expenditure
p.u.	Per-unit
P2G	Power-to-gas
PV	Photovoltaic
PyPSA	Python for Power Systems Analysis
TSO	Transmission system operator
VRE	Variable renewable energy

List of Figures

List of Tables

1 | Introduction

1.1. Background

Globally, energy systems face major restructuring at different scales due to a combination of factors including technological development, environmental concerns, markets and regulations. International agreements reinforce this movement: the Paris Agreement of the COP21 (Conference of the Parties, part of the United Nations Framework Convention on Climate Change) in 2015 aims to limit global warming to a maximum increase of 2 °C by curbing greenhouse gas emissions [16] and has been adopted by over 190 countries. The European Union builds upon this with its long-term strategy to be climate-neutral by 2050 [17].

These greenhouse gases are emitted when fossil fuels are used directly as fuels or indirectly for electricity generation, chiefly to support the energy needs of industry, agriculture, mobility and the built environment. The goal to reduce emissions is approached in several ways, i.e., through increased renewable energy generation, increased energy storage, decentralisation, and the electrification of mobility and heating [18]. These changes also lead to more interactions and coupling of different energy sectors and carriers.

Historically, there have been connections between energy sectors through storage and conversion units such as combined heat and power (CHP), heat pumps and power-to-gas [15]. However, the infrastructure and operation of different energy carriers have typically been planned independently, without accounting for these interactions on a system scale [19]. This approach leads to a loss in capacity utilisation and efficiency [20] and can be improved by integrated energy system planning.

Energy system integration broadly refers to thinking of the energy system as one interconnected whole rather than as individual systems of carriers. Known by various other terms such as *multi-energy systems*, *energy sector coupling* and *smart energy systems*, this concept can refer to the combined planning, operation, control and protection of multiple energy carriers and their corresponding infrastructure. Integrated energy systems typically comprise some combination of electricity, heat and fuel (such as natural gas or hydrogen) infrastructures, which could also include (electric or fuel-based) transport [21]. Figure 1.1 shows an example of an integrated energy system with generation, demand, storage and conversion among electricity, heating and gas networks.

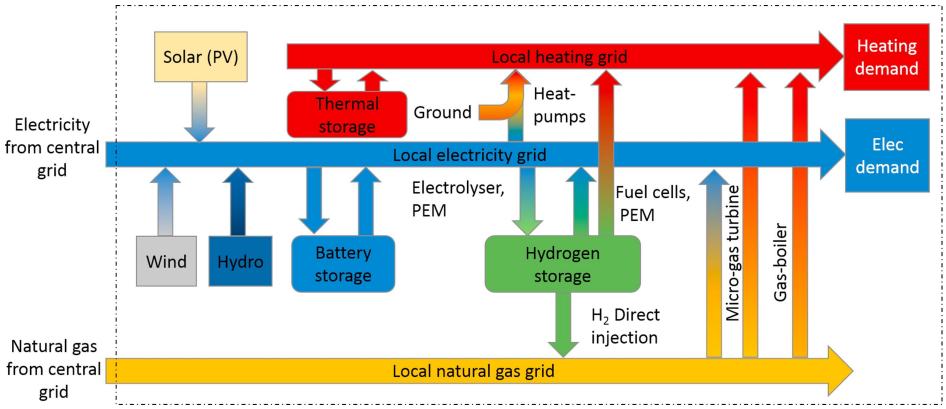

Figure 1.1: Example of energy flows in an integrated system with electricity, gas and heating [1].

Energy system integration is increasingly important since all energy sectors are facing a transition. At an international level, the European Commission published a strategy on energy system integration in 2020 [22]. As mentioned in the report, the decisions taken in the coming 5-10 years are crucial for the energy system of 2050, as energy infrastructure investments typically have lifetimes of 20-60 years. Within the Netherlands, there are studies and plans which consider multiple energy sectors

(but not explicitly the integrated planning thereof). Some examples include the *Integrale Infrastructuurverkenning* based on different scenarios of energy developments from 2030 to 2050, and the "Investeringsplannen", which are 10-year investment plans for gas and electricity (currently planned independently) of Dutch distribution system operators (DSOs) and transmission system operators (TSOs). At a regional scale, there are *Regionale Energie Strategieën* (RES) of 30 regions' high-level energy infrastructure plans for 2030 made in collaboration with network operators and industry stakeholders, and the *Transitievisie warmte* in which 355 municipalities outline plans for electricity, gas or district heating for their locality in 2030 [23].

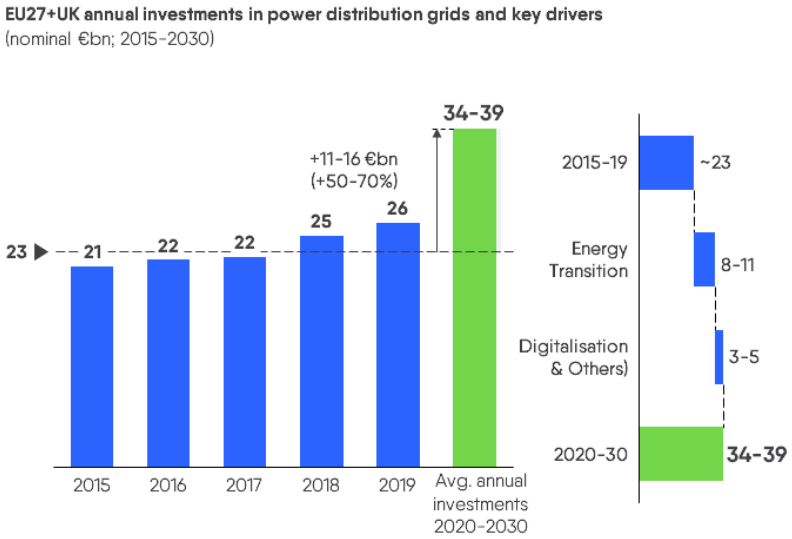

Figure 1.2: A projection of the increase in the annual distribution grid investments within the EU27 + UK until 2030 [2].

Given the rapid energy transition and large scale of energy investments, it is crucial to improve the long-term planning of energy networks and account for the interactions within the system. Particularly electric distribution networks, which connect end-users to distribution substations, face major changes and uncertainty on two fronts. Firstly, the increasing electrification of energy demand (such as heating and mobility) leads to a considerable increase in electricity demand in the following decades. Secondly, the increased adoption of renewable energy generation also affects distribution grids where demand was predominant before, notably the distributed generation at sub-transmission and distribution voltage levels. Instead of power flowing only from higher to lower voltage levels, the flows may be reversed with the distribution system flows depending on loads as well as generation [24]. Figure 1.2 shows the investments in power distribution grids between 2015 and 2019 in the EU27 countries and the UK, as well as a projected average annual investment amount for the period of 2020-2030. The figure, from a study by Eurelectric and E.DSO [2] shows that in this region, the average annual investments in distribution grids for 2020-2030 are projected to increase to 34-39 billion euros per year, which is 50-70% higher compared to the average between 2015 and 2019. This increase is chiefly due to the energy transition, and it highlights the (rising) importance of grid expansion planning.

1.2. State-of-the-art

Many works related to system integration have emerged in recent years, with a diverse range of methods, scopes and research questions. Some researchers analyse the role of specific technologies or applications within an integrated energy system. For example, [25] focuses on data centres that serve as waste heat sources with responsive demand. Studies [26–29] look into electric vehicles and their impact on energy infrastructure through controlled charging and as potentially coordinated storage devices (smart charging and demand-side response/management). Other studies specifically focus on the uncertainty involved in energy infrastructure operation and planning, such as [30–33].

Many research works include or focus on operational aspects (multi-modal energy flows, operational costs, unit commitment, optimal dispatch), while some also include long-term planning. Typically, the electricity network is considered along with some combination of natural gas, hydrogen [33], mobility, storage [18, 34], and heat networks [35, 36]. Plans and strategies in these works are typically made using the optimisation of (operational and investment) costs, and sometimes emissions are included in the objective to be minimised, or as a constraint. Many studies involve optimising a mixed-integer linear programming (MILP) problem [28, 33, 37], while combinations are also used, such as MILP, dynamic programming (DP) and linear programming (LP) in [35]. Alternatively, heuristic methods such as genetic algorithms are used to optimise the energy system [29, 34].

The spatial scope is often international, such as in [18, 38, 39] at European level, or national, e.g. [27] for the UK, [40] for Switzerland, [41] for China, and [35] for Germany. Nevertheless, studies are also carried out for smaller scales, such as districts [42], cities [43, 44], and at distribution level [32, 34].

1.3. Thesis objectives

The objective of the thesis is to gain insight into energy system integration at distribution level, with joint supervision from TU Delft and the distribution system operator (DSO) Stedin. It is of an early-stage, exploratory nature and involves developing a model to answer the research questions for a specific case study, which are listed below. First, the scope of this work is outlined.

1.3.1. Scope

The case study in this thesis is based on the Sterrenburg region which lies in South Holland, a province of the Netherlands. This region includes 186 neighbourhoods, covering about 400 km^2. Electricity and gas infrastructures are considered within this work, which at distribution level are both operated by Stedin. Furthermore, the electricity demand and generation profiles, and gas demand profiles are taken from four different 2050 scenarios from an existing work, based on different possible policy directions. The electric grid is considered between 13-150 kV, i.e., the high-voltage (HV) to medium voltage (MV) parts of the distribution network. A simplified gas network, assumed to be repurposed for hydrogen in 2050, is considered only at the 40 bar/8 bar city gates.

1.3.2. Research questions

The following research question and sub-questions are formulated to be answered in this work.

How can the flexibility provided by energy system integration in network planning lead to benefits compared to only electric infrastructure reinforcements for the 2050 generation and demand scenarios for the Sterrenburg sub-network?

a. To what extent do the economic costs and savings due to system integration vary between different 2050 scenarios?

b. What effect does integrated planning in the Sterrenburg case have on the spatial use of the energy infrastructure?

c. Are there intermediate investments made for the 2030 scenario that become unnecessary in any of the 2050 solutions?

d. How robust is the optimisation result in terms of sensitivity to model parameter values?

These questions are answered by first carrying out a literature review of relevant theory and methods, developing an expansion planning model, and applying this to the case study of the Sterrenburg area for 2050.

1.4. Report outline

The remainder of this report is structured as follows. In Chapter 2, different energy infrastructure subsystems and concepts related to system integration are introduced. Chapter 3 elaborates on the theory and methods of energy system expansion planning based on literature, focusing on electricity grids. In Chapter 4, the development of this work's model is outlined. This model is applied to a case study which is introduced in Chapter 5, followed by the results in Chapter 6. Chapters 4 and 6 also contain targeted discussions pertaining to the model and case, respectively. Finally, in Chapter 7, the results are reflected upon and discussed as a whole in order to answer the research questions, along with recommendations for future works.

2 | Energy systems and integration

In this chapter, energy networks are introduced along with their main components, characteristics and methods to model them. Section 2.1 contains an introduction to electrical networks, focusing on the distribution network level and how networks are modelled. In Section 2.2, an overview of gas and heating infrastructures is given, among which hydrogen infrastructure is most relevant to this work. Section 2.3 briefly covers energy storage at utility scale, and Section 2.4 presents ways through which energy systems are integrated. Finally, in Section 2.5, the structures and characteristics of energy markets are described.

2.1. Electrical infrastructure

The electrical power system can broadly be divided into generation, transmission, distribution and consumption, each with the corresponding control and protection mechanisms. Generators and loads are located at various voltage levels of the network, with large conventional plants at the highest voltages and smaller generators and loads at lower voltages. When power is transported at higher voltages, it is more economical due to lower electrical losses (per transported unit of power). However, equipment at higher voltages also tends to be more expensive, and this trade-off causes it to be beneficial overall to transport larger quantities of power at higher voltages, which is typically also done over larger distances [45]. Figure 2.1 shows a schematic of an electrical power system. The transmission network connects large power plants to distribution networks, which bring power to the end-users. The voltages levels in the figure are indicative; these vary between countries and even within countries. The lower part of the figure shows a single-line diagram of the same system, and it illustrates the components and their connections.

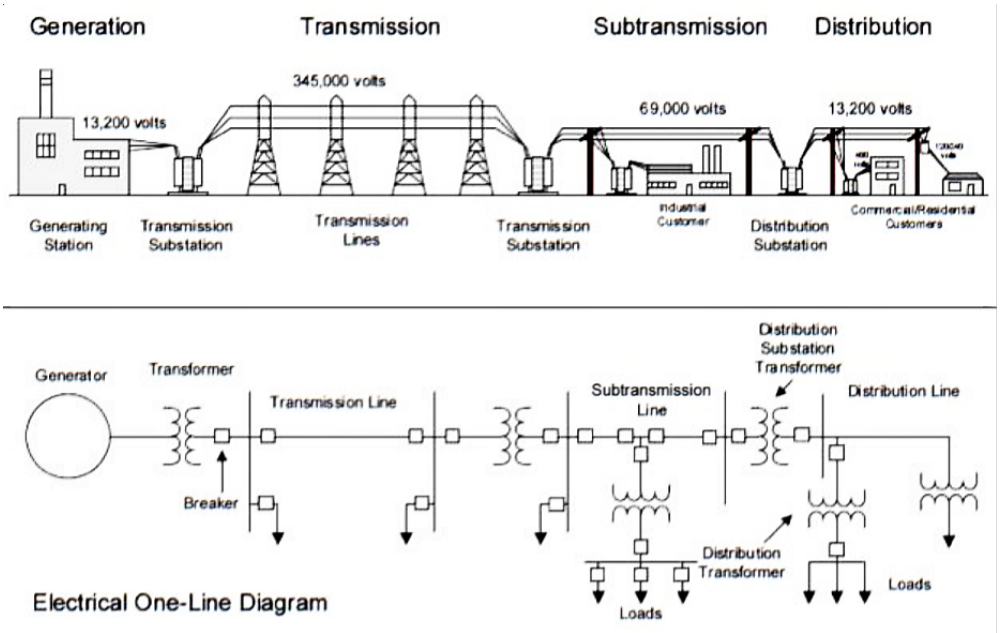

Figure 2.1: Schematic showing the structure of the electrical power system [3].

In the Netherlands, distribution system operators (DSOs) typically operate grids at voltages below 66 kV, whereas transmission system operators (TSOs) operate grids at higher voltages [46]. The Netherlands has one transmission system operator – TenneT, and several distribution system operators, of which Stedin is one.

There are some notable differences between transmission and distribution networks. Most importantly, transmission networks are tasked with the transfer of large amounts of power over long distances, and they do this at high voltages. Distribution networks connect the transmission network to larger (industrial) and smaller (residential) consumers. Distribution networks tend to have a radial structure, while transmission networks are meshed. There is only one path between any two points in a radial network through which power can flow. Meshed networks, on the other hand, contain loops. Nevertheless, the same fundamental expansion planning principles can be used in both cases [47]. In the Netherlands, power at high voltages is typically transmitted through overhead lines, and at lower voltages through underground conductors, usually referred to as cables.

Transformers in substations facilitate the various voltage conversions in the power system, along with other components like bus bars, circuit breakers, control equipment, protection equipment and current transformers. Switchgear is especially important to safely disconnect these components which accommodate large power flows, for example for maintenance, installing new components or for containing faults. In the Netherlands, the transmission level has high voltages of 110/150 kV up to 380 kV, and the distribution network has lower voltages down to 400 V (line voltage) at a residential level. For example, the HV-MV station connects the high voltage transmission system side of 110-150 kV to the medium voltage (MV) distribution system side of 20 kV [12].

The global standard for electrical networks today is to use alternating current (AC). Direct current (DC) provides some advantages over AC. For instance, it can be cheaper over distances that are long enough because it only requires two conductors, rather than the three conductors required for three-phase AC. There are already some DC cables in use today at high voltages and over long distances, such as the NorNed cable spanning 600 km between Norway and the Netherlands. On a smaller scale, DC could be advantageous because many household appliances use it [12]. Nevertheless, in this work, the scope is restricted to AC electricity networks.

Historically, distribution systems are 'fed' by (sub-)transmission networks; lines known as feeders then distribute the energy further into the distribution network. The technological development of distributed generation (DG), especially renewable wind and solar energy generation, is leading to significant levels of generation at the distribution level. Due to climate policy, distributed renewable generation is expected to keep growing, especially with targets for (near-) carbon neutrality in 2050. DG units have smaller capacities than traditional power plants and tend to be located closer to the consumers. The DG technologies are often renewable energy sources (RES), such as wind turbines, solar panels and small-scale hydropower, but they may also be based on fossil fuels, such as micro gas turbines. Some advantages of DG include increased reliability (by spreading risks) and decreased (transmission) losses [48]. However, a large proportion of solar and wind generation decreases the flexibility of a power system since the sun and wind cannot be dispatched. Such weather-dependent sources are also referred to as variable renewable energy (VRE) or intermittent renewable energy sources (IRES).

In a power system, a mismatch between supply and demand causes deviations in the system frequency and voltages, which can cause instability, damage equipment and even lead to outages. Power system flexibility describes the measures which can be taken to ensure the demand and supply match each other closely at all times. Figure 2.2 shows some sources of flexibility in power systems. In systems with low VRE, the primary source of flexibility is usually from the generators. Generators known as peaking generators have characteristics such as high ramping capabilities (changing the output level quickly), quick start-up, and low minimum operational level. However, these typically depend on fossil fuels. With VRE depending on external circumstances such as the weather, they cannot be predicted perfectly ahead of time, and their control is also limited. The output can be (partly) decreased by "curtailment", but this is usually not a desirable solution since it decreases revenues and the utilisation of renewable generation investments. Instead, the task of flexibility shifts to other sources shown in Figure 2.2 in systems with high VRE, such as the power systems expected in 2050. The sources of flexibility also reflect some of the emerging activities of distribution system operators due to the energy transition: managing increased demand from electric vehicles (EVs) and heating, supporting distributed generation and managing demand-side response.

Robust transmission and distribution networks increase the flexibility of systems by allowing power to be transported further across regions, which can balance out spatial mismatches in supply and demand. Grid flexibility also involves automatic control of generators or advanced power flow control

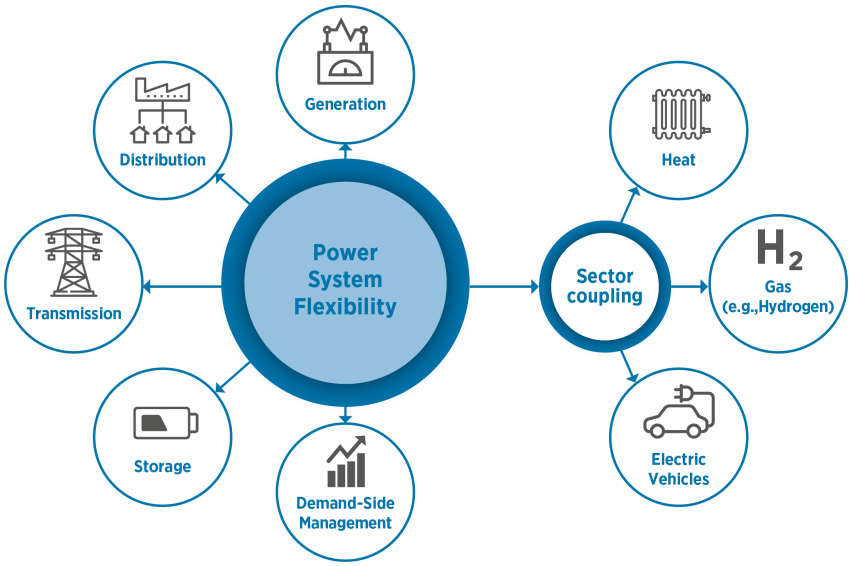

Figure 2.2: Different sources of flexibility in a power system [4].

such as using flexible alternating current transmission system (FACTS) devices. Energy storage, which is discussed in more detail in Section 2.3, facilitates flexibility by decreasing temporal mismatches in demand and supply: energy is stored when there is excess supply and released at times of excess demand [4].

Demand-side management includes a variety of measures taken to control the loads rather than the generation to maintain their balance. This management could be through direct control by the grid operator of, for example, industrial loads. Another method is via price signals; in a simple form, this could be a time schedule (i.e., time-of-use, when the price is lower at off-peak hours), or this price could vary in real-time. Sector coupling also provides the potential to increase flexibility by making use of additional infrastructure and components to overcome the limitations of a single sector. For example, when there is an excess of electrical generation and limited capacity to transport this in the electrical grid, this power can be converted to heat or gas. Coupling the sectors improves the flexibility across energy carriers by combining the demand for power, heat, fuel and mobility in one system.

Liberalised energy markets treat flexibility as a service that can be traded. Energy market trade takes place at different time scales; this way, the baseload can be met with generation ahead of time, and more energy trades are made closer to real-time, as more becomes known about the demand profile and generation. Additionally, control reserve products are traded on ancillary services markets, including primary/secondary/tertiary frequency control reserves [49]. The market is explained further in Section 2.5.

2.1.1. Electrical network representation and simulation

Many types of analysis are carried out on electrical networks, with different corresponding modelling approaches. Power flow calculations (also known as load flows) are used to determine the steady-state power flowing through each point of the network, and this is most relevant for long-term expansion planning, as is done in this thesis. Power flows are elaborated on later in this section. Other types of analyses are, for example, short-circuit simulations to estimate fault currents (for protective equipment requirements) and reliability simulations to predict outages [45].

In standard steady-state power flow analyses, and in the rest of this thesis, it is assumed that the three phases are balanced, i.e., that loading and generation are evenly distributed over the three phases. This assumption allows a single-phase equivalent representation of the network to be used. The power flow analysis that follows applies to the steady-state solution of networks, as is appropriate for long-term expansion planning models (but not, for example, for fault analyses).

The per-unit (p.u.) system is often used to simplify power system calculations, and it makes deviations from nominal values more apparent. Per-unit normalisation involves dividing voltage, current, impedance and power by their corresponding base value. These four quantities are physically related, so when base values are chosen for two (typically the nominal voltage and rated apparent power), this sets the base for the remaining variables. For example, if $|V_b|$ is the base voltage and $|S_b|$ the base power, then the base impedance $|Z_b| = |V_b|^2/|S_b|$.

Furthermore, per-unit normalisation with the following base choices simplifies transformer-related calculations: the base powers at the primary and secondary sides of the transformer are chosen to be equal, and the base voltage ratios correspond to the winding ratio of the transformer. If the transformer is ideal (no core losses or leakage flux), and the per-unit normalisation is implemented in this manner, then the per-unit transformer voltages and currents are the same on the primary and secondary sides. This method avoids having to compute across different voltages [12].

For analysing networks of interconnected components, the junction between where components are joined can be referred to as a node, and components spanning two nodes are called branches. When modelling sources as current injections, Kirchhoff's current law can be applied to the nodes: the current through each branch equals the product of the branch admittance (reciprocal of impedance) with the voltage difference. The sum of all the branch currents connected to a node equals the current injection. This relation can conveniently be written in matrix form [50].

There are four variables of interest at each bus i when calculating the power flows through each line of an AC network, namely the net active power injection P_i, net reactive power injection Q_i, voltage magnitude $|V_i|$ and relative voltage angle θ_i. By generalising Kirchhoff's laws to describe a network using vectors and matrices, the vector of current injections at buses $\mathbf{I}$ is described by Equation 2.1. Here, $\mathbf{Y}$ is the bus admittance matrix, and $\mathbf{V}$ is the vector of bus voltages.

$$\mathbf{I} = \mathbf{YV} \quad \therefore \quad I_i = \sum_{k=1}^{n} Y_{ik} V_k \tag{2.1}$$

The net current injected at a bus I_i is also shown in Equation 2.1. The mutual admittance, Y_{ik}, is a complex property consisting of conductance G and susceptance B as follows: $Y_{ik} = |Y_{ik}|e^{j\delta_{ik}} = G_{ik} + jB_{ik}$. The apparent power S_i injected at a bus i is the complex sum of real and reactive power $S_i = P_i + jQ_i$. Equation 2.2 shows how S_i can be calculated from the bus voltage and admittance values. These are separated into the real power and reactive power components in Equations 2.3a and 2.3b, respectively [47].

$$S_i = V_i I_i^* = V_i \sum_{k=1}^{k} Y_{ik}^* V_k^* \tag{2.2}$$

$$P_i = \sum_{k=1}^{n} |Y_{ik}||V_i||V_k| \cos\left(\theta_i - \theta_k - \delta_{ik}\right) \tag{2.3a}$$

$$Q_i = \sum_{k=1}^{n} |Y_{ik}||V_i||V_k| \sin\left(\theta_i - \theta_k - \delta_{ik}\right) \tag{2.3b}$$

Depending on the type of bus, there are usually two known quantities and two to be calculated among the net active power injection, net reactive power injection, voltage magnitude and voltage angle. Load buses have known values for net active and reactive power injections, and are also known as PQ buses (P_i and Q_i known). At voltage-controlled buses, a controllable generator maintains the bus voltage magnitude at a steady value. Therefore, the power injection and bus voltage are known, at these buses, also referred to as PV buses (where $|P_i|$ and $|V_i|$ are known, not related to *photovoltaics*). Finally, a slack bus serves as a reference for the voltage angle (since these are computed relative to a certain value), and its voltage magnitude is assumed to be at 1 p.u. The real and reactive powers at the slack bus are determined such that the rest of the system is in balance [50].

Equations 2.3a and 2.3b are non-linear and computationally complex to solve. These are solved through iterative methods such as Newton-Rhaphson or Gauss-Seidel [51]. With this formulation, the

convergence of the solution is not guaranteed. In practice, a linearised version of power flow equations is often used, also known as "DC load flow". This is derived from the non-linear equations, neglecting the reactive flows and using the following assumptions.

1. Line resistance is negligible compared to reactance, i.e., $R \ll X$.
2. The voltage angle differences are small, such that $\sin(\theta) \approx \theta$ and $\cos(\theta) \approx 1$.
3. The voltage profile is flat, i.e., all voltages are close to 1 p.u.

Based on these simplifications, the remaining expression for power at bus i is shown in Equation 2.4. Without active power and voltage magnitude terms to consider, the computations here are considerably simplified in this linear form. The form of the expression also matches that of DC power flows (hence the term DC load flows), where reactance is in the place of resistance and voltage angle in place of voltage.

$$P_i = \sum_{k=1}^{n} B_{ik}(\theta_i - \theta_k) \tag{2.4}$$

Since the linearisation assumptions made are never perfectly satisfied, there is also a (slight) loss in the accuracy of the flows compared to the non-linear formulation. Particularly, in distribution networks, it is less accurate to assume that resistance is negligible: at lower voltages, the resistance tends to be bigger with respect to the reactance. That being said, the distribution networks are also typically radial, which simplifies power flows as there is only one path power can traverse between two points. The linearised power flow method is sufficient for this thesis, as a very high accuracy for the hourly power flows is not necessary, and only a good approximation of the magnitudes of flows is required.

2.2. Gas and heating infrastructure

Natural gas, a fossil fuel consisting primarily of methane, currently plays a very important role in the Dutch energy system. In 2018, 42% of the total primary energy supply in the Netherlands was sourced from natural gas (followed by oil at 37%, coal at 11% and smaller amounts of biofuel, nuclear, wind, solar, hydropower and geothermal). In fact, 51% of the electricity in 2018 was generated from natural gas, and 90% of residential household heating was by means of natural gas [52]. However, there are plans to gradually decrease the use of natural gas to lower carbon emissions, and to phase out extraction from the Groningen gas field in the Netherlands.

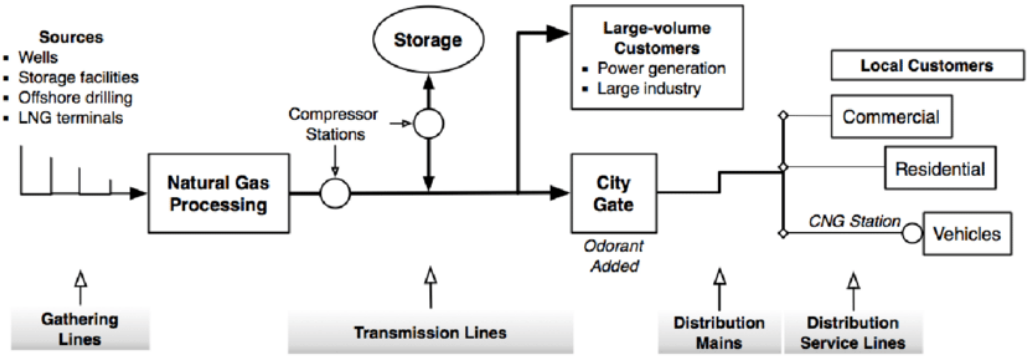

Figure 2.3: Schematic of natural gas supply infrastructure [5]

Considering the importance of natural gas in the Netherlands, there is an extensive network of gas infrastructure. This includes over 130,000 km of gas pipelines, and connections to 95% of the residences as well as most other properties. Like with the electric network, gas is also transported throughout the

country by a transmission system operator (in the Netherlands, this is Gasunie Transport Services – GTS), and distributed to end-users via the distribution network through the gas distribution network. Similar to higher voltages in the electric transmission network, the gas transmission network makes use of higher pressures (up to 87 bar) to transport large amounts of gas over long distances. Figure 2.3 shows a schematic overview of natural gas infrastructure. The natural gas transmission network connects to the distribution network at city gates, which are typically found at the outskirts of cities. The pressure at city gates in the Netherlands drops from 40 bar at the transmission level to 8 bar for distribution, and further decreases in pressure down to 100 mbar for residences.

Remarkably, the Dutch natural gas infrastructure contains separate infrastructure for high-calorific (H-gas), which is sourced from imports and smaller gas fields, and low-calorific (L-gas) natural gas, which is extracted in Groningen. H-gas is mostly used by industry and gas-fired power plants, while the remaining commercial and residential consumers make use of L-gas. The H-gas is also converted to L-gas at one of the four blending plants in the Netherlands which add nitrogen to reduce the calorific value.

Energy storage is treated in Section 2.3, but it is worth mentioning that natural gas is suitable for long-term storage of large amounts of energy, and this used to meet seasonal variations in demand. The Netherlands has five underground gas storage locations (depleted fields and salt caverns) with a sizeable capacity of 14.4 bcm (billion cubic metres – using a gross calorific value of $35.17\,\mathrm{MJ\,m^{-3}}$ for natural gas, this equals 140 TWh of storage). For context, this is comparable to the total electricity consumption of the Netherlands in 2018 (114 TWh) [52].

Considering the scale of natural gas infrastructure available, and the intention to phase out natural gas in the following decades in favour of more sustainably sourced gases, there is discussion on repurposing the existing infrastructure. Specifically, hydrogen is envisioned to play an important role in the future carbon-neutral energy systems, both as feedstock for industry, and as a fuel (including for heating and mobility). For example, the *EU Hydrogen Strategy* released in 2020 mentions: "The repurposing of existing gas infrastructure for transporting hydrogen or hydrogen-based fuels also needs further research, development and innovation activities" [53, p. 15-17]. The same report also posits that a future hydrogen network in the Netherlands and Germany may consist of up to 90% of repurposed natural gas infrastructure. This is, however, expected to take place only after 2030 when the natural gas use is scaled down and hydrogen is more established.

Depending on the production methods, hydrogen is broadly classified as grey, blue or green hydrogen. Most hydrogen used today is grey hydrogen: it is produced via steam methane reformation (SMR) using high-pressure steam to react with methane, which produces hydrogen and carbon dioxide. Blue, or low-carbon hydrogen refers to grey hydrogen for which the resulting carbon dioxide has (mostly) been captured and stored. However, the most sustainable form of hydrogen production is using electricity from renewable sources to split water into oxygen and *green* hydrogen. Section 2.4 contains more information on the coupling of electricity and gas networks. The right-hand side of Figure 2.4 shows how the supply of these different types of hydrogen could develop until 2050 in Europe.

Figure 2.4 shows the possible change in the composition of gases in the European gas supply between 2020 and 2050 in a study of accelerated decarbonisation pathways [6]. As depicted in the figure, natural gas (light grey in the left-hand plot) plays a prominent role until 2030. Between 2030 and 2050 the supply of natural gas rapidly declines, and is largely replaced by blue and green hydrogen. In the transitional phase leading up to 2030, the blending of hydrogen with natural gas in existing networks could be beneficial. This might help kick-start decentralised renewable hydrogen production projects rather than, for example, the more costly transport of hydrogen by road. Nevertheless, only a limited amount of hydrogen can be mixed with natural gas when the devices (like boilers) connected to this network are made to be used with natural gas [53].

Hydrogen has different physical properties than methane, including a lower energy density and a faster diffusion speed in air. It seems that with some minimal modifications, existing natural gas infrastructure can be repurposed for a hydrogen network [54]. A 2018 study on the future of gas networks in the Netherlands concluded that existing gas networks are suitable for sustainable gases (hydrogen and biomethane) with only minor modifications in the gas transmission and distribution network components. The biggest changes would have to take place regarding metering, and by

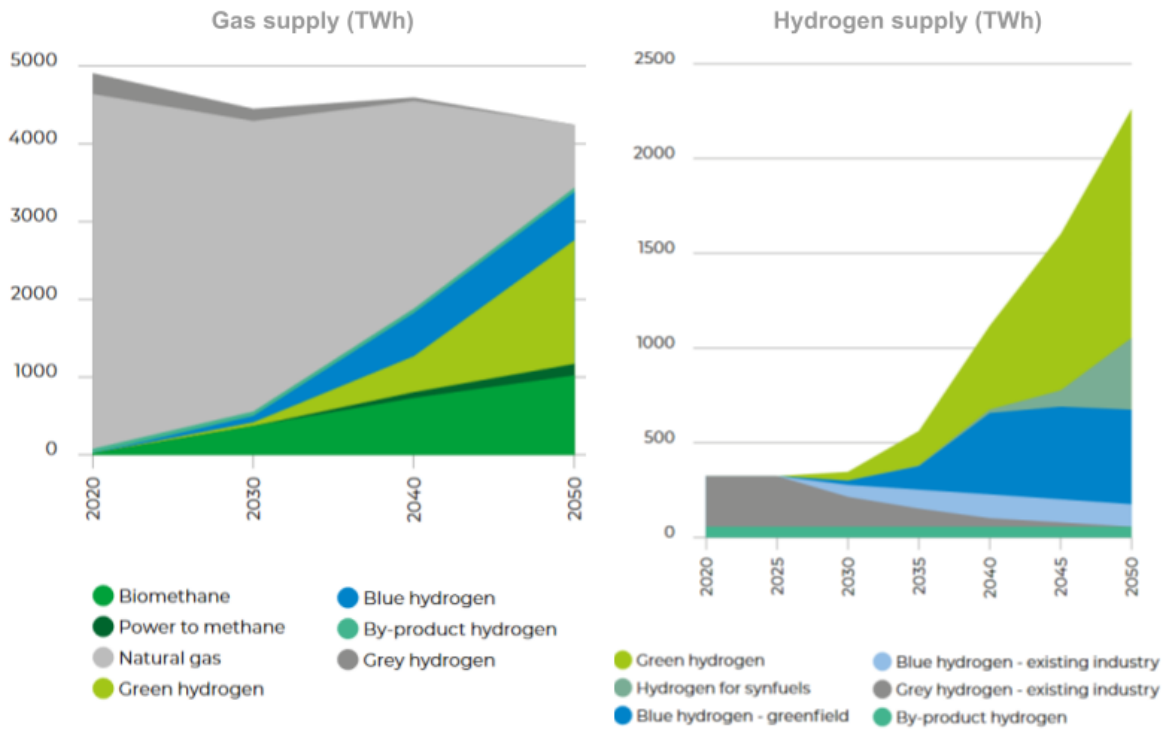

Figure 2.4: EU supply of all gas (left) and only hydrogen (right) between 2020 and 2050 in an accelerated decarbonisation pathway [6].

replacing the natural gas-based equipment of the end-users [55]. Practical and experimental studies are being carried out to investigate the operational, economical and safety aspects of repurposing natural gas infrastructure for hydrogen. One recent example is a 2021 study conducted in the Australian Capital Territory on the feasibility of repurposing nylon and polyethylene pipes and fittings from the medium pressure distribution network for hydrogen [56].

2.2.1. Modelling gas networks

Gas is transported from supplies to customers through pipes, and the pressure difference between the upstream and downstream nodes of a pipe determines the gas flow rate. Gas pressure drops along pipelines due to frictional resistance, which is compensated by compressors along the network. Unlike with electricity, the supply of demand does not have to closely match demand at all times. Gas is compressible, and the concept of *linepack* is used to describe how more gas can fit in the volume of a pipeline at times of high supply, which can be withdrawn for short-term local demand [57].

When modelling gas networks, the main variables of interest are pressure, volume, density and temperature. The dynamics of gas flows are computationally complex and non-linear, and network expansion models typically make assumptions such as horizontal pipelines with constant temperature and velocity profiles along their length, and one-dimensional flows. The Weymouth and Panhandle equations are simplified approaches for computing steady-state gas flows. Aside from flows in pipelines, gas network models also include compressors, storage and constraints based on the physical limitations of the components. More details of modelling gas networks can be found, for example, in [58–60].

At Stedin, the commercial IRENE Pro gas pipeline analysis software is used for the gas network. It includes functionality for network design and reliability analysis in addition to computing gas flows. Other dedicated, commercial software such as Synergi pipeline also exists for gas network-related simulations. One potentially relevant open-source resource is *fluids*, a Python library with extensive modules for pipings, pumps, tanks, compressible flows and more [61].

Because this thesis is a high-level and early-stage exploration Sterrenburg of the case study with a

focus on the electrical aspects, the gas network is heavily simplified by modelling the gas network as conceptual energy flows (rather than physical flows through pipelines). Future works can extend the gas model for more insight into the opportunities, limitations and costs related to the gas network.

2.2.2. Heat networks

Although heat networks are not modelled in this thesis, they are worth mentioning at least briefly because of their relevance to sector coupling and system integration. Much of the final energy demand in the built environment is for heating, especially during the winter in cold climates such as in the Netherlands. Currently, this heating is often done by combusting fossil fuels on-site, such as with natural gas boilers. One alternative to this is to electrify the heating, for example using a heat pump, and to lower the demand by means of better insulation. The idea behind heat networks, also known as district heating, is to supply buildings with heat directly by using a network of insulated pipelines carrying a heated fluid.

Heat is injected into the heat network through fossil-based, renewable and waste sources of heat, for example: geothermal and solar thermal heat, CHP plants, waste-to-heat, and residual heat from industry. Heat losses from the pipelines become substantial over longer distances; therefore, heat networks are typically contained within neighbourhood or city scales. The heat losses are also higher when the network operates at a higher temperature; different generations of heat networks have progressively operated at lower temperatures. The first generation used steam, the second and third used pressurised hot water above and below 100 °C respectively, and the fourth generation uses water at lower temperatures, combined with diverse heat sources, integration with other carriers and sometimes also providing cooling [62]. Major district heating systems are operational in cities across the world, including Moscow, Beijing, New York, Stockholm and Paris, with the total number of such systems estimated at 80,000 [63].

2.3. Storage

Energy storage comes in many forms and scales. Its importance at the grid level is expected to increase in future energy systems with an increasing proportion of intermittent renewable energy, especially following the expected development in storage technologies. Figure 2.5 shows an overview of energy storage types, along with an indication of their typical power ratings and discharge times.

Some of the most important properties of an energy storage system that determine its applications are the capacity and the rate at which energy can be stored/released. Other important considerations include cost, energy density, standing losses, scalability, round-trip efficiency, lifetime, mechanical robustness and safety aspects. As Figure 2.5 shows, energy storage technologies can be categorised according to the type of energy stored: electrical, electrochemical, thermal, mechanical and chemical (hydrogen). Pumped hydropower and compressed air can be used to store large amounts of energy (in the range of GWh), but these also rely on geographical features such as mountains for pumped-hydro and underground caverns for compressed air. Hydrogen is another form in which lots of energy can be stored, for example as a compressed gas or in liquid form. At this scale, energy storage can be used to meet seasonal variations in energy demand [7].

Storage can provide different services to energy networks. In terms of ancillary services to support electrical power grids, energy storage can facilitate frequency regulation, voltage support and black starts. These services are typically provided by electrical and electrochemical storage systems [64]. On a scale of minutes and hours, storage systems can facilitate arbitrage, or time-shifting by levelling loads and shaving peaks in demand. This also helps in avoiding load shedding and the curtailment of renewable energy generation, and storage systems can with high ramp rates can provide peaking capacity. These services can help defer or even avoid grid reinforcement investments altogether by moderating moments of high net demand or supply.

Several overviews exist which compare the properties and suitable applications of different energy storage forms in more detail, such as [65], or focusing on battery energy storage, such as [64]. Batteries are becoming more cost-competitive, especially lithium-ion batteries. These systems are especially

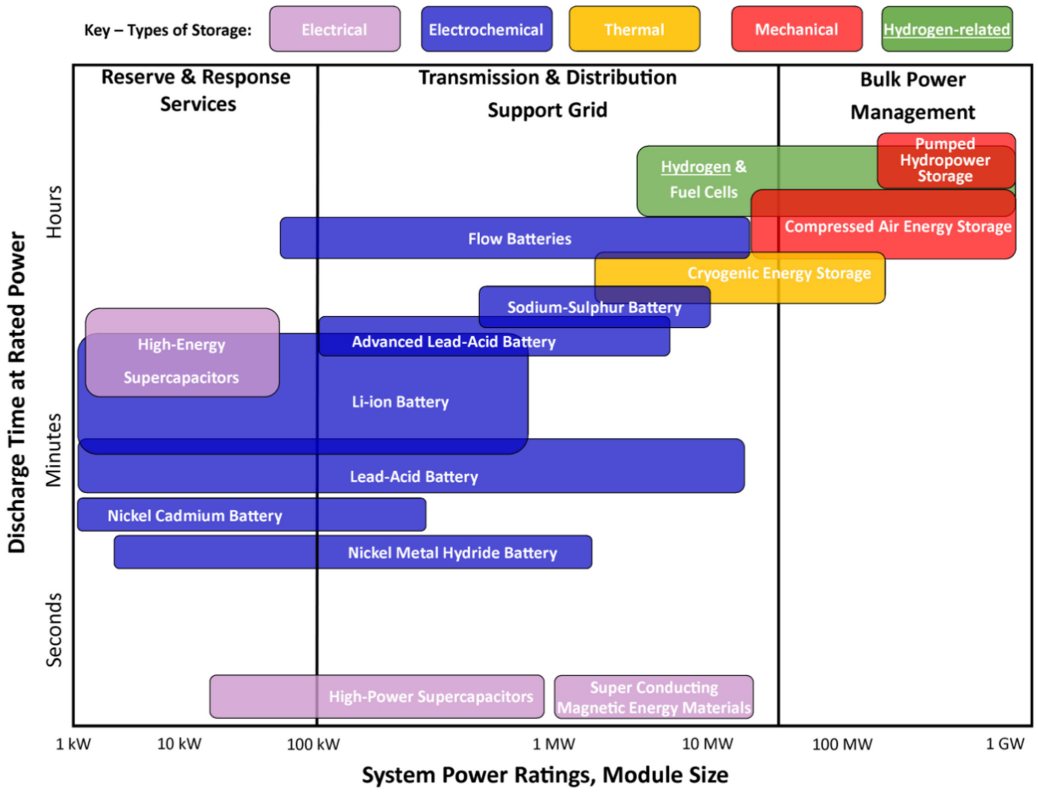

Figure 2.5: Comparison of energy storage technologies and their power ratings and capacities [7].

cost-effective for up to 4-8 hour capacities (of energy storage at their rated power). For example, this study by Denholm et al. [66] shows that 4-hour batteries are a valuable alternative to fossil-fuel based peaking capacity in the United States, especially in systems with a high penetration of photovoltaic generation.

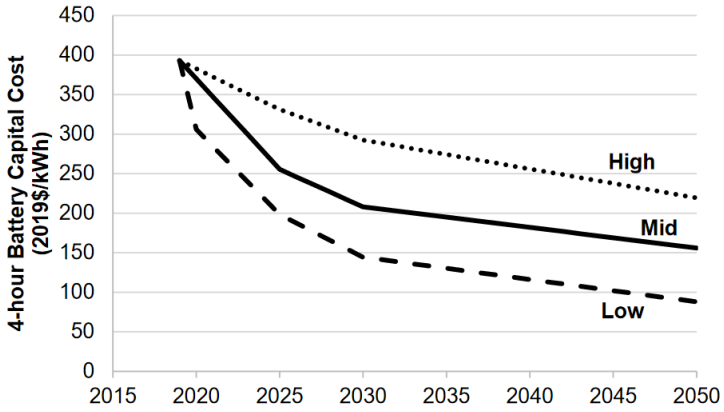

Figure 2.6: Cost projections for 4-hour lithium-ion battery systems until 2050 [8].

Moreover, expected decreases in the prices of battery energy systems will support their large-scale deployment in future grids. In fact, [67] predicts that after 2030, lithium-ion batteries will be the most competitive energy storage type for a variety of applications including arbitrage, power quality, grid investment deferral and congestion management. At this stage, larger systems in the range of 10–100 MW will also be feasible with lithium-ion storage. Figure 2.6 shows the expected decrease in the capital cost of 4-hour lithium-ion batteries between now and 2050, with the mid-range expectation showing a substantial decrease from about 400 $/kWh to just 150 $/kWh.

The rising popularity of electric vehicles is also relevant in the context of system integration and power grids. Using smart and coordinated charging technologies, electric vehicles can provide

flexibility to the electricity grid and offer ancillary services, including peak shaving, voltage and frequency regulation under a concept known as vehicle to grid (V2G). Electric vehicles collectively add a substantial load, but also dynamic storage capacity to the grid, and investigations into their challenges and opportunities will be important in designing future power grids [68].

2.4. Energy system integration

Energy system integration refers to an approach of energy system planning and operation where different forms, carriers and infrastructures of energy are treated as an interconnected system rather than separately. Energy system integration is also known as multi-energy systems, sector coupling or smart energy systems. The main benefits of the system approach include a reduction in primary energy use, decreased need for capital expenditure, more flexibility in the electrical power system and increased security of supply [9].

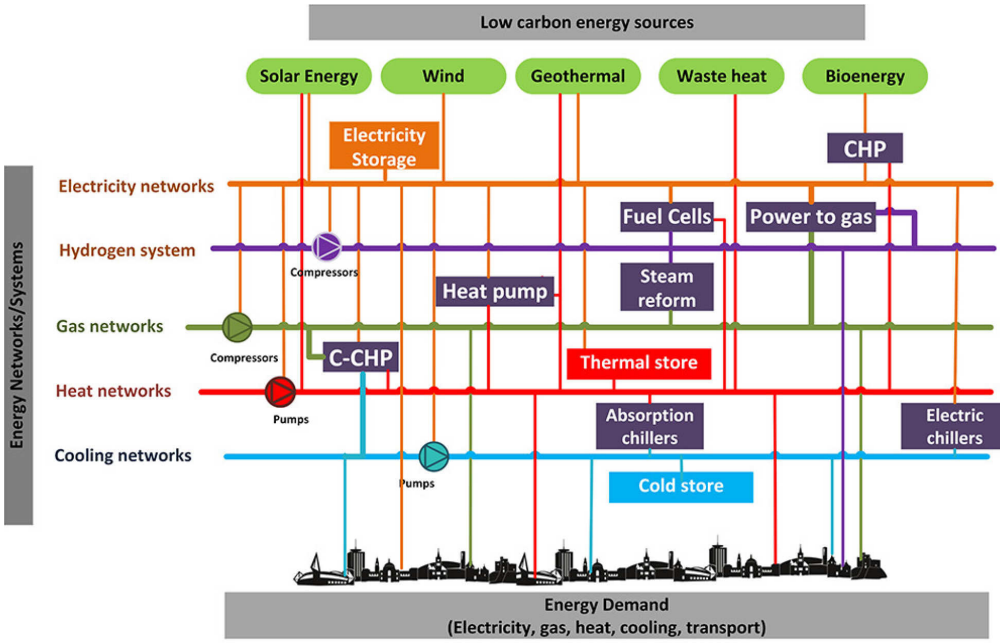

Figure 2.7: Schematic showing the integration of different energy networks, local generation and storage components [9].

Often, energy storage is also included within the scope of energy system integration since the interconnection of different carrier infrastructure also increases the interconnection between their respective storage system, and enhances the benefits of system integration. Figure 2.7 shows an example of the networks and components in an integrated energy system, as a more elaborate version of Figure 1.1. It shows networks for electricity, hydrogen and (natural) gas, heating and cooling. These networks are interconnected through energy conversion devices. Electricity and gas networks interact through fuel cells, gas turbines and power-to-gas which convert energy between electrical and gas forms, and steam reform is used to convert natural gas to (grey or blue) hydrogen. The electrical network connects to heating/cooling networks via heat pumps and electric chillers. Combined heat and power (CHP) or even combined cooling, heat and power (C-CHP) uses gas to generate electricity and heat (and cooling). Such a system, also known by co-generation or tri-generation, makes use of a gas turbine, a heat exchanger and an absorption chiller.

The multi-energy systems can be applied at different scales, ranging from a single building to districts, regions and up to country-level. Multi-energy systems can be modelled as energy hubs, an input-output concept. Vectors of different forms of energy flowing in and out of a system like a building or a city, and the hub itself is represented by a coupling matrix containing terms of the conversion efficiency and connections between energy types; see for example Zhang et al. [69].

Multi-energy system models tend to focus on operational or expansion planning (network design) aspects. Especially with operational planning, it may be important to take dynamics into account rather than just steady-state models; for example, gas and thermal energy networks have more storage capacity in their transport infrastructure, and different transient behaviour. Modelling these together can help to develop more efficient scheduling and control algorithms for the operation of multi-energy systems.

In this thesis, the focus is on long-term expansion planning with links between the electricity and gas (hydrogen) networks. For power-to-gas, electrolysers are considered, and hydrogen turbines for conversion from hydrogen to power. Both these technologies are still being developed, and projected 2050 parameters are used to model them.

Electrolysers use electric power to split water into hydrogen and oxygen. When this is carried out with power from renewable energy sources, the resulting hydrogen is referred to as green hydrogen, since it does not result in any carbon dioxide emissions. Different types of electrolysers exist, of which the main types available at an industrial scale are alkaline, proton exchange membrane (PEM) and solid oxide, mainly differing in the material separating the anode and cathode. Additionally, alkaline and PEM electrolysis are carried out at near-ambient temperatures, whereas solid oxide electrolysis is operated between 700 and 950 °C [70]. Figure 2.8 shows how [10] projects the investment costs for different electrolysis technologies to drop between 2020 and 2050.

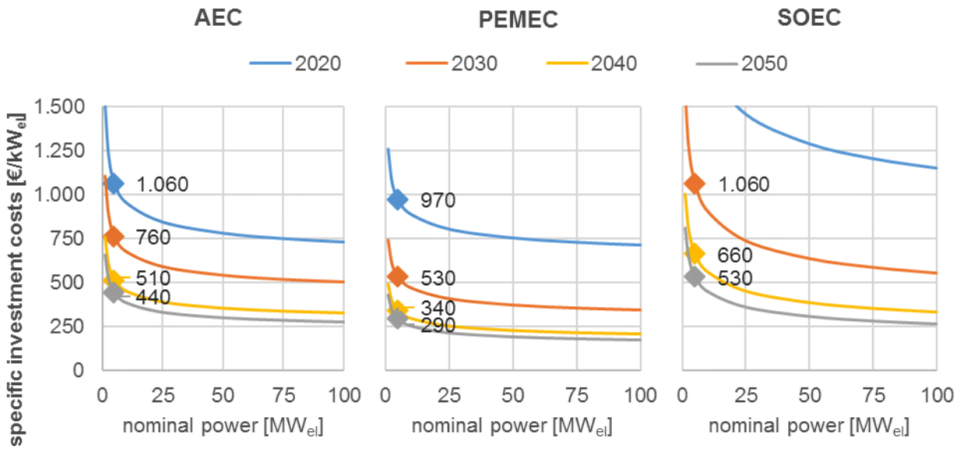

Figure 2.8: Projected investment costs for three different electrolysis technologies between 2020 and 2050, at installed capacities up to 100 MW [10].

Figure 2.8 shows that at the moment, alkaline electrolysis cells (AEC) and proton exchange membrane electrolysis cells (PEMEC) are cheaper than solid oxide electrolysis cells (SOEC). However, by 2050, all three technologies will have become substantially cheaper, and the price differences among them will be smaller. The plots also show that the specific investment costs are lower for larger electrolysis systems. Regarding the efficiency of electrolysers: this reflects the ratio of hydrogen energy produced per unit of electric energy. However, there are multiple ways of determining the energy content of a gas. The higher heating value (HHV) or gross calorific value measure the upper limit of thermal energy released through complete combustion of the fuel. The lower heating value (LHV) or net calorific value assumes that water resulting from the combustion process is in a vapour state at the end of combustion. Depending on the application of the fuel use, one of the definitions may be more suitable. In this work, the LHV is used for electrolysis efficiency since this gives a more conservative estimate.

Hydrogen produced from electrolysis can be used in industry, heating or mobility. As Figure 2.5 shows, large amounts of energy can also be stored effectively as hydrogen. Conversely, hydrogen can be converted back to power, using technologies such as stationary and mobile fuel cells (especially for mobility), and gas turbines. Today, the contribution of hydrogen in generation power is negligible at less than 0.2% of all electricity generation. Existing gas turbines can handle hydrogen shares of 3-5%, and gas turbines using only hydrogen are being developed. At grid scale, gas turbines might be more favourable than fuel cells considering their longer lifetimes and larger output powers [54].

2.5. Energy markets

The following section focuses on power markets, but many of these concepts also extend to other commodity markets including gas. The ownership of energy transmission and distribution infrastructure is a natural monopoly in a spatial region: system operators tend to own all of the transmission or distribution infrastructure within an area. These monopolies are regulated by authorities such as governments, to oversee the cost and quality of the infrastructure. In Europe, there has been a shift towards unbundling, which means that the ownership of transmission and distribution assets is separated from energy generation [71]. This unbundling has been accompanied by the deregulation, or liberalisation of the energy market. Profit-seeking energy suppliers compete at energy trade markets.

The goal of liberalisation has been to encourage diversification, efficiency and innovation among energy generation companies, while providing reliable energy to consumers at a low cost. Electricity markets also aim to stimulate efficient long-term investment decisions. Electricity markets are distinct for a number of reasons: the supply must match demand closely at any time, storage is limited (with current technologies), and the demand has a very low price-elasticity (customers respond very little to short-term price variations, partly due to the fact that retail prices are kept stable while wholesale prices vary much more) [72].

The system operator is responsible for keeping the voltage and frequency steady, maintaining the balance between demand and supply, managing congestion, and black-start capabilities. These are obtained in the ancillary services market, and provided by spinning, supplemental and replacement reserves, which are able to respond within different time-frames [73].

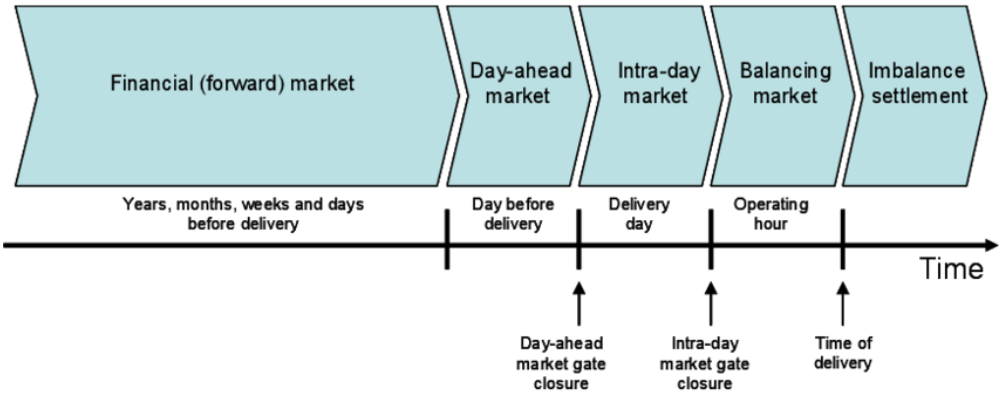

Figure 2.9: Time horizons and structure of wholesale power markets [11].

Trade between buyers and sellers can occur directly, which is known as bilateral or over-the-counter (OTC) trade, and this form tends to happen be used more for longer-term (forward) contracts. Alternatively, trade can be mediated by power pools and power exchanges where an auction is run at regular times to set a uniform market price that all buyers pay and all sellers receive. As shown in Figure 2.9, power exchanges operate at different time scales to spread risks and to match supply to consumption as closely as possible. The forward, or futures market involves trade in contracts for delivery at a future date [73]. This will only represent a part of the ultimate power flows, since demand and supply based on predictions.

Day-ahead and real-time markets are referred to as spot markets, where bids can be placed until the moment of gate closure. Day-ahead markets typically trade hourly or block contracts for the following day by means of a double-sided auction in which both buyers and sellers place bids. Trade can also take place on a continuous basis, in which demand and supply bids are immediately finalised when a match takes place. Intra-day markets facilitate trading on the day of delivery itself, and balancing markets occur in real-time to ensure the power generated matches the load. Imbalance settlement takes place ex-post, in which parties are penalised for physically deviating from the contracted energy amounts [74].

Energy markets can encompass different sizes. In a uniform market, physical infrastructure limitations are neglected using a “copper-plate” assumption. In this case, the system operator must apply

re-dispatch in case of congestion by reallocating the (market-determined) generation based on network constraints. Conversely, in systems with frequent congestion, capacity can be allocated between each set of nodes, i.e., a nodal market system. Between these two concepts lies the zonal system, where the inside of a zone is treated as a copper plate, and trade between zones is constrained by capacity. Many European countries are grouped in markets which use such a system, for example in the EPEX (European Power Exchange) SPOT exchange. Coupling the zones between European countries has led to some convergence in their respective day-ahead power prices, but it is still limited by interconnection capacities [12].

In power exchanges with double-sided auctions, the demand and supply bids are aggregated for each period and the market-clearing price (MCP) is set where the aggregate demand and supply curves intersect. See for example Figure 2.10: at the indicated MCP, the demand is exactly equal to the supply, and there are no more buyers or sellers who are willing to trade at that price (i.e., the market "clears").

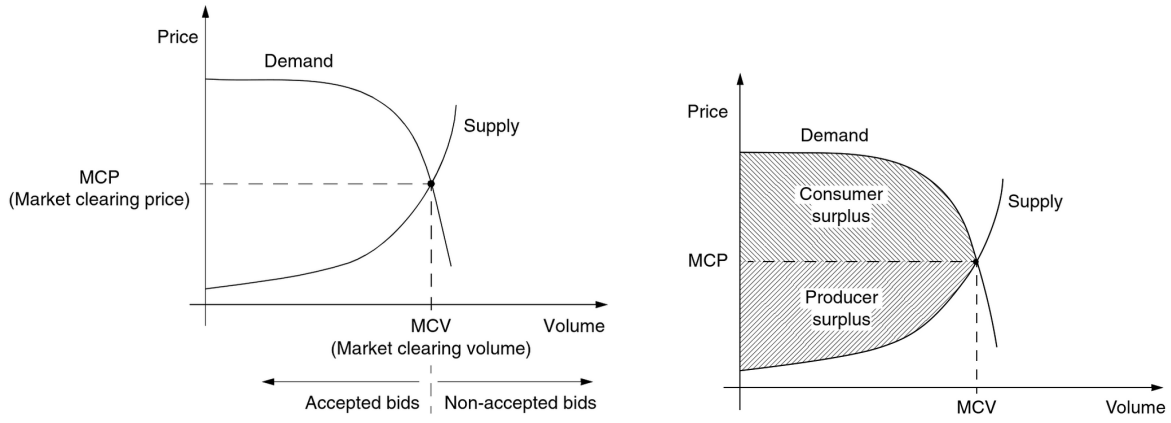

(a) Market equilibrium (b) Economic welfare

Figure 2.10: Competitive market clearing mechanism with demand and supply bids [12].

The competitive system as illustrated in Figure 2.10 shows the merit-order effect: suppliers with lower price bids are the first to be dispatched, while those with higher bids are not accepted except in times of extremely high demand. This also leads to economic dispatch: a given amount of power is supplied at the lowest possible cost since the cheaper supply bids are accepted ahead of the more expensive ones. In a perfectly competitive market, the participants are price-takers, and that they cannot influence the price since there are assumed to be infinitely many buyers and sellers in the market. Under perfect competition, buyers bid a price equal to the marginal value they place on the product. Sellers bid a price equal to the short-run marginal cost of production, this can include start-up, fuel and possible emission costs. The market price will equal the marginal cost of the last-dispatched (most expensive) generator. Under perfect competition, bidding above the marginal cost would decrease the frequency at which suppliers are dispatched (and decrease revenue), while bidding below marginal cost could force them to operate at a loss-inducing price [75]. In 2.10b, the market equilibrium is shown to maximise the sum of consumer surplus and producer surplus, which together equal the economic welfare (the shaded area). Any other combination of price and volume would decrease the consumer surplus (area between the demand curve and price) or producer surplus (area between the supply curve and price) [12].

In reality, the number of participants in power exchanges is limited, and suppliers can influence their prices and profits for example by withholding capacity, or bidding above marginal cost price in an oligopolistic market structure. Another approach is fixed-cost bidding, in which a supplier adds a fixed mark-up to each bid based on CAPEX and OPEX costs. There are also other complicating factors in practice, such as pricing the Value-of-Lost-Load, scarcity pricing, congestion, and the price elasticity of demand, see for example [72] for more details.

Another consideration is whether the current supply bids based on marginal costs are still suitable in future energy systems with a high proportion of intermittent renewable generation. Considering that solar and wind renewable technologies do not require fuels for their operation, their marginal

costs are close to zero. Due to the merit-order effect, this will cause these generators to be dispatched preferentially, and cause electricity prices to plummet in markets with abundant renewable energy generation. This is also complicated by the fact that that intermittent renewable generation can have high fluctuations, and the exact capacities are not known ahead of time. While there is not yet a consensus on how to approach these challenges and redesign power markets if necessary, there is active discussion in literature.

For example, [76] stresses the need for sufficient mid and peak load generators and suggests that subsidies might stay necessary to increase wind and solar power capacities. Another study suggests two main possible solutions: returning to a centralised market, or redesigning the market-clearing mechanisms to accommodate intermittent renewable energy [77]. Similarly, [78] also suggests to either keep subsidies such as feed-in tariffs, or to redesign power exchange markets. On the other hand, [79] argues that fundamental market principles need not change. It is reasoned that the market will encourage investment in large-scale energy storage, which will have sufficiently dropped in price by the time renewable energy forms a substantial proportion of energy generation. This would be in combination with active demand involvement in the market, and scarcity pricing.

Keeping in mind these expected changes in the energy infrastructure and markets, there is much uncertainty regarding the future energy prices. Figure 2.11 shows the historical annual average day-ahead electricity price in the Netherlands from 2000 to 2010 (solid line), and the projected price until 2030 (dashed line) along with a margin of error (*bandbreedte*, light green shading), based on the current and expected policy developments. Electric energy is expected to become more expensive in 2030, with the expected price range between 30 and 70 €/MWh.

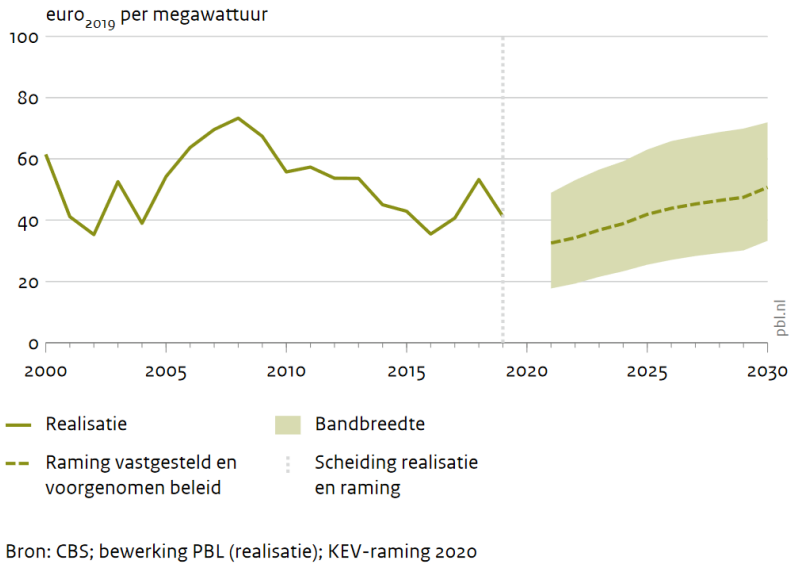

Figure 2.11: Historical and projected average day-ahead wholesale electricity prices in the Netherlands between 2000 and 2030 [13].

In this thesis, a simplistic approach is taken with regard to modelling the market, as will be explained in Chapter 4. In brief, marginal cost bidding is used for the local generators within the region of the case study, and three discrete bid levels are used to model exchange with the rest of the grid. The sizes of these bid levels vary (linearly) with local demand and supply. Local and external bids compete in the market. Local demand within the case region is price inelastic and essentially an infinite bid, so it will always be met.

See also for example in Bent et al. [60], where an endogenous gas pricing function is formulated using historical price and operating data, which in turn affects the electricity prices. Fitting parameters to this data results in a quadratic function of total zonal demand, where the spot prices rise when demand is higher at that location. This is subsequently used for joint electricity and natural gas transmission planning.

3 | Network expansion planning

This chapter outlines the process of network expansion planning with a focus on optimal planning. In Section 3.1, the fundamental concepts of the expansion planning problem are explained. Section 3.2 describes some of the stochastic and contingency considerations that have to be kept track of in power system planning. Finally in Section 3.3, the process of formulating and solving an expansion planning optimisation problem is described, along with a review of some tools available for energy system planning.

3.1. Power system planning fundamentals

Expansion *planning* or *design* refers to decisions on future modifications of infrastructure such as new investments, rather than the *operation* which involves decisions such as dispatch and maintenance in the context of the existing system. Grid expansion planning is complex, in view of interactions between networks, loads, generators, and different energy carriers; the reliability in case of contingencies; and the future time periods in question with accompanying uncertainty. The power system must allow energy demand to be met while staying within constraints imposed by generator, storage and network capacities. In the short term, decisions need to be made on how to dispatch and operate components, and in the long term planning decisions are made on how to add, reinforce or decommission components of the network to allow it to serve its functions.

Power system planning processes are typically carried out by first developing future load and generation scenarios, and then determining how to (best) modify the existing infrastructure to meet the future power system needs. The planning decisions can include the timing, siting and capacity of each modification [80]. In this thesis, the focus is on *expansion* planning (i.e., the addition of components), and not on evaluating the status of the existing network, or planning the removal/replacement of the components which are already in place.

Expansion planning takes place on the scale of years and comprises decisions on future network modifications including the addition and reinforcement of substations and lines. System operators typically outline their investment plans in a Ten-Year Network Development Plan (TYNDP), which is periodically updated (for example, every two years). Due to the rise of distributed generation throughout power systems, it can be beneficial to consider network expansion and generation planning together, even when these are carried out by different decision-makers [48]. System operators can also use their investment plans to advise decision-makers on suitable locations for renewable energy projects.

Section 3.3 describes the processes related to optimal expansion planning. However, expansion planning is not always optimised in practice. For example, an expected system inadequacy at a particular location might be foreseen by the system operator, based on the announcement of a new investment project. In a radial system especially, there might only be one location at which a reinforcement investment can solve the inadequacy. Based on the magnitude of the deficiency, or on standardised component size, an investment decision could be made, or a set of investment alternatives could be generated manually and evaluated against the relevant objectives [81]. The algorithmic optimisation approach is especially useful when trade-offs are being made between different alternatives.

3.2. Uncertainty and contingencies

Power systems are vital infrastructure, and it is important that they are reliable. System adequacy evaluates the steady-state performance of a system when faced with minor disturbances such as load variations [82]. Power system stability is a time-varying characteristic which describes its ability to

withstand adverse circumstances or disturbances known as contingencies by continuing to operate as intended. Security relates to stability; it relates to not only the occurrence of failure under contingency but also the extent thereof. Finally, reliability aggregates the stability and security of a power system over time [83].

Building redundancy into the power system involves a trade-off as it will improve reliability, but also increase costs. Considering the trade-off between the cost of investing in networks and their reliability, indices and criteria exist to evaluate the reliability of power systems. A deterministic approach typically assigns a fixed redundancy requirement for a system. This could be a fixed reserve margin for components which must be left unused. Another way is to require the presence of redundant components. For example, N - 1 requires that the power system is able to deliver all required power to end-users even when any one component fails or is out of commission. N - 2 describes the same, but for two components. Deterministic requirements might also be conditional, for example N - 2 during regular conditions and N - 1 during maintenance [84]. Alternatively, N - 1 redundancy could be required for times of net demand, and N (no redundancy) could suffice for net generation.

Alternatively, there are probabilistic approaches to evaluating system reliability. These include the loss-of-load expectation (LOLE), expected energy not served (EENS), system average interruption duration index (SAIDI) and system average interruption frequency index (SAIFI), of which the latter two are often used for power distribution systems. In expansion planning, reliability requirements can be set as constraints which have to be met, and the reliability indices can be evaluated by considering the effect of various outages. Probabilistic analyses can be carried out, for example, using Monte Carlo simulations. For more details, see for example [69, 85].

Since expansion planning is concerned with the future system, there are unavoidable uncertainties involved. This includes, for example, the hourly generation capacities of weather-dependent generators. Additionally, some parameters depend on many subsequent processes and decisions, for example the prices of electrical storage devices which depend on the research and development activities leading up to the time which is modelled. Many dedicated approaches exist for characterising, modelling and optimising probabilistic systems. For example, model parameters can be treated as random variables drawn from a probability density function. Alternatively, approaches like fixed-interval analysis exist, which consider parameters to be distributed within a set of limits. A solution is *robust* if it meets the reliability criteria for all extremes of the parameter intervals considered [86]. Another aspect of uncertainty due to unbundling and deregulation, such that generation, transmission and distribution are carried out by different parties. While there is coordination between these parties, each still faces some uncertainty from the actions of the others [47].

In this thesis, a deterministic model is developed. An N - 1 approach is approximated by leaving a redundant set of components out of the initial model simulation. The uncertainties in the future parameters are addressed firstly by the use of different load and generation profile scenarios, and secondly by performing a sensitivity analysis on a selected set of input parameters. These aspects of the model are explained in Chapter 4.

3.3. Optimal planning

It is worth noting that numerous factors affect expansion planning including regulations, societal acceptance, coordination with other construction works, acquisition of permits, maintenance, and decommissioning of ageing components. A mathematical optimisation model will likely omit several of these factors, but it nevertheless provides insights into the factors which are considered, and the optimisation results can always be manually modified for any practical considerations if necessary.

Mathematical optimisation problems are defined by decision variables subject to constraints, and an objective function to be minimised (or maximised). The decision variables are the independent factors which are varied to obtain an optimum, for example the decision of whether or not to build an additional cable in the case of expansion planning. Investment decisions can be represented by binary (integer) variables which indicate whether or not a certain candidate investment is carried out. Constraints limit the solution space of the decision variables, based on limitations of technical, economic or environmental nature. The remaining solutions are known as the feasible region.

To determine the optimal solution from among the feasible solutions, an objective is defined as a function of the decision variables. For expansion planning, this objective typically includes time-discounted investment and operational costs, and potentially other factors such as a penalty for unserved energy. A generic mathematical optimisation is expressed as in Equation 3.1, where $\boldsymbol{x}$ is a vector of optimisation variables, $C(\boldsymbol{x})$ is the objective function, and $\boldsymbol{f(x)}$ and $\boldsymbol{g(x)}$ are the sets of equality and inequality constraints respectively. The objective function can contain terms of just one type (for example, cost) or multiple types (such as costs and a reliability index). The terms in a multi-criteria objective function can be weighted to reflect their relative importance.

$$\begin{aligned} &\min_{\boldsymbol{x}} C(\boldsymbol{x}) \\ &\text{s.t. } \boldsymbol{f(x)} = 0 \quad \text{and} \quad \boldsymbol{g(x)} \leq b \end{aligned} \tag{3.1}$$

3.3.1. Modelling expansion planning problems

Expansion planning problems have in common an objective function and constraints, but there are many different aspects that can distinguish how they are modelled. This includes the planning horizon (static or dynamic), the (non-)linearity of the problem and possible integer variables, and whether the problem is modelled as deterministic or probabilistic. In literature, there tends to be more focus on the planning of transmission networks than on distribution networks, but as mentioned in Section 2.1, many of the same principles apply. Aside from transmission and distribution networks, expansion planning can also include generation assets, non-electricity networks and conversion devices, or a combination thereof. The expansion planning formulation considerations are elaborated on below.

In *static* expansion planning, a single investment stage is considered, independently of other years. A semi-static or quasi-dynamic expansion plan builds on this by considering multiple sequential stages during which investments can be made, and feeds the result from each stage into the following one. With *dynamic* expansion planning, different investment stages are considered together to determine an overall optimal investment plan [47]. A semi-static investment planning algorithm is closer to reality than dynamic expansion planning, since in reality investments are made while the developments of the following investment cycle are still uncertain. That being said, dynamic expansion planning leads to solutions which are more optimal than semi-static solutions.

When the objective function and constraints are all linear functions of the optimisation variables, the problem is said to be a linear programming (LP) problem. Often, some simplifications have to be made to linearise a model (such as using linearised power flows), but this leads to benefits in solving the optimisation problem as explained in the next section. Expansion planning problems often have a discrete aspect to them, for example when only a fixed cable capacity can be chosen rather than any value. Integers are used in optimisation problems to model discrete decisions, such as binary variables (0 or 1), to indicate whether or not an investment is chosen. Many expansion planning problems use a linear formulation in which some of the decision variables are limited to integer values, i.e. a mixed-integer linear programming (MILP) problem. Non-linear formulations, such as using non-linear power flows or quadratic generation costs, can also be used for their increased physical accuracy.

In deterministic formulations, all input parameters have fixed values, and this always results in the same optimal solution. Probabilistic approaches can include varying some input values within a fixed range, or drawing parameters values from probability density functions. Stochastic programming is used to optimise the mathematical expectation of the objective function, based for example on scenarios weighted by their probabilities [87]. In [88], a stochastic approach is taken using Monte Carlo simulations to generate scenarios.

Regarding the investment possibilities (candidate components) in expansion planning problems: these are usually predetermined manually, i.e., a set of possible components with designated costs and physical properties is included in the input parameters. Mixed-integer formulations can use binary variables in combination with these candidates to let the optimiser indicate whether or not the candidate is invested in. In expansion planning problems with a large scope, manually including a set of investment candidates at each location can lead to excessive computational complexity. Methods exist to automatically determine a set of potential candidates, and to reduce the size of this set before

optimising the investments [81]. Expansion planning algorithms usually take an existing network into account (Brownfield). Making an investment plan for a case without considering any existing network (starting "from scratch") is also referred to as a Greenfield approach.

To highlight some more expansion planning formulation examples, [30] develops a static, MILP formulation with stochastic considerations of renewable generation capacity and prices to plan the integration of gas and electricity networks. In [32], probabilistic methods are used to generate scenarios for an otherwise deterministic non-linear expansion planning model (a mixed-integer second-order cone programming model). A dynamic formulation is used in [89] for a multi-year transmission expansion optimisation using a MILP problem.

3.3.2. Solving expansion planning optimisations

Various methods exist to solve optimisation problems, which also depend on the properties of the problem. The methods can be classified as mathematical methods and as heuristic methods. In convex problem formulations, the convergence of a mathematical solution is guaranteed. Linear problems are convex. Moreover, a globally optimal solution is also guaranteed for linear problems using mathematical solutions. On the other hand, heuristic methods have less strict requirements on the problem formulation. They might lead to solutions faster than mathematical methods, especially in non-linear cases. Heuristic methods might lead to local rather than global optima, and their convergence is not guaranteed. Non-heuristic methods may also lead to local optima and face non-convergence for non-linear problems [47, 90].

Heuristic algorithms are often inspired by natural processes, as reflected in their names. Many forms exist, and they often start with a set of solutions, moving incrementally to better ones. Evolutionary algorithms are popular among heuristic solutions, and they do not require explicit formulations of an objective function with constraints. Instead, an initial population of solutions is modified using methods for mutation, recombination, crossover and selection, and the best among these are chosen with a fitness function. Evolutionary algorithms include genetic algorithms and evolutionary strategy, e.g., [91]. Other heuristic methods include simulated annealing (based on thermodynamic principles) [92], particle swarm optimisation (based on bird and fish movements) [93], tabu search (inspired by memory response) [94] and ant colony (drawing from ant behaviour) [95].

Different mathematical solutions can be used depending on the type of optimisation problem. These can be solved with both commercial (e.g. Gurobi) and open-source (e.g. CPLEX) software tools. Using differential calculus, the method of Lagrange multipliers can be used to find the optimal solution of an optimisation problem with equality and inequality constraints, using Kuhn-Tucker conditions [47].

Linear programming problems have a convex solution space for which convergence to the global optimum is guaranteed. Two mathematical algorithms for solving linear programming problems are the simplex and interior point algorithms, which make use of the convex solution space's properties. Linear programming problems also have an associated dual problem, which can provide insights into the solution. Another advantage of linear programming formulations is that infeasibility can be identified relatively quickly (because, in theory, convergence is guaranteed) [47, 96].

Non-linear programming (NLP) problems including quadratic programming may be more accurate representations of physical systems, such as optimal power flow problems. Non-linear programming problems are typically solved iteratively, using direct or gradient-based approaches. Newton's method is suitable for a special case of non-linear programming problems: quadratic problems [96].

Mixed-integer problems are often decomposed into simpler sub-problems. For example, the branch-and-bound method is used by first applying an LP relaxation (removal of integer restrictions). For each integer variable, branches are made from this relaxed optimum to fixed it to the most optimal integer value, using a search tree [97]. Benders decomposition is another method for decomposing large optimisation problems into smaller problems. In [98], a mixed-integer disjunctive formulation is developed for expansion planning, using Benders decomposition in conjunction with the branch-and-bound decomposition to solve mixed-integer investment problems.

3.3.3. Modelling power systems operation and expansion

Many models and digital tools exist for analysing and optimising power systems. These vary in technical, temporal and spatial scope, as well as the purpose of their analysis and the solving methods. In this thesis, the requirements for modelling the energy include:

1. Operational and investment decision-making support,
2. functionality to model power flows,
3. modelling of network constraints,
4. possibility to model non-electrical networks,
5. an hourly time resolution.

To elaborate on these requirements: investment decisions are based in part on operational requirements. Moreover, system integration components also involve operational decisions, such as deciding at each time-step whether or not to convert power to gas. For this reason, the energy system model must support operational and investment decision-making. The electrical distribution system plays a prominent role in this system, making power flow calculations desirable. The capacities and other physical characteristics of the components must also be present in the model. Additionally, the gas network is considered in the case study. Demand and supply profiles are available at an hourly resolution (for a whole year). The modelling tool must also be suitable for modelling at a regional level, considering that some are focused on large scales (such as an international level) or small scales (such as a building).

Furthermore, there is a preference for open-source software. Access to the source code allows the freedom to alter this code if necessary, and often open-source software has an active community for discussions and new developments.

Table 3.1 shows an overview of selected models by comparing some of their relevant characteristics. Some of the models, for example EnergyPLAN and DER-CAM, do not account for the network infrastructure and capacities in sufficient detail. Others have a low time resolution (RETScreen) or lack of operational modelling (eTransport). For more exhaustive comparisons, see [99–101].

Table 3.1: Comparison of selected energy system modelling tools, adapted from [15].

	RETScreen	**EnergyPLAN**	**DER-CAM**	**eTransport**	**PyPSA**
Operation	Yes	Optimisation	Optimisation	No	Optimisation
Planning	Yes	No	Optimisation	Optimisation	Optimisation
Network	Yes	No	No	Optimisation	Optimisation
Resolution	Monthly	Hourly	Hourly/Variable	Hourly	Hourly
Time scale	Annual	Annual	Lifetime	Lifetime	Lifetime

For this thesis, PyPSA is chosen. PyPSA (Python for Power System Analysis) is an open-source energy modelling tool based in Python [14]. PyPSA supports the optimisation of investment and operational decisions, and has (limited) functionalities for modelling energy conversion and non-electrical networks. The optimisation uses linearised power flows, and as a branch of the main code (i.e., not yet part of the main code distribution), there is an integer implementation of investment planning for lines, which can be (and has been in this work) extended to cover integer investment planning for transformers.

4 | Model formulation and methods

In brief, the model is an investment and operational optimisation of an energy system, with generation and demand profiles based on 2050 scenarios. This chapter details the components, assumptions and methods related to the development of this model. A general description of the technical aspects of the model is provided in this chapter. The specific values used in the case study and results obtained are covered later, in Chapter 5. The model and its input/output aspects are visually summarised in Figure 4.1, and the details hereof are further explained in this chapter.

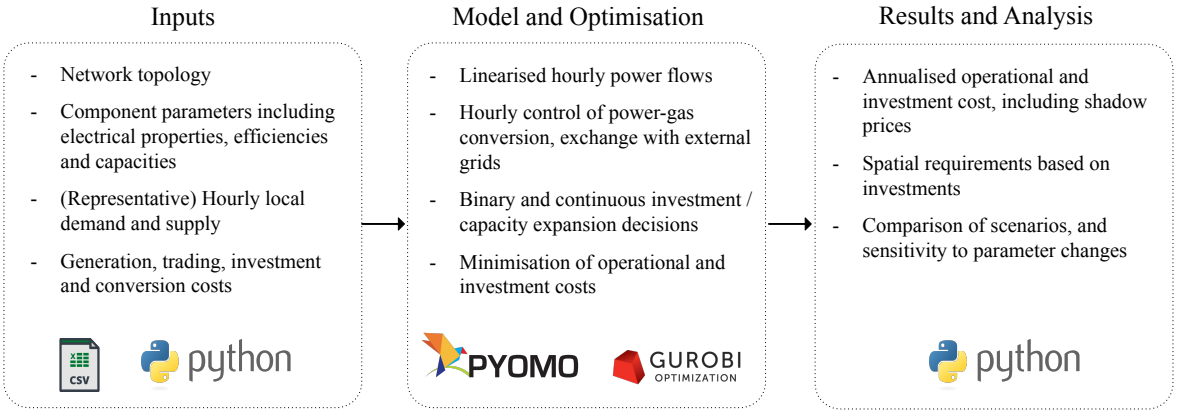

Figure 4.1: A visual summary of the model inputs, process and outputs.

In Section 4.1, the PyPSA model in Python and its different components are introduced. Next, in Section 4.2, the financial aspects of the model are described, including the investment costs and the model for trading with external grids. The objective function and constraints corresponding to each type of component are elaborated on in Section 4.3. The processes in the model relating to solving the optimisation problem are described in Section 4.4. In Section 4.5, the method for selecting representative time steps is explained, and the approach to the sensitivity analysis is covered in Section 4.6.

4.1. Grid representation and sector coupling

The open-source software toolbox PyPSA (Python for Power System Analysis) [14] is used for modelling the energy system and the optimisation problem. PyPSA includes code to translate static and time-varying input parameters of components into constraints and an objective function, which are optimised using a separate solver, and PyPSA is used again to interpret the optimisation results.

The model comprises the following component types, each with its own properties: buses, generators, lines, links, loads, storage units and transformers. Buses are the fundamental nodes to which all other components are attached and where energy conservation is enforced. A visualisation of this is shown in Figure 4.2, where energy flows f occur between buses m and n with generation g (s and w for solar and wind generation) and loads d. The equations at the bottom of the figure show that all the energy flows into any bus equal energy flows out of a bus.

Each bus has a "carrier" type, and in this model, AC (alternating current) and gas are used. This property merely indicates at which buses components with electrical properties (such as resistance) are found and at which to implement electrical power flow constraints. Buses of AC type also have a voltage property. Generators, loads and storage unit are one-port components, i.e. each component is connected to a single bus. Conversely, lines, links and transformers are two-port components that are connected to different buses at their two ends.

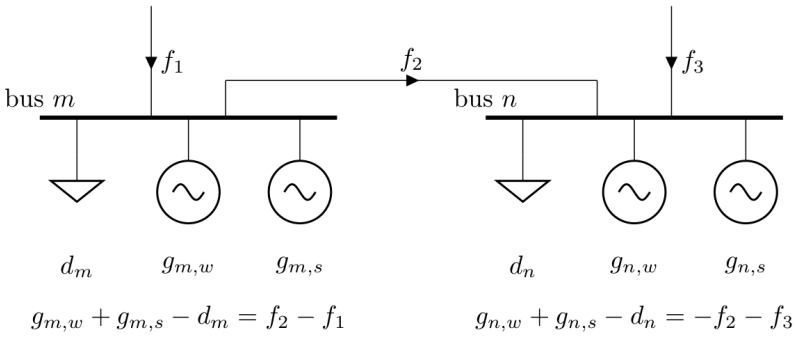

Figure 4.2: Schematic showing energy flows between buses with loads and generators [14].

A generator is an energy source with a marginal cost, nominal power capacity and static or time-varying minimum and maximum power values, of which the dispatch is an optimisation variable. A load is an energy sink with a predetermined power set-point for each time step. The load at each time step must be met regardless of the cost. Time steps in PyPSA are also referred to as snapshots. Storage units are both sources and sinks of energy, with parameters for nominal power, nominal energy capacity and efficiency. Moreover, storage units have a state-of-charge which is constrained by its previous value in the time sequence. The operation of storage units (charging or discharging) is also determined by the optimisation.

Lines and transformers are passive branches, which means they are components through which the power flow is determined by physical (electrical) parameters —the impedance in the case of linear power flows. Transformers connect buses of unequal nominal voltages, whereas lines connect buses of the same nominal voltage. The power flows are limited by the nominal power values. Links are active branches, which means that the power flow is an optimisation variable (and is assumed to be actively controlled). The flow is still constrained by a rated power. The link component is also able to connect buses of different carriers (such as electric and gas), with conversion occurring at a fixed efficiency. Links are therefore used to model energy conversion devices, such as power-to-gas and gas-to-power.

The electrical part of the model includes a range of voltages (13-150 kV in the case study, see Chapter 5). The loads throughout the lower voltage parts of the network are aggregated at the lowest voltage included in the model, and the same is done for generation. Local generation and demand profiles are exogeneous values, and they are taken from scenarios modelling hourly demand and generation for different technologies and sectors, for 2050. Different technologies of distributed generation are modelled as different generators, each with a marginal cost corresponding to the technology.

Figure 4.3 illustrates an example electric bus m, with a load (d_m), three generators ($g_{m,\text{wind}}$, $g_{m,\text{PV}}$ and $g_{m,\text{CHP}}$), a transformer, and candidate components for conversion and storage. At each time snapshot, the set-point of the loads and generators will match the sum of the loads and generation of all the lower voltage parts of the network attached to this bus. The transformer is connected to the rest of the network through a higher voltage bus (not pictured). Electrical storage is, as mentioned, a one-port component, while the potential converter could be an electrolyser for power-to-gas conversion, which is attached to a gas bus.

A minimal version of a gas network is implemented in the model. Gas pressures and flows are not directly modelled due to the complexity and the lack of PyPSA functionality for this. Rather, non-electrical buses are considered in PyPSA to have abstract energy and power flow (not specific to the carrier). In the model, a city gate closest to each of the substations is chosen and a possible conversion (power-to-gas) component placed between the electrical bus and the gas network. The gas network comprises two buses (representing 40 bar and 8 bar on either side of the city gate in the case study, but in practice not assigned any pressure values; see Chapter 5), and a link component (with 100% efficiency) representing the city gate. At the "lower" pressure bus n, loads are attached with their set-points equal to the aggregated demand of the areas they serve. The "higher" pressure gas bus is attached to the external gas grid and is also fed by the potential electrolyser which is assumed to have an output pressure of 40 bar.

It is assumed that today's existing natural gas distribution infrastructure is repurposed for hydrogen gas, and for simplicity, all gas demand (hydrogen and natural gas) in the scenarios is assumed

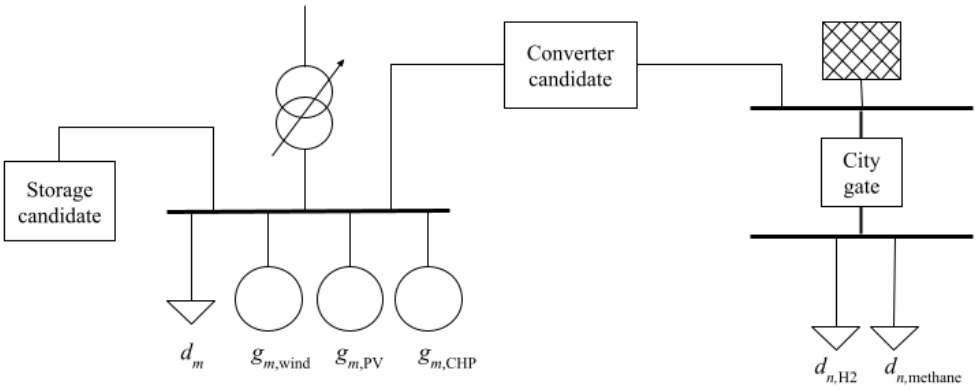

Figure 4.3: Example of components connected at electricity and gas buses.

to be for hydrogen. This way, the gas network is only for hydrogen, and the electrolyser can directly feed hydrogen into the network. In Figure 4.3, the loads d_{H2} and d_{methane} are based on the scenario demand profiles for hydrogen and natural gas respectively, but in the model it is added up and treated as demand for a single carrier (hydrogen). The various component parameters mentioned above are loaded into a PyPSA network from CSV (comma-separated values) files.

4.1.1. N-1 and redundancy

The N-1 criterion describes the requirement for system redundancy such that the power supply is maintained (even at peak flows) despite any one component being out of commission. There is discussion, including at Stedin, on whether to keep applying this deterministic criterion for maintaining redundancy in future energy systems when there is such high variability introduced by renewable generation. One proposed alternative is to guarantee N-1 redundancy in the distribution network for situations when there is net demand, but to let go of this condition (effectively moving to N-0) for net supply, when power is being fed back into the grid. This could mean there would be fewer redundant components in the network connection of a solar field with net generation compared to the connection of an industrial area with net demand. There are also probabilistic variations such as N - 0.9.

In the model, however, a simpler approach is taken to redundancy in the following manner. N-1 is enforced by leaving one component out of the initial starting point for each position: for example, instead of the two 52.5/13 kV transformers present at Oud-Beijerland, only one is modelled as part of the existing components in the simulation. When calculating the costs or spatial requirements, however, this is added back in. So if the optimisation determines that three transformers are necessary at this location based on the power flows, it will indicate that two transformer investments are made in addition to reinforce the existing transformer capacity. In the subsequent analysis, four transformers are counted at this location, so that there is sufficient power infrastructure even if the fourth transformer were not functional. In this approach, no distinction is made between net demand and net generation.

4.2. Financial model

4.2.1. Investment and operational costs

In large-scale investment problems, financial aspects to consider include the expected lifetimes, large up-front costs, depreciation, and recurring (operation and maintenance) costs. Typically, the one-time initial investment costs are called capital expenditure (CAPEX) and recurring costs like operation and maintenance fall under operational expenditure (OPEX).

The net present values (NPV), one approach to evaluating investments, is the sum of all costs and revenues expected from a project discounted back to their present values using an interest rate. The NPV for a component c that is purchased in year 0 can be calculated according to Equation

4.1, where r is the discount rate and T is the planning horizon (here, incomes are not considered and costs are positive). When calculating annualised investment costs for the model, the revenue from the component is not considered, in that case the present value is specifically a net present *cost*. In this thesis, a fixed discount rate of 3% is assumed whenever costs are annualised, based on [102].

The net present cost does not, however, account for differences in lifetimes. This is why the one-time CAPEX is converted into an annual equivalent. Multiplying the present value with an annuity factor converts it to the amount that would be paid each year on a recurring basis. The annuity factor A_c as expressed in Equation 4.2 converts the capital expenditure (investment cost) to an equivalent annual cost, where L_c the component lifetime in years. This equivalent allows for the comparison of energy infrastructure assets with different lifetimes since they would be decommissioned and reinvested in at different times [103, 104].

$$\mathrm{NPV}_c = \sum_{t=0}^{L_c} \frac{\mathrm{cost}_t}{(1+r)^t} = \mathrm{CAPEX} + \sum_{t=1}^{L_c} \frac{\mathrm{OPEX}_t}{(1+r)^t} \tag{4.1}$$

$$A_c = \frac{1-(1+r)^{-L_c}}{r} \tag{4.2}$$

Note that inflation is not taken into account here. However, assuming that inflation affects the different investment options equally, this would not change the optimisation outcome. The costs are taken to be in present euros (rather than the euro value of 2050). It is, however, assumed that the (operating and reinvestment) costs stay the same, which can weaken the comparison especially for investments with substantially different lifetimes. In the model, component performance (such as efficiency) is assumed to be constant throughout its lifetime.

The CAPEX and fixed OPEX costs are converted into annualised costs and entered in the PyPSA model as the capital costs. For transformers and lines, the capacity investment is a fixed amount since the investment is determined by a binary (rather than continuous) variable. In cases where the capacity investment is a continuous variable (for electrolysers and storage), a fixed capacity cost per megawatt is modelled, and it is assumed that this cost scales linearly with capacity (i.e. that the marginal investment cost per megawatt is constant). Additionally, there are variable operational costs which depend on the operation, such as the fuel cost for fuel-based electricity generators. These are included in the model under marginal costs, and are assumed to be a constant value throughout the operational range of the component.

4.2.2. Exchange with external grids

The model is developed for a part of the distribution network with local electrical generation. At any hour, this region could have a surplus or deficit of energy which is exchanged with the external grid connecting the region to the rest of the country. The optimisation in the model involves trade-offs between investment and operational costs. For this reason, setting the exchange of power and gas at a fixed price indicates that any amount can be exchanged with the external grids at the same price (as constrained by infrastructure), and this leads to unrealistic behaviour. The consequences of a lack of market signals for the exchange of energy with the external grid are explored further in the context of the case, in Section 5.4.

A simple market model is developed to simulate the trading of power and hydrogen between the local and national networks (via the higher voltage/pressure connections). The model contains three main elements: i) supply and demand for energy, ii) bids at different price levels to indicate increasing marginal costs and decreasing marginal utility, and iii) bid sizes varying with time to reflect temporal aspects like daily cycles, seasons and weather. This market is implemented at each location where there is exchange with the national grid: at 150 kV in the electricity network, and at each city gate location in the gas network.

The structure of such an external market model is depicted in Figure 4.4. The bid levels (price) are constant, and some of the bid sizes (MWh) are made to vary with the time-steps of the simulation, (as indicated as blocks shaded in blue in the figure).

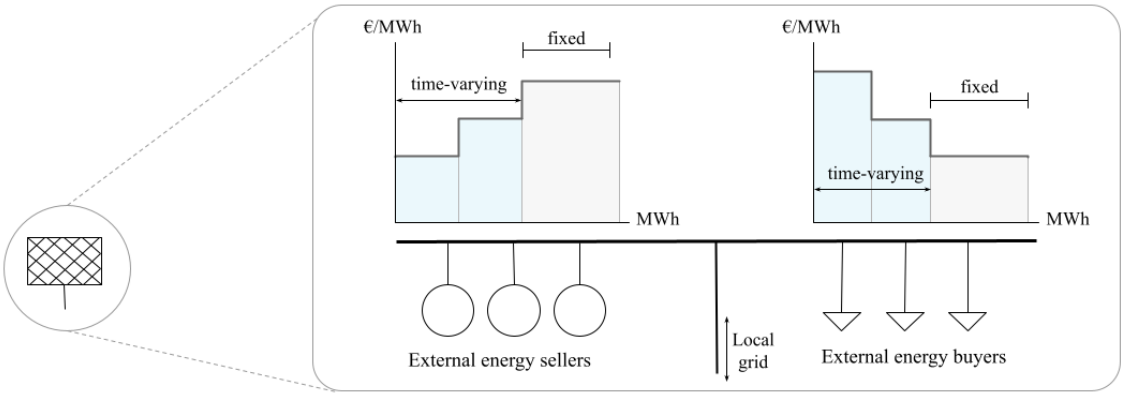

Figure 4.4: Illustration of the bidding model at the external grid bus.

The bids are assumed to be at three price levels, as shown in Figure 4.4. The mid-level bid is 50 €/MWh for electricity and 90 €/MWh for hydrogen [102]. Electricity prices are assumed to be more volatile than hydrogen prices, based on the assumption that existing large-scale natural gas storage is also repurposed for hydrogen. If there was not much hydrogen storage available, these prices would probably also vary more. The electric bids have low and high-level bids at 40% lower and higher respectively (30 € and 70 €). Hydrogen price bids vary by 20%, resulting in low and high bidding block prices of 72 € and 108 €.

The bid sizes at each price level have a fixed nominal value (in MWh), and a per-unit capacity which can vary with time. For electricity, the nominal capacity (1 p.u.) of each block is 1000 MW to ensure sufficient external demand and supply at any time. For hydrogen, each of the three bid sizes has a nominal value which is one third of the (current) city gate capacity. Some bid sizes are constant in time, specifically the "favourable" bid levels of which there are assumed to be enough through at all times: buyers at the low price and sellers at the high price for hydrogen and electricity (the grey blocks in Figure 4.4.

The low-level gas buyer bid size is constant at 1 p.u. (one third of the total city gate capacities). The external gas supply bid sizes are also modelled as constant: 0.5 per-unit for the low- and mid-level blocks each (i.e., one sixth of the city gate capacity). The high-level supply bid sizes are set at a higher capacity (multiple times the city gate capacity), to be able to supply more in case the city gate capacity needs to be expanded at locations with extreme local gas demand (especially in the 2030 scenario). For the constant electric bid sizes, the expensive supply and low-price buyers are both fixed at 1 p.u. (1000 MW).

The time-variation of the market bid sizes is generated based on the total hourly demand and supply of the region modelled in the case. This is achieved by varying the hourly per-unit capacities for each bidding block. Starting from per-unit values which vary between 0 and 1 directly proportional to the corresponding total supply/demand in the case region, some modifications were made to obtain reasonable average prices throughout the year which are close to the mid-level bids. This is done as follows.

To generate the time-varying per-unit values for the bid sizes, first the total electric supply, demand and gas demand are calculated for the Sterrenburg sub-network. These values are normalised by the maximum value of the year so that they vary between 0 and 1. The electrical demand is additionally scaled by a factor of maximum demand divided by maximum generation (to maintain the correct ratio of electrical demand and supply, since the nominal values of their bid sizes are the same). These proportional per-unit values are used for low-level electrical power supply bid sizes, and the high-level demand bid sizes of gas and electricity. Finally, the mid-level bid sizes are assumed to be a bit more steady (varying between 0.333 and 1 instead of 0 and 1); this is achieved by scaling the time-varying values down by a factor of 0.667 and adding 0.333 to each value.

In the model, local (i.e., within the case region) gas and power demand are price-inelastic, which means they must be met regardless of the cost. At time-steps when local generation is insufficient to meet local demand, extra power will be drawn from the external grid. In the market model, the

local demand is the first to be met since the bid is essentially at an "infinite" price, while the external energy buyers have a set price at which they bid. The local generation is chiefly from PV and wind, which have lower marginal costs than the external bidders. This way, any excess renewable energy is also the first block to be dispatched from among the sellers. However, when energy is purchased for electrolysers, or gas is sold back to the national grid, the bids must compete with the others among the market, as the price level of the bids depend on the energy mix and values of other components at that time.

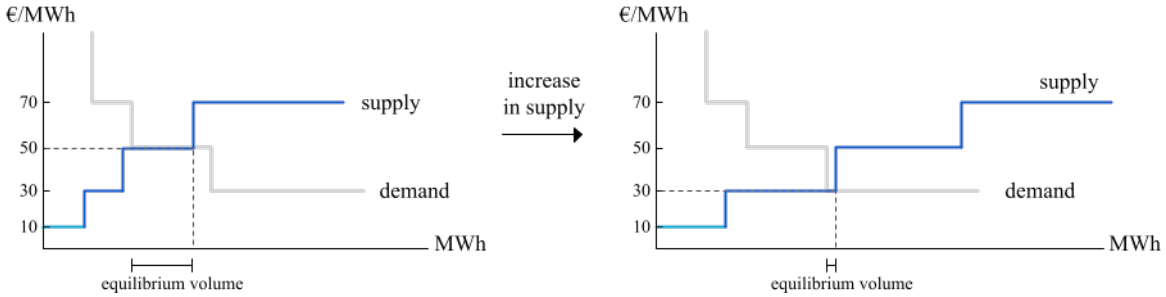

Figure 4.5: Visualisation of the market model for an increase in low-cost electricity generation.

Figure 4.5 shows an example of how the market price varies in the market model of this work. Demand for electricity is plotted in grey as a downward sloping curve, while supply is upward-sloping in blue (these slopes represent decreasing marginal utility and increasing marginal costs respectively). The initial part of the demand curve is vertical, which is from the price-inelastic local electricity demand. The local electricity supply is represented by a lighter blue, and in this example it has a marginal cost of €10/MWh. The remaining bid blocks represent the external grid buyers and sellers, with bids at 30, 50 and 70 €/MWh, of which the size is determined based on the case region's demand and supply as has been explained in this chapter. The market price and trade volume are determined by the intersection of the demand and supply curves. Note that, unlike the continuous curves of Figure 2.10, the demand and supply curves comprise a small number of bid blocks at the same prices. This causes there to be not a single point, but possibly a range of trading volumes at which the demand and supply curves intersect (as marked by the equilibrium volume range in Figure 4.5).

In terms of optimisation, market clearing is achieved when the sum of consumer and producer surplus (i.e., social welfare) is maximised. In Figure 4.5, this is the area between the demand and supply curves (see also Figure 2.10). For this objective, the different points along the intersection of demand and supply along the equilibrium volume have no effect on the social welfare, since there is no producer or consumer surplus (since marginal cost and marginal utility are equal to each other and to the market price). For more on market clearing and economic welfare, see for example [12, Chapter 7]. In practice, in PyPSA the market clearing is implemented such that the trading volume is maximised, i.e., at the higher end of the equilibrium trading volume range. The market price and trading volume are marked in Figure 4.5 by dashed lines (horizontal and vertical, respectively).

The plot on the left of Figure 4.5 shows a market equilibrium with a price of 50 €/MWh. The plot on the right shows the same demand curve in grey, but an increase in supply. The local generation, in light blue at 10 €/MWh, is higher in the right-hand side plot. In the model, this also increases the sizes of the external market supply bids at 30, 50 and 70 €/MWh, according to the method explained earlier in this section. As seen from the figure, the market equilibrium for the increased low-cost electricity supply is at 30 €/MWh. This demonstrates that at simulation hours with, for example, high amounts of PV and wind generation in the case region, the market price for electricity tends to be low. Similarly, high demand for electricity would tend to increase the electricity price by causing the demand curve to shift to the right, and setting a higher equilibrium price at the intersection of the curves.

Optimal market assumptions

Using cost minimisation to optimise the combined investment and operational costs of the power system involves certain assumptions, i.e. conditions required for there to be optimal investment decisions. Suppliers are assumed to be price takers, that is, they have little individual influence over the market price due to their competitors. This causes them to bid at marginal cost price. Another assumption is perfect knowledge and foresight: it is assumed that for each time step, the demand, generation

and corresponding costs are known to all parties. Specifically, the optimisation is carried out for all time-steps of demand and supply in the simulation at once, so the "future" demand and generation profiles are known at the moment of optimisation. Each operational time-step is optimised at the same time, making this model a dynamic optimisation from an operational perspective. There is only one investment moment (at the beginning of the simulation), making it a static investment optimisation. The actors' behaviour is assumed to be rational (maximising utility) and risk-neutral (i.e. decision-makers in the model do not take risk into account, when in reality they are often risk-averse) [72, 105].

Spot markets facilitate deals close to delivery time, whereas in a futures or derivative market, trades take place further in the future such as in the following year (see Section 2.5). As markets are not the central focus of this work, there is no provision for these markets at different time scales; rather, a simple market is simulated where prices and dispatch are determined (instantaneously) at each time step. Furthermore, in real life, there is uncertainty in power demand, but this is taken to be deterministic and known (fixed) for each time step in the model. Inconsistency with these assumptions in real life would cause the market outcomes to deviate from the cost optimum.

4.2.3. Financial scope of the model

It is important to be clear on what is, and what is not included in the financial scope of the model. This scope influences the results based on the objective function. Table 4.1 shows a summary of the main costs which are modelled, and related costs which are not modelled. The local generation placement is exogeneous to this model, based on the scenarios. Therefore, this optimisation is not concerned with planning or changing the presence of PV, wind or other local generation. The cost of the locally generated energy, however, is modelled as a fixed marginal cost. This makes it attractive for the optimisation to convert cheap surplus local generation to hydrogen instead of having to build extra infrastructure to transport this power elsewhere.

The model also covers only a finite part of the network, which excludes investments and operational costs from other parts. In the case study, this covers the infrastructure connected to the Sterrenburg 150/52.5 kV substation, down to the 52.5/13 kV substations. For gas, only selected 40 bar city gates are modelled. When this infrastructure needs to be reinforced, this is typically accompanied by investments in other parts of the grid. For example, if many houses in a neighbourhood install solar panels, the lower voltage infrastructure will likely need to be reinforced. Similarly, when new transformers are placed at the 150/52.5 kV level, TenneT will also need to place additional infrastructure at 150 kV to facilitate this. The results are, however, aligned: investments at one level typically require investments at other levels, and savings at one level also tend to translate to savings at other levels. The main consideration here is that the results of the optimisation represent only a part of the network, and it is to be kept in mind that changes in this part also affect the bigger surrounding network.

Table 4.1: Summary of the financial scope of the model.

Included	**Not included**
• Marginal costs of local generation	• Investment costs for local generation
• Annualised network investment costs at 13-150 kV and for sector coupling	• Network investments at transmission or below 13 kV level
• Cost estimates of annual operation and maintenance	• Cost of decreasing performance over lifetime and of decommissioning components
• Simplified costs of trading energy with national grids	• Possibility for congestion pricing, curtailing or local demand response
• Selected gas city gate costs at 40 bar	• Gas pipeline costs

As Table 4.1 also shows, the costs included are relatively simple (fixed estimations of OPEX costs, and energy trade with the external grid at three price levels). These modelled costs could be made

more complex, for example with a more detailed market model, or by adding parameters such as to change the performance over the lifetime. Additionally, the costs of decommissioning components are not included. Furthermore, the optimisation allows for investment in network reinforcement or conversion of energy, but not for example curtailment, or local demand response. All demand must be met, and all generation must either be used locally or fed into the national network. This goes to say that there exist alternatives to the actions modelled in the optimisation, and this model specifically explores the effects of reinforcement and system integration.

4.3. Objective function and constraints

The energy network expansion planning problem is defined mathematically as a set of equations and inequalities. The goal of optimisation is to minimise or maximise a function referred to as the objective function. In this case, the objective function describes the operational and investment costs, which are to be minimised.

An optimisation problem's goal is to minimise the cost function. This objective function comprises investment and operational costs as expressed in Equation 4.3. This includes costs from the whole system, including those of the grid operator, energy consumers and potential private investors. Here, n and t are indices representing the buses and time-steps, while the indices s, r, b and l represent the sets of storage units, generators, passive branches and links respectively.

$$\begin{aligned} C(\boldsymbol{x}) = &\sum_{n,s} c_{n,s} \cdot E_{n,s} + \sum_{b} u_b \cdot c_b \cdot F_b + \sum_{l} c_l \cdot F_l \\ +\beta &\sum_{t} w_t \left[\sum_{n,r} o_{n,r} g_{n,r,t} + \sum_{n,s} o_{n,s} h_{n,s,t} + \sum_{l} o_l \cdot f_{l,t} \right] \end{aligned} \tag{4.3}$$

The symbols for indices are used to represent sets; for example, the index n along with a summation symbol is used to indicate a summation over all buses. In the optimisation problem, there are fixed parameters which are inputs to the model (such as component costs and capacities), and there variables whose values are determined through the optimisation. The objective function $C(\boldsymbol{x})$ is minimised by determining the optimal values of the optimisation variables $\boldsymbol{x}$. The investment optimisation variables are the energy storage capacity $E_{n,s}$, conversion (electrolyser/gas turbine) capacity F_l, and the passive branch (transformers and cables) investment decision variable u_b. These are continuous variables, except for u_b which is binary, i.e., it takes only values of 0 or 1. The binary formulation is used for transformer and cable investments, because it is more realistic to model these as having discrete capacities, rather than freely scalable capacities (i.e., investments can occur in fixed blocks of capacities rather than any continuous value). Binary variables are a specific type of integer variables, since 0 and 1 are a subset of integers. The operational investment variables are all continuous variables: generator dispatch $g_{n,r,t}$, storage charging/discharging $h_{n,s,t}$ and state-of-charge $e_{n,s,t}$, energy conversion operation $f_{l,t}$, voltage angles $\theta_{n,t}$ and passive branch (transformer/cable) power flows $f_{b,t}$. Some of these operational variables are not included directly in the objective function, but they still influence the objective function indirectly.

The first line of Equation 4.3 comprises investment costs, which are a one-time decision (rather than at every time-step). This part contains the sum of each type of investment decision multiplied by its cost, starting with capital cost per MW $c_{n,s}$ of energy storage times the invested capacity $E_{n,s}$. Note that the costs of energy storage depend on both the power and the capacity, but these costs are lumped together in the model. The next term is for branch investments (transformers and cables), which is the product of *binary* decision variable u_b, branch cost per MW c_b and branch capacity F_b for each candidate branch. Finally for each link l (used to model conversion devices such as electrolysers), the cost per MW c_l times the invested capacity F_l is added to the objective. The next line of the objective function contains the time-bound terms related to operational costs: the per-MW operational costs o are multiplied by the amounts dispatched ($g_{n,r,t}$, $o_{n,s}$ and $h_{n,s,t}$ for generators, storage units and links), summed over the different components and weighted by the weight w_t of the corresponding time-step. The time-steps can be weighted to express their relative frequency of

occurrence (and thereby their relative contribution), and a set of time-steps can also be weighted to represent a bigger number of time-steps. The use of weights for time-steps is elaborated on in Section 4.5. The factor β in Equation 4.3 represents a weighting which can be given to the operational cost terms, to express their relative importance in the objective. In this thesis, $\beta = 1$.

Aside from the binary investment decision variables, the variables are continuous variables, which means that they can take any (real) value. The objective function in Equation 4.3 and the constraints as listed in the following sections are all linear functions of these continuous and integer variables. This means that the optimisation problem uses a mixed-integer linear programming (MILP) formulation. The number of variables, constraints and time-steps used in typical power system expansion planning problems makes it favourable to use formulations with lower solving times, and as discussed in Section 3.3, linear formulations tend to be more straightforward to solve than nonlinear formulations.

Note that in the model of the external grids, the energy buyers are represented by "negative generators". When these are dispatched, the cost is negative (and is, in fact, a revenue). Consequently, the cost minimisation optimisation preferentially dispatches the buyers with a higher marginal "cost", i.e., the one who is willing to pay the most (unlike for regular generators or the energy suppliers, where the cost minimisation preferentially dispatches those with lower marginal costs). Another relevant property is that summations are commutative, and therefore the objective in Equation 4.3 does not depend on the actual order of the time-steps. This will also apply to the constraints that follow, with the exception of the storage units' state-of-charge. Therefore, in the formulations without storage units present, the discontinuities introduced by selecting time slices (as explained in Section 4.5) have no effect on the solution.

Finally, it is also worth discussing the relative weighting of terms in the objective. All the one-time and recurring decisions which are included as optimisation variables are traded off against one another in the simulation. A one-time investment is viable if it saves an amount in hourly dispatch throughout the year which is greater than the investment cost, i.e., one euro spent on investing in infrastructure is equally important as one euro spent on dispatching a generator. If the goal of the optimisation is explicitly to reduce network investments for example, these components can be given higher weights in the objective function (but in this case, hourly costs summed over the whole year have the same weight as one-time costs). If, for example, operational costs are considered less important than investment costs, the value of β in the objective could be set to 0.5, or a value greater than 1 could be used to express greater importance. In this thesis, the equal importance of operational and investment costs are indicated by the lack of weighting, i.e., $\beta = 1$.

4.3.1. Power balance and branch flows

Power in a network is injected or withdrawn at buses, and flows through branches which are active (power flows actively controlled, known as links and used to model energy conversion) or passive (power flows determined by impedance, i.e. transformers and cables). At each bus, the power balance as shown in Equation 4.4 applies to ensure the conservation of energy. The first two terms denote power being injected by generators or storage units. The third term describes flows $f_{l,t}$ from other buses. If branch l is a cable, then the term $\alpha_{l,n}$ equals -1 or 1 depending on whether the branch is defined to start or end at bus n. Similarly for links, depending on whether l starts or ends at bus n, $\alpha_{l,n}$ equals $-\eta_l$ or $+\eta_l$, which is the efficiency of the link. As shown in the constraint, the demand of a load at bus n, $d_{n,t}$ must always be met (regardless of the cost of energy) and therefore the load components have a perfectly inelastic, fixed demand.

$$\sum_r g_{n,r,t} + \sum_s h_{n,s,t} + \sum_l \alpha_{l,n} \cdot f_{l,t} = d_{n,t} \qquad \forall n, t \tag{4.4}$$

This power balance constraint maintains energy conservation, and therefore Kirchhoff's Current Law holds. Additionally, each branch has a limited capacity for power flow as expressed in Equation 4.5. For electrical power flows, the limit F_l is the rated cable capacity, and for links this is the invested capacity at the input bus (e.g., for electrolysers this is the electrical capacity).

$$-F_l \leq f_{l,t} \leq F_l \qquad \forall l, t \tag{4.5}$$

In active branches (links), the flow f_l is freely determined by the optimisation, and bounded only by the capacity. For passive branches (transformers and cables), the flow is determined by the linearised power flow equations. PyPSA offers several formulations (equivalent, but with different computational complexities) of these equations. In this work the "angles" formulation is used, where the flow in a passive branch spanning buses n and m is given by Equation 4.6. $\theta_{n,t}$ and $\theta_{m,t}$ are the voltage angles at the buses n and m at time-step t, and x_b is the series reactance of the branch.

$$f_{b,t} = \frac{\theta_{n,t} - \theta_{m,t}}{x_b} \tag{4.6}$$

The constraints set by Equations 4.4, 4.5 and 4.6 together ensure that the optimal flows are representative of the physical characteristics of the network [14].

4.3.2. Generators

Generators inject power at the bus where they are connected, and this power is an optimisation variable. It is constrained by the capacity of the generator, which can further be defined by time-varying per-unit capacity values, as expressed in Equation 4.7.

$$\bar{g}_{n,r,t,\text{lower}} \cdot G_{n,r} \leq g_{n,r,t} \leq \bar{g}_{n,r,t,\text{upper}} \cdot G_{n,r} \qquad \forall n, r, t \tag{4.7}$$

The lower and upper generation per-unit values are set as fixed input parameters for each simulation time step. The scenario generation profiles of local generators are implemented by setting the lower and upper per-unit values ($\bar{g}_{n,r,t,\text{lower}}$ and $\bar{g}_{n,r,t,\text{upper}}$) such that they are equal, and that their product with the nominal generator capacity $G_{n,r}$ equals the power output derived from the scenario. This way, the output for these local generators (within the case area) is fixed for each hour to match the case profiles. The generation output is modelled to match that of the scenarios at each hour, which excludes, for example, having reserves or curtailment. The upstream generators representing the external market, however, are dispatchable by the optimisation. The per-unit capacities are modelled as described in Section 4.2.2. For generator components representing buyers (dispatchable loads), the per-unit limits lie between -1 and 0, and for the generator components representing sellers, the per-unit limits are positive. For all the generator components, no additional constraints such as unit commitment or ramp rate constraints are considered.

4.3.3. Storage units

As mentioned previously, the energy storage units have a sequential time dependence. The state-of-charge, $e_{n,s,t}$ depends on the previous time step value as the state-of-charge constraint in Equation 4.8 shows. In this expression, the charging power $h_{n,s,t}$ is separated into positive (charging) and negative (discharging) values, each of which has a corresponding efficiency. It is also assumed that there are no standing losses.

$$e_{n,s,t} = e_{n,s,t-1} + \eta_{n,s,+} \left[h_{n,s,t}\right]^{+} - \eta_{n,s,-} \left[h_{n,s,t}\right]^{-} \tag{4.8}$$

Note that the snapshot weightings w_t are used to indicate the relative importance of that snapshot in the overall time period simulated. Each snapshot still represents a single hour in terms of charging and discharging energy storage. The state-of-charge is bounded by the total energy capacity $E_{n,s}$ of the storage unit, and its lower limit is zero, as shown in Equation 4.9. Furthermore, the charging and discharging are bounded by the rated power of the battery, $H_{n,s}$, which is indicated in Equation 4.10. Furthermore, in this work, it is assumed that the batteries have a 4-hour storage capacity, namely that $E_{n,s} = 4H_{n,s}$. The batteries can be placed at 13 or 52.5 kV level, i.e., at a utility scale. In the case study, the battery input parameters are based on lithium-ion batteries, see Section 5.3.

$$0 \leq e_{n,s,t} \leq E_{n,s} \qquad \forall n, s, t \tag{4.9}$$

$$-H_{n,s} \leq h_{n,s,t} \leq H_{n,s} \qquad \forall n, s, t \tag{4.10}$$

4.3.4. Investment candidate components

In this expansion planning model, the optimiser can make continuous capacity investments in links, and discrete capacity investments (with binary variables) in transformers and cables. These two forms are also modelled distinctly. Specifically, some extra steps are required to include the integer constraints, as explained in this section.

The discrete optimisation candidates have a binary optimisation variable which can be set to 1 (invest) or 0 (no investment) by the optimiser. Multiplying this investment variable with constraints corresponding to the candidate component enforces the presence or absence of the component in the model. For example, in Equation 4.11, the binary investment variable u_b is zero when the branch b is not chosen. This constrains the power flow to be zero, and the constraints are still linear since $u_b F_b$ is the product of a variable (u_b) and a fixed parameter (F_b). When the branch is invested in, $u_b = 1$ and the flow in the branch is bounded by the branch capacity F_b. The same is applied to other constraints relating to the discrete investment components.

However, this can also lead to non-linearities due to the product of variables. For example in the voltage angle constraint in Equation 4.12a, which is the investment candidate equivalent of Equation 4.6, there is a product of the voltage angle and investment variables. Here, u_b is the binary investment variable for a candidate branch between bus n and m.

To avoid this non-linearity, the non-linear mixed-integer constraints are reformulated in PyPSA using a big-M parameter (see also Section 3.3.2 and [106]). This code was already present for candidate lines in a branch of the PyPSA source code, and it was extended in this work to include candidate transformers.

$$-u_b F_b \leq f_{b,t} \leq u_b F_b \tag{4.11}$$

$$f_{b,t} = \frac{u_b \cdot (\theta_{n,t} - \theta_{m,t})}{x_b} \tag{4.12a}$$

$$-M_b(1 - u_b) \leq f_{b,t} - \frac{(\theta_{n,t} - \theta_{m,t})}{x_b} \leq M_b(1 - u_b) \tag{4.12b}$$

The big-M reformulation is used to convert a logical, non-linear constraint such as in Equation 4.12a to a set of linear inequality constraints. Looking more closely at the voltage angle constraint: if the investment is chosen and $u_b = 1$, Equation 4.12a is the same as the constraint in Equation 4.6. Similarly, when $u_b = 1$, the M_b terms of Equation 4.12b equal zero, and therefore the same equality constraint for the voltage angles and flow hold. This shows that when the investment is chosen, the appropriate physical constraints are implemented.

When the investment is not chosen, $u_b = 0$ and the right-hand side of Equation 4.12a equals zero. The flow through this non-existent branch is constrained to zero as desired, and no additional constraint is placed on the voltage angles since this component is not present. The same effect is approximated by Equation 4.12b. As long as the M_b value is big enough (compared to the central term), the flow and voltage angles are left unconstrained by this expression (and the flow is still set to zero by Equation 4.11). If M is too small, this would, however, place unwanted constraints on the voltage angles. For this to work, the M value must be large enough (hence "big"-M). The big-M values are chosen in PyPSA according to [98].

Finally, among the investment candidates, some components are dependent on others. For example, some transformers are more expensive because the cost of building a substation is included in them. These need to be invested in if the existing substations are already at full capacity, and additional equality constraints as shown in Equation 4.13 are introduced to implement this dependence wherever necessary. This ensures that the investment variable of the dependent component, $u_{\text{dependent}}$ can only be 1 if the corresponding independent investment has been made.

$$u_{\text{dependent}} = u_{\text{dependent}} \cdot u_{\text{independent}} \tag{4.13}$$

4.4. Optimisation and solvers

Using PyPSA, the energy system and its components are translated into an optimisation problem in Pyomo, an open-source optimisation modelling language for Python. The Pyomo optimisation problem comprises sets of parameters and variables to form objectives and constraints, using equality and inequality expressions [107]. These expressions are based on the objective and constraints mentioned previously in Section 4.3.

There are several different solvers available to solve the Pyomo optimisation problem, including open-source models. However, commercial solvers tend to be more powerful with better solving times, and in this work, the commercial solver Gurobi is used (with an academic license) [108]. Nevertheless, even with this solver, the time solve the optimisation for the full year (8760 hours) is excessive (over 30 minutes solving time). This is a common issue in power system optimisations, and is one reason why linear models (which are faster to solve) are preferred over non-linear models.

Another approach is to relax the mixed-integer programming gap (MIP gap) parameter. This parameter limits the relative difference between the lower and upper bounds of the objective (the primal and dual objective bounds), which in essence sets a requirement for the accuracy by which the solver has converged to the optimal solution. The default value is 0.0001, and setting this to a higher value can decrease the solving time. However, the effect of this on solving time is limited: a value of 0.001 is chosen, but higher values are avoided as this was observed to affect the optimality of the results. A more effective approach to bring down solution time is by reducing the number of time-steps. In this work, the solving time is improved by choosing a subset of the snapshots which is still representative of the entire year. The snapshots of the subset can be weighted in PyPSA so that their total weight adds up to 8760; this way, the annualised investment cost can appropriately be traded off against the weighted operational costs. The method for choosing the representative days is described further below, in Section 4.5.

The optimisation problem is originally a mixed-integer problem, due to the binary investment variables. After solving this once, the integers are fixed (to be known parameters rather than binary variables), and the solution is rerun as a linear programming (LP) problem. From this second round's LP solution, it is possible to obtain marginal values, including shadow prices, which are used to analyse and interpret the results. The shadow prices are the Lagrange multipliers corresponding to the power balance constraint (Equation 4.4) at each time-step and node. This shadow price at each time step reflects the change in the objective function resulting from one unit increase in demand at that bus. When the infrastructure is not limiting, this shadow price equals the marginal cost of the last dispatched (i.e., most expensive) generator (after accounting for any weighting in the objective function). However, at some times the shadow price may spike, for example because additional infrastructure would need to be invested in to accommodate an extra unit of demand. If the shadow price is used as an indication of energy prices for analysing the results, these spikes need to be filtered out. In Section 5.4, it is explained how this is implemented in the case study.

4.5. Selection of representative time slices

The method used in this work to choose representative time steps is based on the paper by Nahmmacher et al. [109]. In brief, the steps are as follows. First, all the time series are normalised; this includes the different generation profiles and load profiles at electric and gas buses. The data is then restructured into observations: each observation consists of 24 hours of each original time series (each observation is a concatenation of a single day's profiles for wind, PV, CHP generation and each type of demand, at each location).

The observations are then clustered together into groups using an agglomerative hierarchical clustering algorithm using the sklearn library in Python. Agglomerative hierarchical clustering starts with each observation initially as its own cluster; at each clustering step, the two closest clusters are merged until only the desired number of clusters remains. The "distance" between clusters is defined using Ward's method, which minimises the within-cluster variance [110]. This is done by joining clusters in such a way that the increase in the overall sum of squared errors (sum of Euclidean distance squared

from each observation to the centroid of its cluster) is minimised.

In simpler terms, days with similar load and generation profiles are grouped together into clusters. Having formed these clusters, a representative day is chosen from each of them. The centroid of a cluster is the arithmetic mean vector, and the observation closest (in Euclidean distance) to the centroid is chosen as the cluster representative. The representative observations are still normalised, and to obtain the representative days, each technology of the representative observation is scaled such that its average equals the original average (for example, the average value of PV generation for the representative days will equal the average PV generation value for the entire original year). Finally, each observation is also weighted by the number of days in the cluster, so that more commonly occurring profiles have more weight in the optimisation. This way, the weighted total number of representative hours equals the original 8760.

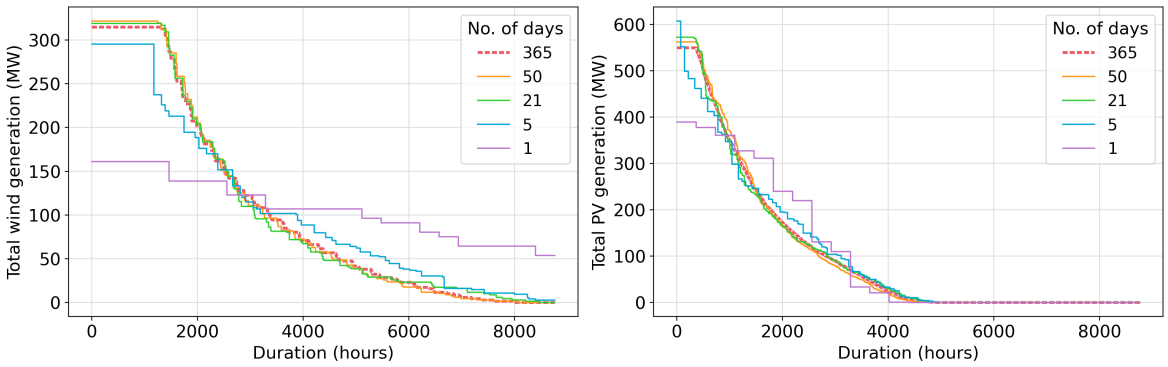

(a) Wind generation curves

(b) PV generation curves

Figure 4.6: Wind and solar load duration curves for different numbers of weighted representative days.

Load duration curves can serve as a visual tool to evaluate the clustering results and to estimate a reasonable number of days to use. Figure 4.6 shows the load duration curves for different numbers of selected representative days time series from the regional scenario, aggregated for the whole Sterrenburg sub-network. The dotted red line is the original data (365 days = 8760 hours), while orange, green, blue and purple are for 50, 21, 5 and 1 day, respectively. The representative days are weighted by the size of their corresponding clusters, such that the total sum of weighted hours equals 8760. From the figure, it can be seen that 1 or 5 days are poor representations of the full year's data, and the difference is especially pronounced at the peak power (hour 0). For the purposes of this work, 21 days provide a reasonable approximation of the original profile, and the increase in accuracy for 50 days is minimal. Therefore, 21 days (504 hours) are chosen from each scenario's annual hourly profiles as a representative subset to bring down simulation time.

4.5.1. Time slice selection with storage

If energy storage is included in the problem formulation, this complicates the selection of time slices since energy storage relies on the time-steps being adjacent in time (see the state-of-charge in Equation 4.9). However, the selection of a subset of representative time slices is still desirable in view of the solving time.

In the formulation which includes storage, a different approach to selecting time slices is taken. Instead of selecting the most representative days (i.e., the 24 hours of a day in the original data stay together as a block in the same order in the slices), the most representative *weeks* are chosen. This way, the effect of, for example, several consecutive summer days is investigated in the system with energy storage. By choosing the most representative weeks using the method described in this section, the hours within the week remain in the same order as in the original scenario. However, at the end of each week, there is still a jump in time in the simulation to a different selected week. This time jump is addressed by introducing an additional constraint on the state-of-charge as follows: the states-of-charge of the last hour in each weekly block must be equal. This way, there is a "cyclic" effect, i.e., the battery cannot start with a high state-of-charge at the beginning of a week and end

with a low state-of-charge or vice versa.

The main issue with choosing weeks instead of days as the basic representative units which are selected is that this drastically decreases how well the selection represents the whole year. This is firstly because the granularity is decreased by a factor of seven: instead of selecting days which are spread throughout the year and have typical temporal profiles, weeks are chosen even when all of the consecutive days might have redundant information or be less representative. Moreover, for the same number of total hours, the larger week blocks also decrease the number of weights which can be assigned to the time slices.

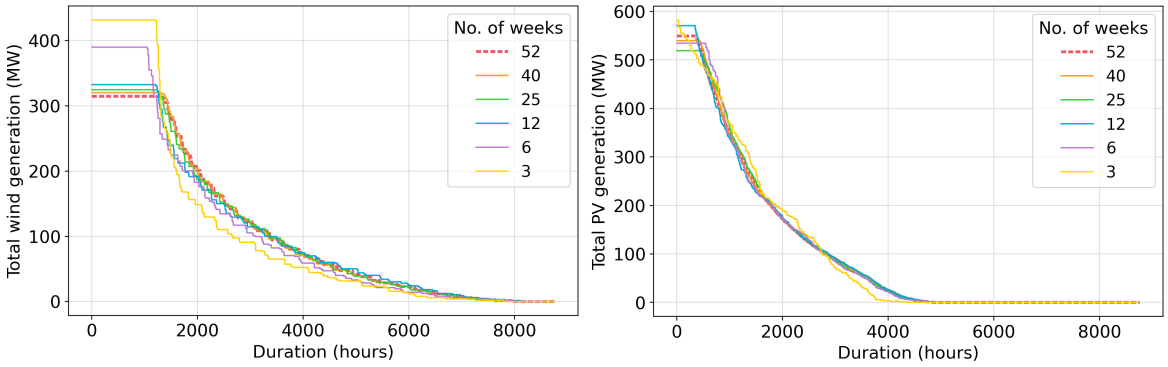

(a) Wind generation curves

(b) PV generation curves

Figure 4.7: Wind and solar load duration curves for different numbers of weighted representative weeks.

The load duration curves of the weighted chosen weeks can again give some impression of how representative they are of the entire year. Figure 4.7 shows the load duration curve for total wind and PV generation within the case region for the Regional scenario. The coloured curves are for different numbers of selected representative weeks, as indicated in the legend. Looking at the figure, it is clear that 3 weeks (i.e., 21 days or 504 hours) is a poor representation of the entire year (by comparing the yellow curve to the dashed red curve. The difference is especially clear when looking back at the match for 21 days in Figure 4.6. Choosing 3 or even 6 weeks gives an insufficient representation of the whole year, especially for the wind generation profiles. For this reason, 12 weeks are chosen. The representation provided by 12 weeks is still worse than that of 21 days (in part because the algorithm can simply provide a better selection when allowed to choose 21 units rather than 12), but this is traded off against a substantial solving time which makes choosing any more weeks unreasonable.

4.6. Sensitivity analysis

The optimisation itself is deterministic, with fixed input parameters. However, these values are not actually known, considering they are projections for 2050. The uncertainty in demand and generation profiles is approached by the use of different scenarios. For a selected set of remaining input parameters, the uncertainty is addressed by carrying out a sensitivity analysis. In this sensitivity analysis, a single input parameter is changed while all others are kept at the standard value. Any effect on the optimisation outputs then reflects the effect of the parameter change. If the effect is large, then the optimisation is sensitive to this parameter.

From among the input parameters, a selection is made to carry out the sensitivity analysis on, as listed in Table 4.2. These parameters to be varied chosen to represent variables that are both considerably uncertain and of importance to the optimisation model. For example, the prices of electrical components such as transformers and cables are left out of this analysis because they depend on relatively established technologies. On the other hand, electrolysers, hydrogen turbines and utility-scale storage are not yet widely used today, but their prices are expected to drop following their technological development and increased uptake (see for example Figures 2.6 and 2.8).

The electricity and hydrogen prices of 2050 are very uncertain; these depend on developments

Table 4.2: Overview of sensitivity analysis parameter variations

Parameter	**Variation**	**Range**
Electricity (median) price	± 50 %	25–100 €/MWh [111]
Hydrogen (median) price	± 50 %	45–180 €/MWh [111]
Electrolyser annual fixed cost	± 25 %	28,486–47,477 €/MW − yr
Hydrogen turbine annual fixed cost	± 25 %	41,582–69,304 €/MW − yr
Battery storage annual fixed cost	−43.6 %/+40.4 %	32,543–80,988 €/MW − yr

in production, transmission and storage technologies, as well as on policy (such as potential carbon pricing) and the demand sectors. For this reason, these inputs are changed by 50% of their initial values, as done in [111]. For electrolysers and gas turbines, a margin of ± 25% of the initial cost is chosen for the sensitivity analysis as this is a sizeable perturbation, but still bounded by reasonable expectations for technological development paths. For battery storage, the costs are based on [8], which reviews several recent resources in literature. The report also lists low and high price projections, which are subsequently used in the sensitivity analysis of this work.

5 | Case study background

In this thesis, a model is developed for optimal expansion planning considering network integration at the distribution level, as detailed previously in Chapter 4. This model is subsequently used to carry out a case study on the Sterrenburg sub-network in the Netherlands in 2050, using different energy mix scenarios. The existing network, scenarios and case study inputs are described in this chapter as follows. Section 5.1 introduces the Sterrenburg region, including the characteristics of the existing network, which is the starting point for expansion planning. Section 5.2 describes the different scenarios used for the future local generation and demand profiles. Next, in Section 5.3, the remaining inputs of the model are reported, including the parameters relating to investment candidate components. The market model and hourly prices are investigated and discussed in Section 5.4 with respect to the case study.

5.1. Sterrenburg and the existing network

The Sterrenburg region is located in South Holland, a province of the Netherlands. When referring to the Sterrenburg sub-network or region, this includes all of the areas served by the 150/50 kV substation at Sterrenburg. Within this thesis, Sterrenburg (region/sub-network) refers to the coloured area on the map of Figure 5.1, and the green area specifically corresponds to the 50/13 kV Sterrenburg substation.

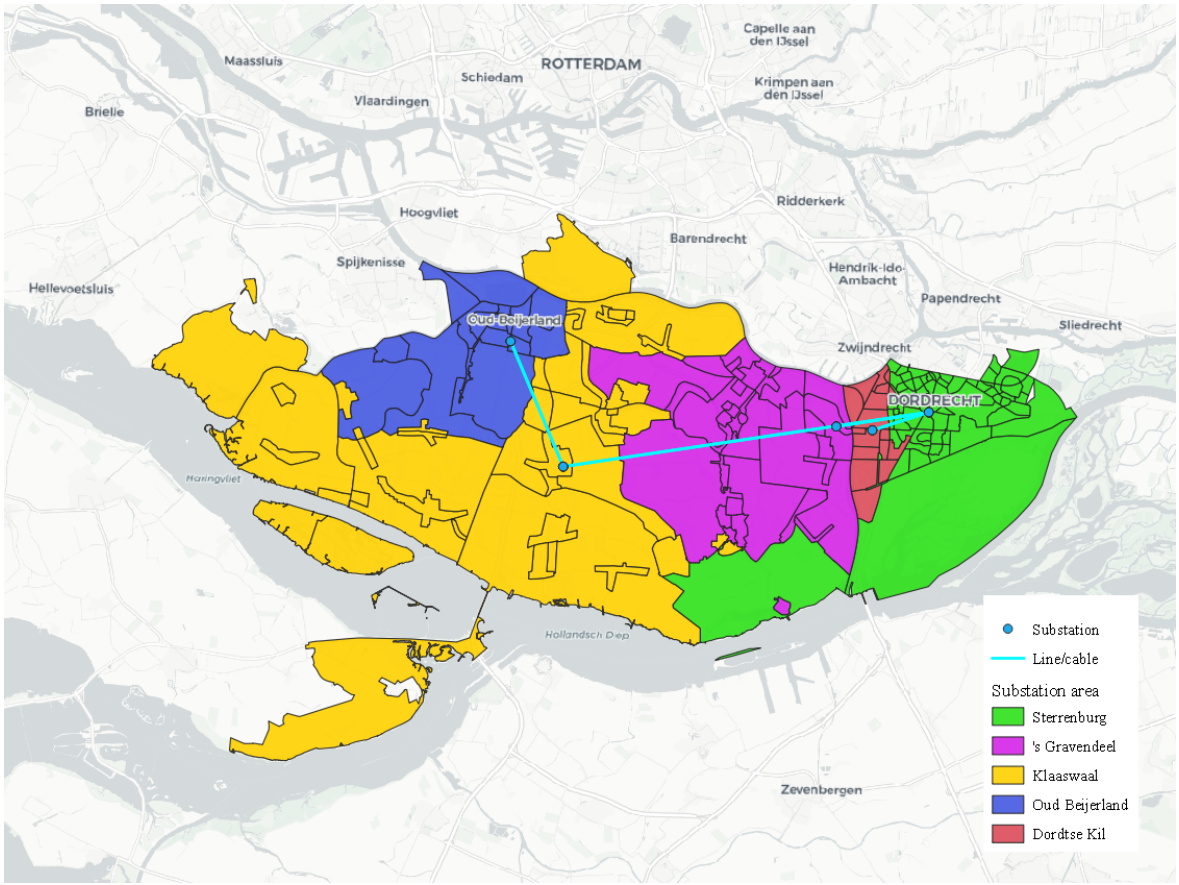

Figure 5.1: Map showing substations and their corresponding areas served in the Sterrenburg region.

This area of about 400 km^2 lies south of Rotterdam and has a population of over 170,000 people (in 2017) [112]. Both the gas and electricity networks are operated by Stedin as the regional distribution system operator, and therefore the information about the current infrastructure is also provided by

Stedin. The region on the map comprises 186 neighbourhoods, each of which has its own code. These codes correspond to a substation, and this information is taken from Stedin's data.

The electric network in this region includes one substation at 150/52.5 kV, and five substations at 52.5/13 kV. The infrastructure at 150 kV and higher voltages is operated by the national transmission system operator, TenneT. As shown in Figure 5.1, the substations are located in Sterrenburg, 's Gravendeel, Klaaswaal, Oud-Beijerland and Dordtse Kil. The neighbourhoods of the map are coloured according to the substation by which they are served. Each of these locations has a 52.5/13 kV substation, and at Sterrenburg there is also a 150/52.5 kV facility. The Sterrenburg substation is in a more densely populated region, as reflected by the large number of neighbourhoods (outlined in black) in the green region of the map. The Sterrenburg substation therefore serves a large number of people, including the city Dordrecht. Also of note is Klaaswaal, which includes many riverside areas that are highly suitable for wind energy generation.

Figure 5.2 shows an electrical schematic of the Sterrenburg region as used in the model. The loads and local generation throughout lower voltages of the network are added up and modelled at the 13 kV point of their corresponding substation. The 150 kV infrastructure is shown in blue, indicating it falls under the responsibility of the TSO TenneT. This is also where the network is connected to the external electrical grid, and where power is exchanged whenever there is a local deficit or surplus.

The transformer at 150/52.5 kV is a three-winding transformer, of which only two windings are in use for the transfer of power between the transmission network and Sterrenburg sub-network — because of this, it is modelled as a two-winding transformer. The horizontal lines in the electrical part of the network represent bus-bars. At two of the substations, Dordtse Kil and 's Gravendeel, the 52.5 kV side of the transformer is connected directly to the cables (*op een steeltje*), rather than via bus-bars and switchgear including current transformers and circuit breakers. For simplicity, this is not modelled differently, and it is assumed that new transformer investments are connected with rails on both voltage sides.

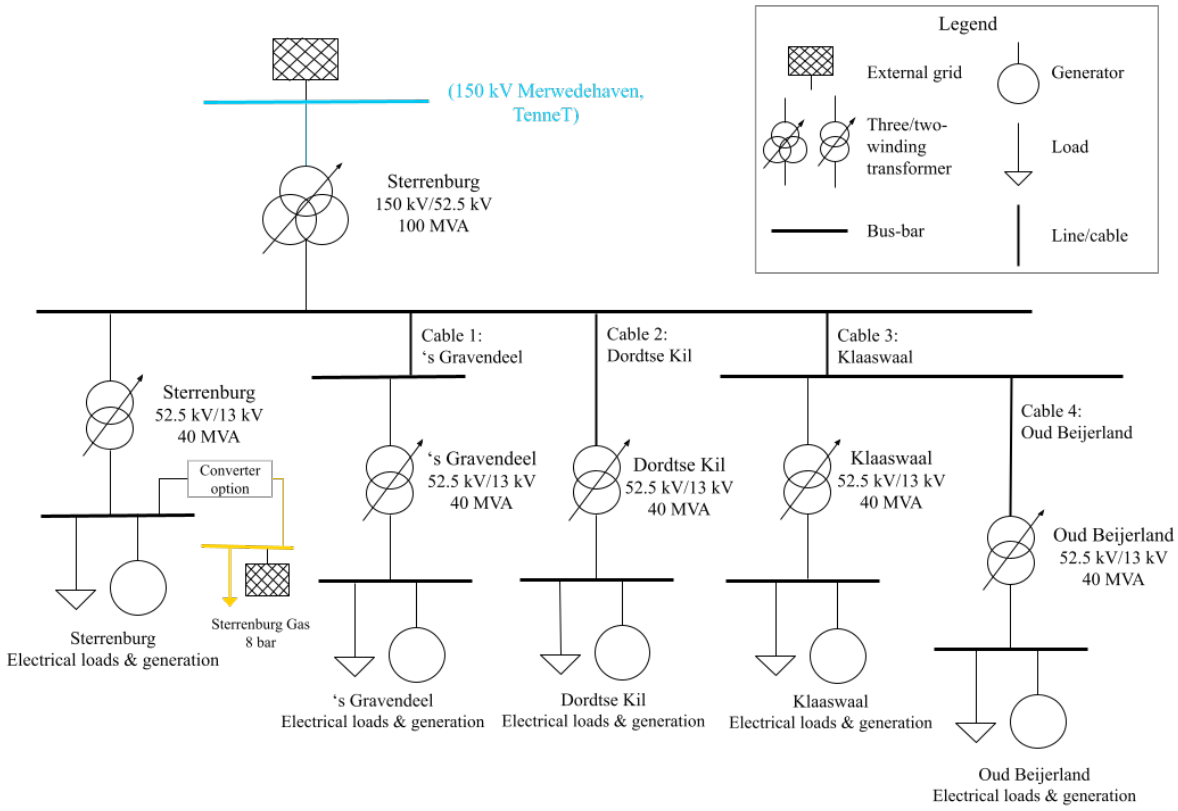

Figure 5.2: Single line diagram showing the extent of the electrical network considered.

Regarding redundancy, wherever a single component is shown in Figure 5.2, there are in practice two identical components to comply with the N-1 rule. For cables, this means that there are two sets of three-phase conductors at each of the four cable locations indicated in the figure. Additionally,

the transformer capacities in MVA noted in Figure 5.2 indicate the capacity of investment candidate transformers at each of those locations.

Table 5.1: Parameters of existing transformers in the Sterrenburg area.

Location	**Voltages (kV)**	**Capacity (MVA)**	**Reactance (p.u.)**
Sterrenburg	150/52.5	150	0.1495
Sterrenburg	52.5/13	31.5	0.154
's Gravendeel	52.5/13	20	0.1027
Dordtse Kil	52.5/13	31.5	0.1495
Klaaswaal	52.5/13	31.5	0.1423
Oud-Beijerland	52.5/13	40	0.149

For the existing transformers, the parameters including their capacities, are listed in Table 5.1 (source: Stedin). Again, each of the components listed is present twice to fulfil the N-1 redundancy. The per-unit series reactance of the transformers is based on the percentage relative short-circuit voltage of the transformer, assuming the resistance is zero (as it is also not needed for linear power flow calculations). At 150/52.5 kV, the fixed annualised cost of the transformers is 1,771 €/MW-yr including the cost of the switchgear, and the additional annualised cost of the corresponding substation is 948 €/MW-yr. For the 52.5/13 kV level the transformer cost is 1,827 €/MW-yr, with an additional annualised cost of 1,951 €/MW-yr for the substation. More details about the transformer and substation costs are found in Appendix A.

Table 5.2: Parameters of existing cables in the Sterrenburg area.

Name	**Reactance (Ω)**	**Resistance (Ω)**	**Nominal current (A)**	**Capacity (MVA)**	**Length (km)**
Cable 1	0.67	0.59	415	37.7	5.0
Cable 2	0.29	0.275	480	43.6	3.3
Cable 3	4.8263	1.2435	700	63.7	15.7
Cable 4	0.68	0.67	480	43.6	8.0

Table 5.2 shows the parameters of the cables in the current network. Cable 3, between Klaaswaal and Sterrenburg, actually comprises two sections, an overhead line of 12.8 km and an underground cable of 2.9 km. The section parameters are aggregated in the table and subsequently in the model. The remaining cables are underground. The line voltage V_{line} is 52.5 kV, and the capacity is calculated as $\sqrt{3} \cdot V_{\text{line}} \cdot I_{\text{nom}}$, where I_{nom} is the nominal current listed in the table. The annualised cost of the cables is 532.62 €/MWkm-yr. The cable costs too are detailed in Appendix A.

As mentioned, a rather simplified version of the gas network is considered in this thesis. Figure 5.3 shows the same Sterrenburg region, this time coloured according to the nearest gas city gate. There are 10 of these city gates in the region, where gas from the national gas network (from Gasunie Transport Services – GTS) at 40 bar is connected to Stedin's gas distribution network at 8 bar. The gas network is meshed, and there is no straightforward mapping of any location to a single city gate, since it could be fed by multiple city gates. Instead, it is assumed that the gas demand of a neighbourhood corresponds to the closest city gate. This is implemented in the open-source GIS (geographic information system) software QGIS, by mapping the centroid of each neighbourhood to the nearest city gate. The geographical data of the neighbourhoods was taken from CBS (*Centraal Bureau voor de Statistiek*) [112].

Considering the investigation of the benefits of energy system integration, the gas city gates are relevant when there is integration with the electrical network. For this reason, the five city gates which are closest to the five substation locations are chosen, as seen by the red markers in Figure 5.3; the substations and cables are also included in blue just like in Figure 5.1, for reference. The neighbourhoods in a coloured region without the red marker, i.e., where the city gate is not close to a substation, do not have their gas demand included in the model (but only their electrical demand).

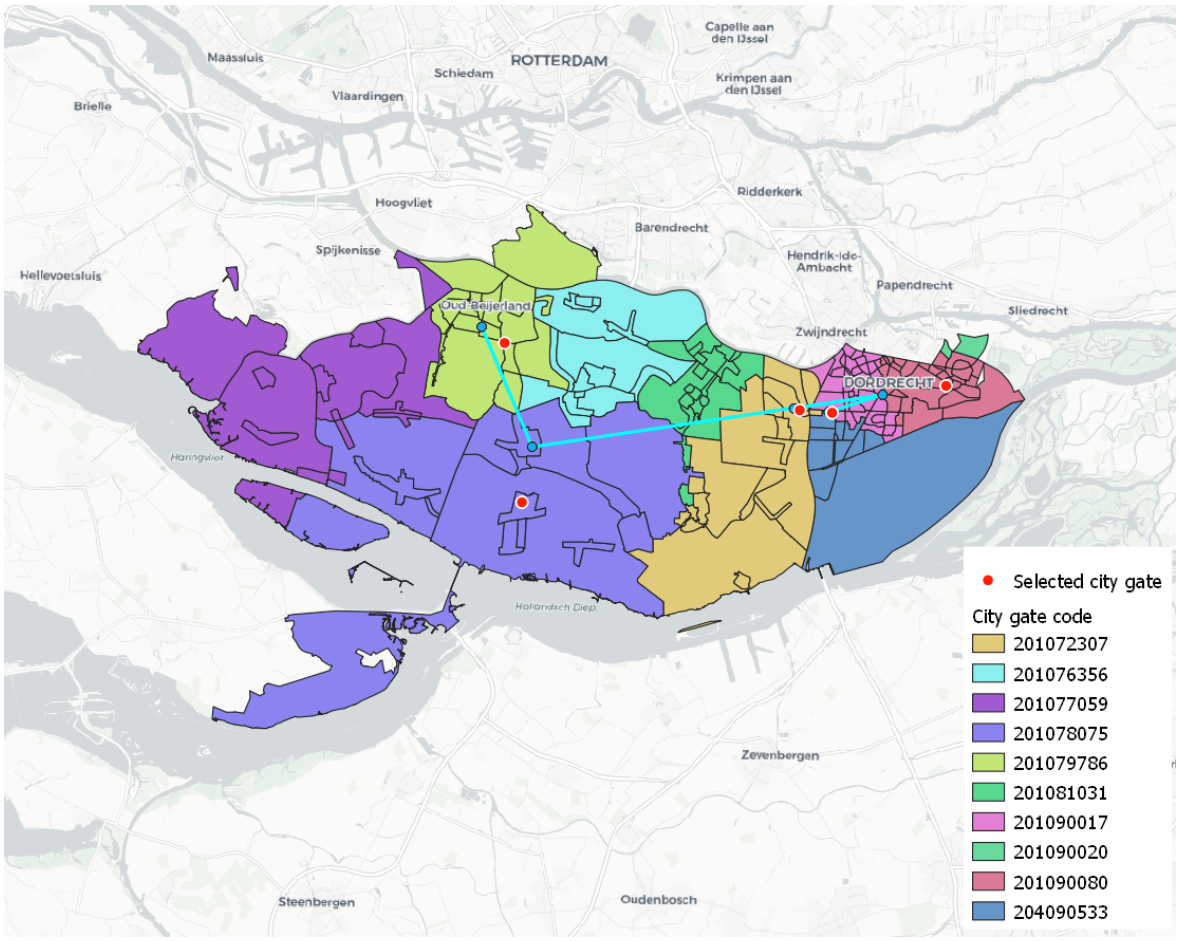

Figure 5.3: Map showing areas corresponding to different gas city gates in the Sterrenburg region.

Table 5.3 summarises the main parameters related to the selected gas city gates. The codes correspond to those in Figure 5.3. It can be seen that the distances from city gate to substation at Klaaswaal (code 201078075) and at Sterrenburg (code 201090080) are relatively long, at 2.506 and 2.386 km respectively. To integrate the two networks, a new connection needs to be laid between the substation and city gate, which adds to the cost of integration. The relatively long distance could therefore be disadvantageous, especially as these are the two substations with high renewable generation and energy demand, respectively.

Table 5.3: Overview of main gas city gate parameters.

Name	**Nearest substation**	**Code**	**Max flow (MW)**	**Distance to substation (km)**
Dubbeldam	Sterrenburg	201090080	57.8	2.386
Oud-Beijerland	Oud-Beijerland	201079786	86.5	1.246
Dordrecht Wieldrecht	Dordtse Kil	201090017	117.5	0.157
's Gravendeel	's Gravendeel	201072307	26.3	0.266
Numansdorp	Klaaswaal	201078075	51.9	2.506

The capacities of the gas city gates are determined from measurements, by using the maximum measured flow value of 2020. Furthermore, the cost for expanding a city gate is approximated in the following manner. The one-time cost of building a city gate is set at €3.5 million based on Stedin figures, and a typical capacity is taken to be 68 MW. With annual OPEX costs at 2% of the CAPEX and a 100-year discount period, this results in 2,658 €/MW-yr costs for city gates. As shown in Figure 4.3, the electrolyser output at 40 bar is connected directly to the transmission network, so the city gate capacity only needs to be expanded when there is excessive demand, and not due to the

electrolysis output.

Table 5.4: Annualised fixed costs of the existing Sterrenburg network infrastructure.

	Units	Price (€/unit)	Quantity	Total (€)
Existing network, annualised costs				
Transformers 150/50 kV	Transformer	177,132	2	354,263
Substations 150/50 kV	Substation	94,813	1	94,813
Transformers 50/13 kV	Transformer	73,075	10	730,748
Substations 50/13 kV	Substation	78,072	5	390,362
Lines 50 kV 43.6 MVA	km	23,222	64	1,485,372
Gas city gate	MW	2,658	340	903,720
				3,959,278

Table 5.4 shows an overview of the total annualised costs for the existing infrastructure within the part of the electrical and gas networks modelled. This includes two transformers (for redundancy) at each of the substation locations, as well as their corresponding substation. Note that while the capacities of existing components vary between the locations (see Tables 5.2 and 5.1), the same cost is assumed among them. For example, the existing cable between 'S Gravendeel and Sterrenburg has a capacity of 37.7 MVA compared to 43.6 MVA for the cable between Dordtse Kil and Sterrenburg, but for the cost estimation, both are assumed to have the same annualised cost per km. For cables, the cost is also assumed to be the same across the varying capacities, but the cost is scaled with the length at each location.

5.2. Future energy scenarios

In terms of investment cycles and infrastructure lifetime, the 2050 goal for climate-neutrality is not too far away. Nevertheless, there is still a lot of uncertainty and an array of different pathways to reach this point. Many initiatives have been set up to explore and plan these transitions, including the Net voor de Toekomst (2017) [111], the *Regionale Energie Strategieën* (RES) of 30 defined regions (a first version planned for 2021), and the high-level Infrastructure Outlook 2050 by TenneT and GTS (2019). With the complexity and uncertainty at hand, it is useful to work with scenarios, which is exactly what was developed by Berenschot and Kalavasta as a part of the *Integrale Infrastructuurverkenning* 2030-2050 (integral infrastructure exploration – II3050) [102]. This study is a collaboration among grid operators, industry, politicians and energy companies, among others.

To explore the possible infrastructure pathways, four different energy-neutral scenarios are developed for 2050 based on different policy directions. The scenarios are referred to in this work as: Regional, National, International and Europe. These four scenarios are also used to compose the hourly demand and supply profiles for this thesis. The scenarios are developed with the *Klimaatakkoord* for 2030 [113] and the Net voor de Toekomst as starting points, using a sociotechnical framework [114].

The Regional scenario is based on principles of regional self-sufficiency. In this scenario, there are no energy imports from other countries, and energy-intensive industries are discouraged. Decentralisation and circularity are also important themes in this scenario. In the National scenario, the Netherlands is envisioned as a European front-runner in meeting emission targets. Imports are still minimised, and energy-intensive industries are electrified but stay roughly at their current scales. Large national projects are also a part of this scenario. Both hydrogen and methane are important gaseous energy carriers, with hydrogen produced with renewable electricity and methane from biomass.

The national governments play less of a role in the Europe scenario, where there is more of a focus on European policies such as a European carbon tax supplemented by carbon compensation costs for imports from outside EU borders. International energy trade takes place, especially within Europe. There is also a role for carbon capture and storage (CCS) technologies in this scenario, as well as in the International scenario. Additionally, in the International scenario, the development of trans-national energy infrastructure is envisioned along with robust international trade. Energy-intensive industries

are expected to grow, along with a globally coordinated striving to meet emission goals, including through CCS [102].

As mentioned, a starting point for developing the 2050 scenarios is the *Klimaatakkoord*, the Dutch climate agreement to decrease national carbon dioxide emissions by 49% with respect to 1990. This leads to an additional scenario: the projected 2030 energy scenario based on the climate agreement.

For each scenario, an hourly profile is developed for various demand and supply categories of different sectors. The demand and supply are modelled using data from the weather of 2015. Based on information like population density projections, land use, expected building age, urban/rural/nature factors, industrial clusters and more, each location is assigned its set of proportions which are multiplied with the corresponding national profiles of different energy categories. At the national level, large flows from, e.g., offshore wind and refineries are included at the transmission level, but these are not used directly in this thesis since the focus lies on the distribution level. Additionally, the scenarios include some options for storage and flexibility, but those are also not included (as fixed inputs) in the model since they are variables to be optimised.

Figure 5.4 shows a high-level overview of the Klimaatakkoord scenario data for the Sterrenburg region: at each substation area, the hourly values for demand and supply are added up for the whole year and plotted. Broad categories for electrical demand, local generation and gas demand are made by aggregating certain categories from the scenario. For example, the built environment electrical demand includes among others, buildings demand, heat pump demand, household demand. Similarly, for industry there are contributions from the demand profiles of data centres, food, paper, and miscellaneous. Specifically, electrical demand is composed of agriculture, built environment, industry, mobility and "other". The generation comprises CHP, rooftop solar, solar farms and onshore wind turbines. In the simulation, the different types of demand and supply categories are not treated differently, but knowing the types helps to gain insight into the region and in analysing the results.

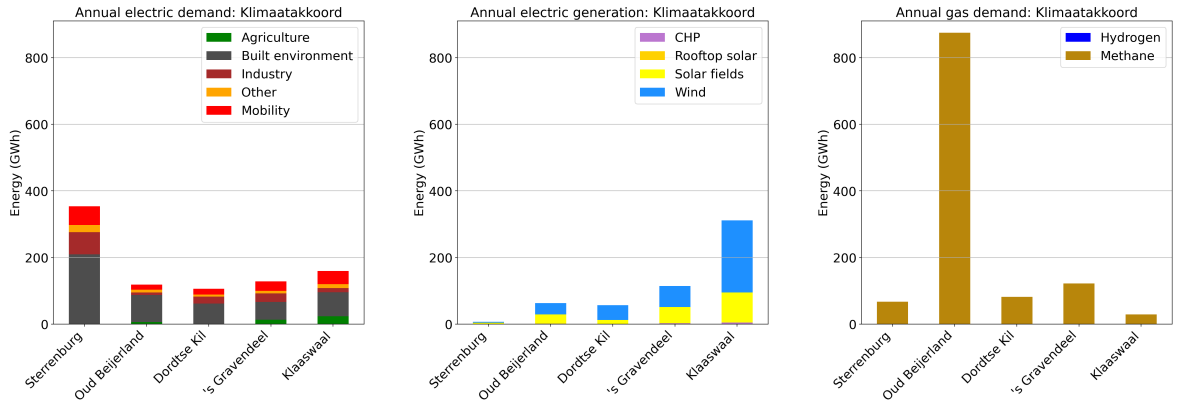

Figure 5.4: Total annual demand and supply at each area in the 2030 climate agreement scenario.

It can be seen that in 2030, hydrogen does not yet play any significant role, but a large amount of the total energy demand is from natural gas. Additionally, local generation predominantly arises from onshore wind and PV fields. Sterrenburg has a high electrical demand and Klaaswaal high electrical generation, both at about 350 GWh for 2030. For natural gas demand, the annual highest is at Oud-Beijerland. In fact, at nearly 900 GWh for the year, this huge demand is anomalous and worth looking into further. Most of this gas demand (over 650 GWh) comes from the household demand for natural gas. Specifically, four neighbourhoods are modelled in the profile to have a large proportion of the national profile. Zoomwijck, Zuidwijk, Oosterse Gorzenwijk and Spuioeverwijk have 0.397%, 0.265%, 0.155% and 0.103% of the national demand profile, which is remarkable as their 2017 populations ranged between 1455 and 5060 per neighbourhood. The gas demand here is higher than in other neighbourhoods and in other areas, but since the source of this high natural gas demand is verified from the scenario, it is used in further analysis without any modifications.

Figure 5.5 shows an overview of the annual total energy demand and supply of the 2050 scenarios. In the figure, the y-axis limits are the same throughout, allowing for a comparison of the relative amounts across scenarios and demand/generation. Comparing the 2050 scenarios of Figure 5.5 with the 2030 scenario of Figure 5.4, some observations are immediately noticeable. Firstly, in all of the

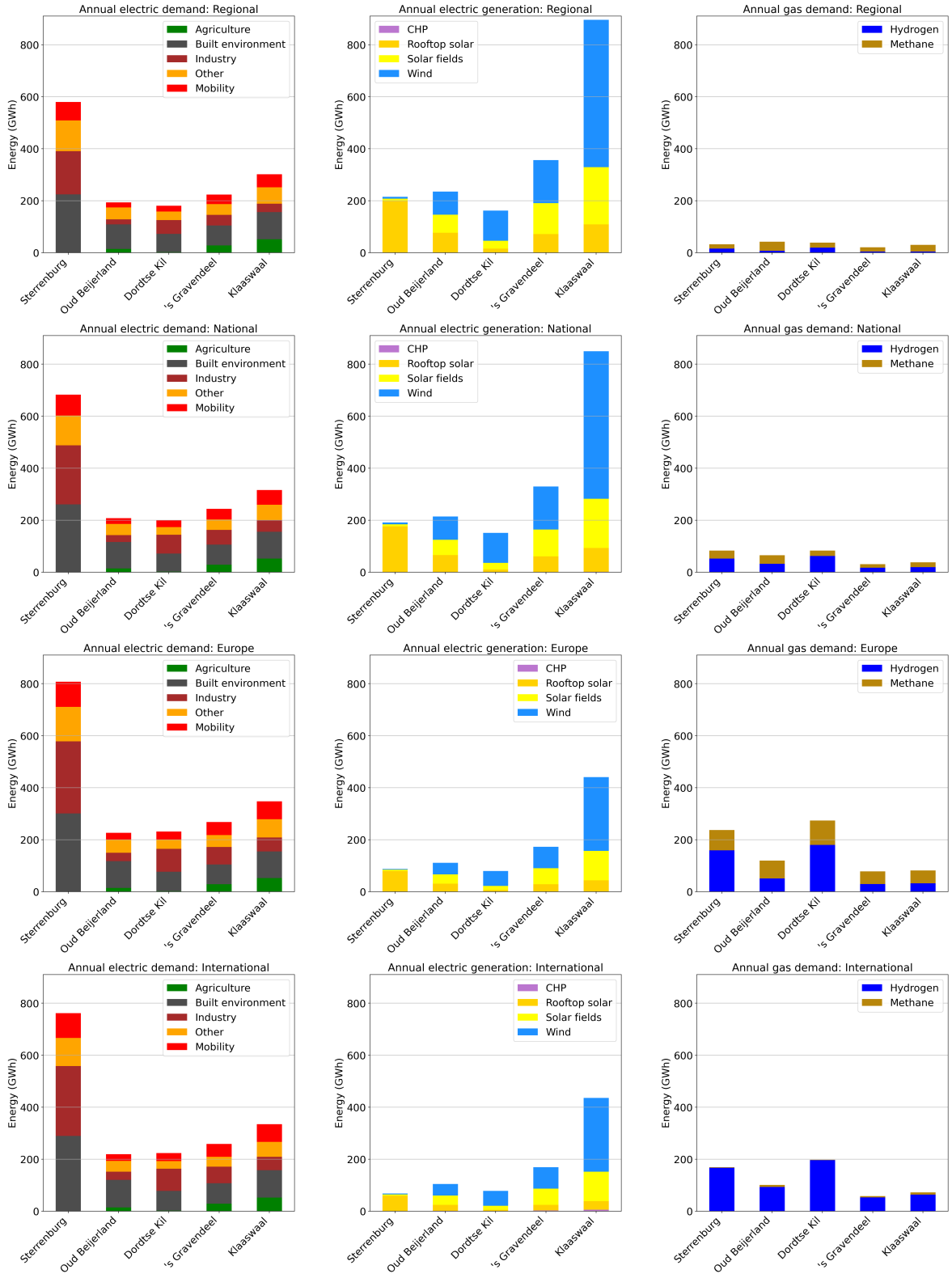

Figure 5.5: Overview of the total annual demand and generation composition for each 2050 scenario, at each aggregation location.

2050 scenarios, the electric demand is expected to increase to different extents, which is consistent with the expected electrification of demand. Additionally, in all 2050 scenarios, the capacity of local energy generation is higher than in 2030, notably through the addition of solar fields in addition to rooftop solar and onshore wind.

In this thesis, the main scenarios used in analyses are the Regional and the International scenarios since these represent some of the extremes in demand and generation. The Regional scenario has the highest capacity of local generation among the scenarios, especially with a lot of wind generation at Klaaswaal. The Regional scenario shares similarities with the National scenario, which does have slightly lower electrical demand and an increased share of hydrogen demand. In the International scenario, both the electrical and the gas demand are relatively high among the scenarios. Specifically, in this scenario, hydrogen plays a strong role. On the other hand, there is less local generation, and the energy exchange between regions is expected to be of more importance.

In Figures 5.6 and 5.7, the annual, daily and weekly characteristics of the demand and supply profiles of the Regional scenario are illustrated. Each of the subplots shows the sum of demand or supply at all locations included in the Sterrenburg sub-network. In Appendix B, the equivalent plots for the International scenario are shown, notably with higher electricity demand, lower local generation and a dominant share of hydrogen demand among the gas consumption.

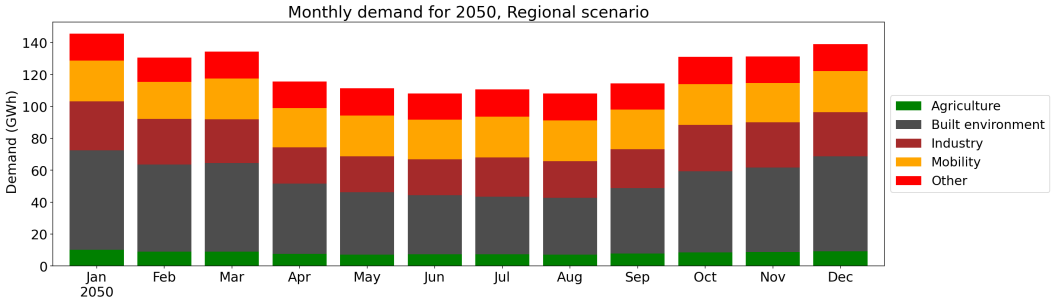

(a) Total monthly electrical demand.

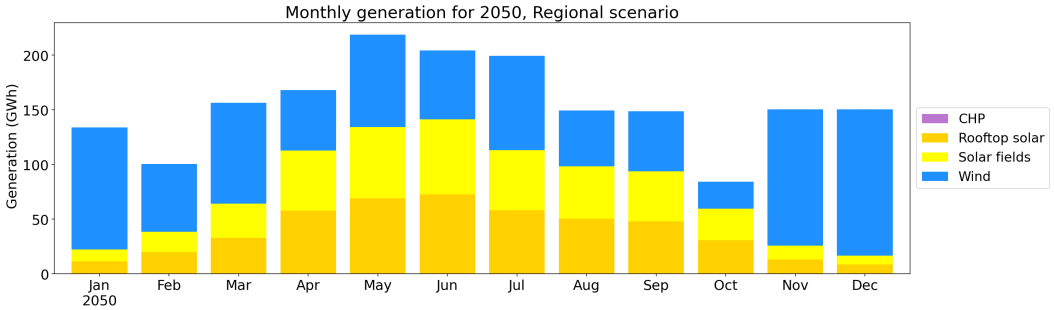

(b) Total monthly generation.

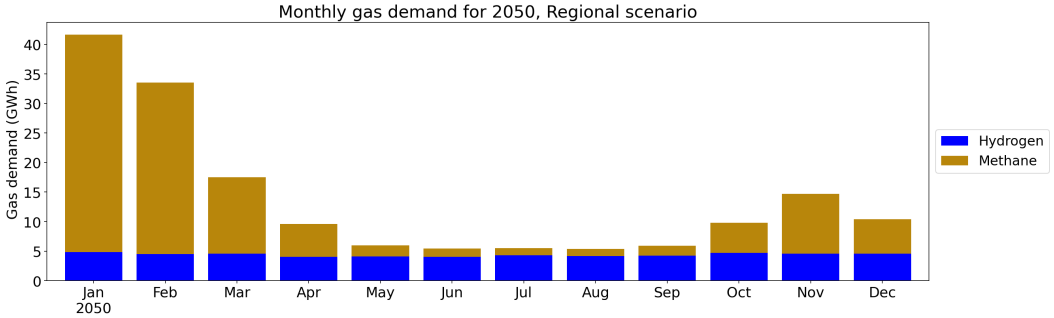

(c) Total monthly gas demand.

Figure 5.6: Total monthly profiles for 2050 in the Sterrenburg sub-network for the Regional scenario.

Figure 5.6a, shows that the total electrical demand is higher in winter than it is in summer: the winter months have about 30 GWh more electrical demand than the summer months. A large part of this difference arises from the change in demand from the built environment, which in turn is explained by the increased energy use for heating buildings in winter.

The local energy generation is shown in Figure 5.6b to peak in summer, due to the solar generation

clearly peaking in June and dropping off in December and January. Wind energy generation fluctuates from month to month, but tends to be higher in the winter months. The gas demand for each month throughout the year is plotted in Figure 5.6c. The demand for hydrogen is relatively stable throughout the year, while the methane demand is higher in the colder months. Biomethane from local biomass is foreseen to play a role in decreasing carbon emissions from methane use. In the Regional scenario, the hydrogen demand is mainly for transport and industry, and the methane demand is largely for households, agriculture and heat networks, i.e., for heating purposes. As mentioned, in the Regional scenario (unlike the International scenario), there is a large proportion of natural gas demand among the total gas demand, challenging the assumption made in the model that all of the gas network is for hydrogen. This shows that the heating transition could occur in different ways and by different extents, e.g., electrification in combination with renewable generation and decreased heating demand by better insulation, the use of alternative fuels such as hydrogen (International scenario), or to some extent still using natural gas (Regional scenario). That being said, the total demand for gas in the Regional scenario is relatively low, peaking around 40 GWh compared to 140 GWh of electrical energy demand in a month (keeping in mind the gas and electricity regions considered are not exactly the same, as explained in Section 5.1). For comparison to the International scenario, the monthly gas demand peaks around 95 GWh, and for electrical demand this is 175 GWh for the case region (see Appendix B).

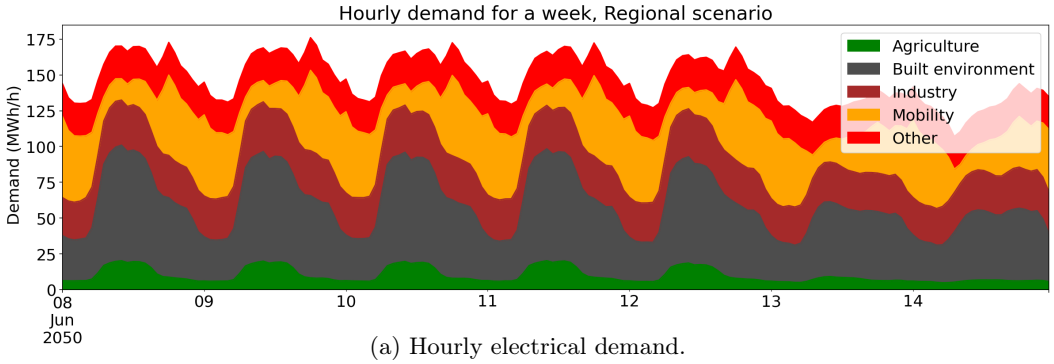

(a) Hourly electrical demand.

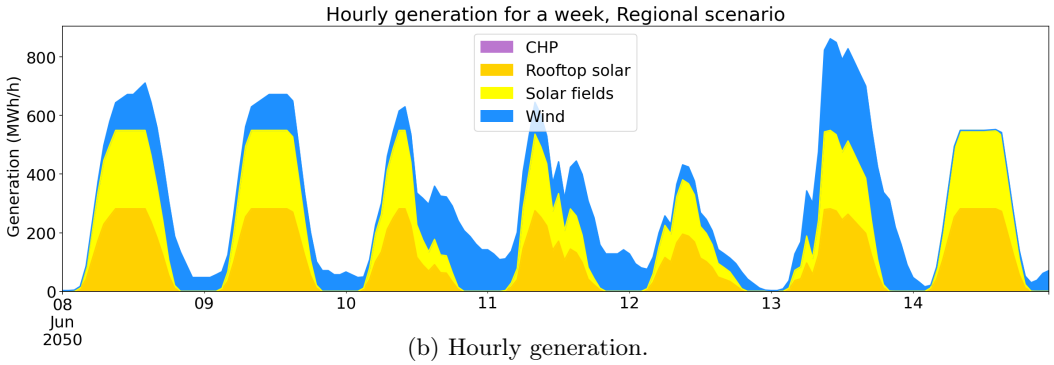

(b) Hourly generation.

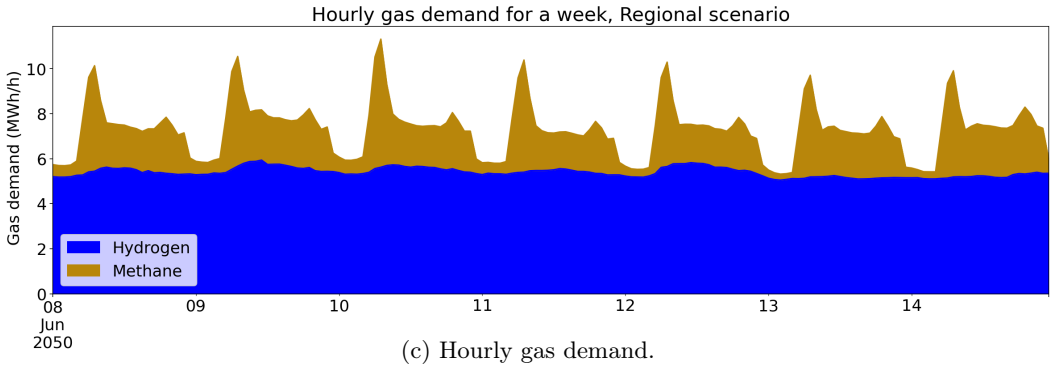

(c) Hourly gas demand.

Figure 5.7: Hourly profiles for a week in the Sterrenburg sub-network from the 2050 Regional scenario.

Figure 5.7 shows the hourly demand and supply profiles for an arbitrary 7-day period in the year, to highlight the daily and weekly variations. While the period of 8 to 14 June is actually Wednesday to Tuesday, it would make sense that in the scenarios (with hourly values labelled 1 through 8760) this corresponds to a week of Monday to Sunday. In the preceding and following 7-day periods of the scenario, it is also seen that in the electrical demand, there are 5 days of higher demand (especially in agriculture and the built environment) followed by two days of lower demand, as plotted in Figure 5.7a. The electricity demand also shows a cycle of being higher during the day, and lower at night.

Figure 5.7b shows the hourly local generation, with fluctuations corresponding to the predicted weather. As would be expected, the daily cycles are indicated by zero solar energy generation at night. The solar generation is seen to level off on some of the days (on 8, 9 and 14 June) which means that at these hours, the solar panels are generating at their full installed capacity, as could be expected from sunny days in June. The gas demand of Figure 5.7c shows a fairly steady demand for hydrogen (as mentioned, mostly from the industrial sector). The fluctuating natural gas demand shows a spike in the mornings, and is fairly constant until taking a dip at nighttime. The natural gas demand is also comparatively low in June, as there is less need for heating spaces during this season (while the industrial component of the demand stays steady).

5.3. Model input data

The inputs for the model are set in a folder containing CSV files which are read into a PyPSA network, and by setting parameters in the main Python script. The CSV files each contain fixed or time-varying parameters for: buses, loads, transformers, lines, links, generators, snapshot weightings, and the time-varying limits/set-points of generators and loads.

The buses are given unique names, and are assigned voltages if electric, or labelled as gas type. Each one-port component includes information on which bus it is attached to, and each two-port on which buses it spans. In the optimisations, the existing component parameters comprise those reported in Section 5.1. The new (candidate investment) component have the properties described as follows.

Table 5.5 shows the electrical and economic parameters of candidate cables at 150 and 52.5 kV, with capacities of 100 and 43.6 MVA respectively. These cables are found at the high-voltage sides of the transformers near loads, as shown in Figure 5.2. In the current infrastructure, these are all at 52.5 kV level, and in the manual expert solution, this would be 150 kV. The resistance and reactance values are multiplied by the respective cable distances before entering them into the model.

Table 5.5: Input parameters for new cable investments.

Voltage (kV)	**Resistance (Ω/km)**	**Reactance (Ω/km)**	**Capacity (MVA)**	**Annual cost (€/MWkm-yr)**
150.0	0.050	0.110	100	1,332
52.5	0.083	0.088	43.6	533

Additionally, new cables need to be invested in to connect electrical substations with gas city gates. This may be at 52.5 or at 13 kV level, and the capacity is determined by the optimisation. For this purpose, the power flow is to an active branch (the electrolyser) and the passive electrical parameters (resistance/reactance) are not used. For the 13 kV lines, the annualised fixed cost is 819 €/MWkm-yr.

The main electrical and economic parameters concerning transformers and substations are summarised in Table 5.6. The reactance is the per-unit series reactance, using the nominal power capacity as the base power, derived from the relative short circuit voltage and assuming resistance is zero. The annual costs reflect the fixed, annualised cost of investing in a single transformer. The cost of switchgear is added to the cost of each transformer type (and it is already included for the 150/21 kV transformer). Furthermore, when the existing substations are at capacity, new substations need to be invested in for any additional transformers. This is modelled by adding the cost of the substation (annualised for a period of 100 years) to that of the transformer, and marking the transformers that fit in this substation as dependent on this investment.

Table 5.6: Input parameters for new transformer and substation investments.

Voltages (kV)	Capacity (MVA)	Reactance (p.u.)	Transformer cost (€/MW-yr)	Switchgear cost (€/MW-yr)	Substation cost (€/MW-yr)
150/52.5	100	0.1495	1,187	585	948
52.5/13	40	0.1490	1,484	343	1,952
150/21	90	0.1800	1,086	-	4,571

Regarding continuous capacity investment variables such as the electrolyser, it is assumed that the costs scale linearly with capacity, i.e. that the cost for each additional MW built is constant. The costs for conversion/storage components are summarised in Table 5.7. The costs listed cover the entire system necessary for the component, for example for the electrolyser, the power electronics, gas conditioning and balance of plant parts are included in the CAPEX.

Table 5.7: Overview of model input parameters for conversion and storage components.

Component	Annual cost (€/MW-yr)	Marginal cost (€/MWh)	Efficiency
Electrolyser	37,982	0	75%
Combined cycle hydrogen turbine	59,718	2	58%
Battery storage	57,690	0	85%

The electrolysis costs are based on alkaline electrolysers in 2050 from [54], but PEM electrolysers are also expected to have similar costs (and in fact, a smaller spatial footprint). The model itself is not specific to any electrolysis technology, since it is modelled as a conversion device with a fixed efficiency. Within the optimisation, electrolysers can be placed between any substation and its corresponding gas city gate. For this, a connection needs to be placed between the two, which is an electric cable at 52.5 or 13 kV. This is modelled by increasing the electrolyser cost at each option by the amount (per MW) corresponding to the electric cable: a factor of 1.5 times the distance between the substation and city gate, multiplied by 533 €/MWkm-yr for 52.5 kV or 1,332 €/MWkm-yr for 13 kV. The factor 1.5 comes from the fact that a redundant connection needs to be placed, but since this is for a single project (at the same time and location), the labour and installation costs are lower, so the cost for redundant cables is less than twice that of a single connection. Moreover, when placing a new connection at a substation, this will require a switchgear bay to be installed as well to facilitate disconnection. This cost depends on the voltage level, and equals a one-time cost of €322,000 at 52.5 kV, or €57,000 at 13 kV. This cost is annualised by a 100-year period (to 10,190.23 and 1,803.86 €/yr at 52.5 and 13 kV) and at each location, the placement of electrolysers is marked as dependent on the switchgear investment. One approximation is made here: the 13 kV switchgear installation is for flows up to 10 MVA, and for higher capacities, additional installations are required. This is approximated as an extra (continuous rather than discrete) cost per MW. At 52.5 kV however, the capacity is 50 MVA. This is a much larger block, and is typically not exceeded at any location for an electrolyser connection. Therefore this is left as a discrete lump sum on which the electrolysis placement depends.

For conversion from hydrogen to power, fuel cells or gas turbines can be used. Gas turbines are an established technology using the combustion of natural gas to generate power; turbines are now being developed to use hydrogen instead. Fuel cells can also be used to convert hydrogen to power, but they are expected to have higher investment costs and lower lifetimes than gas turbines, while operating at a comparable efficiency [115]. Therefore, only gas turbines are considered in this case study for conversion from hydrogen to power, specifically combined cycle hydrogen turbines. For energy storage, lithium-ion batteries are considered as storage units connected to the electrical grids. These can be placed at 13 or 52.5 kV buses. The parameters are based on [8], which considers 4-hour lithium-ion batteries for utility-scale use in future grids. The round-trip efficiency for charging and discharging the battery is 85%, which is notably higher than for converting power to hydrogen and back (which gives an overall efficiency of 42%). More details on the techno-economic component parameters are found in Appendix A.

The time-varying power output of local renewable generation is modelled as a fixed (rather than

dispatchable) value at each hour by setting the minimum and maximum per-unit values at each generator and snapshot equal to the production calculated from the scenario. The generator output cannot be lower than the scenario value because it is assumed that there are no operational reserves (by running below capacity, e.g. to be able to provide frequency control) or curtailment, and the generator output cannot be higher because these renewable generators are limited by their environmental conditions (weather). The generation profiles are derived from the scenario, and the different generation technologies (solar PV, onshore wind and biomass CHP) have marginal costs as listed in Table 5.8, which are elaborated on in Appendix A. Note that biomass CHP is not connected to the hydrogen grid, and it is only present in small amounts in some of the scenarios. The prices for energy exchange with the national grids (as explained in Section 4.2.2) are centred around 50 €/MWh for electric energy and 90 €/MWh for hydrogen.

Table 5.8: Cost overview of the various energy sources.

Source	**Cost (€/MWh)**	
Solar PV	1.2785	
Onshore wind	2.2188	
Biomass CHP	55.0	
Electricity import/export	50.0	(mid-level price)
Hydrogen import/export	90.0	(mid-level price)

To analyse the spatial requirements of each solution, the areas and widths listed in Table 5.9 are used, based on [46] unless listed otherwise. The spatial footprint of the infrastructure is divided into two categories: those of area type and length type. The area type includes the above-ground and location-centred infrastructure like substations and electrolysers. The length type comprises electric cables (usually underground, except at 150 kV), which span two locations such as two substations, or a substation and a gas city gate. The 13 kV cables have a width which varies linearly with the capacity, as approximated in the table.

Table 5.9: Spatial footprints of components.

Type: area	**Capacity**	**Area (m^2)**
150/52.5 kV substation	300 MVA	45,000
150/21 kV substation	180 MVA	30,000
52.5/13 kV substation	80 MVA	10,000
Electrolyser	varies	95.0/MW [54]
Battery	varies	71.4/MWh [116]
Type: length	**Capacity (MVA)**	**Width (m)**
150 kV cable	100	10
52.5 kV cable	43.6/varies	10
13 kV cable	varies	0.3 + 0.1/MW

5.4. Market model validation through case study

Before presenting the 2050 infrastructure plans, the market model is examined a bit more closely. During the model development, trading with the external grid was initially modelled at fixed prices: electric energy could always be bought or sold for 50 €/MWh and hydrogen at 90 €/MWh. With an efficiency of 75%, this means the electrolyser consumes 1.33 MWh of electric power (worth €66.67) to produce 1 MWh of hydrogen worth €90. Even when renewable generation is low, power can be imported from the national grid at a commercially viable rate for conversion to hydrogen at every single hour (when the price is modelled as fixed). This makes it profitable to install large capacities of electrolysers, and import large amounts of power from the national grid to supplement the locally generated power. In the Regional scenario, this still leads to a reduced need for grid infrastructure (compared to no electrolysis), since the large, consistent demand counters the net generation at

many locations. However, the (unrealistic) effect of the fixed prices is especially pronounced in the International scenario, where the option of electrolysis leads to investment in *more* infrastructure than with reinforcement only. The effect is unrealistic because in practice, the electricity price is affected by bids in the competitive markets. When the demand is high, this leads to more expensive generators being dispatched (see the merit order effect in Section 2.5). Moreover, the electricity (and gas) prices fluctuate throughout time, making it more attractive to convert power to hydrogen at some hours than at other hours when the electricity price is high. For small installed capacities of electrolysis, their demand would not have much effect on prices, but when hundreds of MW of electrolysers are installed in the case region (and likely elsewhere in the country), the price variations of electricity become important. Some of the optimisation results are highlighted in Table 5.10.

Table 5.10: Selected results for the International scenario comparing fixed and varied trading prices.

Component investments	**Reinforcement only**	**Fixed price**	**Dynamic market**
New transformers 150/52.5 kV	2	6	2
New transformers 52.5/25 kV	10	7	8
New cables 43.6 MVA, 50 kV (km)	83.4	136.3	55.3
Total electrolysis capacity (MW)	0	534.0	121.3

Table 5.10 shows the investments made in three variations of the model: first, the results are shown in which only new cables and transformers (with substations) can be placed to reach the necessary network infrastructure. In the next column, electrolysers are included as an option, and the trade with the external markets is set with fixed prices as explained previously. Finally, the dynamic model (with time-varying price bids at three levels) is implemented along with the option for gas-electricity integration, for which the main investment results are also summarised in the final column.

Compared to only reinforcement, the fixed price model tends to require more network infrastructure, while the dynamic market model leads to fewer network infrastructure investments. Specifically, this optimisation calls for 6 new transformers at 150/50 kV level (compared to 2 such transformers for the other two models). This highlights the fact that the electrolysers cause more power to be drawn from the national grid, via the 150/50 kV connections. With the fixed market prices, the optimisation chooses for a total of 534 MW electrolysis capacity in the Sterrenburg sub-network, compared to 121.3 MW with the dynamic market. This is also reflected in the cable investments, which are highest for the fixed market price model (136.3 km) compared to the reinforcement-only (83.4 km) and the dynamic market model (55.3). The fixed price model results also include more than five times the electrolysis capacity compared to what is chosen with the dynamic market.

Not only is this result counter-intuitive, it is also unrealistic to assume that any amount of power can always be purchased at the same price, or that hydrogen can always be sold at the same price. The fixed prices make electrolysis seem artificially attractive. Particularly in the International scenario which has less (cheap) renewable generation and higher electrical demand, the electrolysers consume large additional amounts of power.

In reality, prices vary along with changes in demand and supply. The limitations of fixed-price modelling are compounded by the fact that this model covers but one region in the Netherlands, and other regions are likely to have similar energy surpluses and bids at the same time. When the demand for heating is high in Sterrenburg due to the cold weather, this will likely be the same elsewhere, and energy prices are driven up by the high demand. For this reason, the model for exchange with the national market was modified as explained in Section 4.2.2, importantly to reflect two simplified market characteristics: i) the time-variation of demand and supply, and ii) the diminishing marginal utility for consumption/increasing marginal costs for production.

Finally, it is useful to briefly consider the shadow prices. These are used during the analysis of the results to calculate how much it costs to import power from the external grids during times of energy deficit, and how much is earned by local producers when selling the energy surplus back to the national grid. The price is calculated from the Lagrange multiplier of the power balance constraint at a bus and an hour. These prices represent the change in the objective function when the demand at that bus is increased by one unit. This usually is supplied by the generator which was last dispatched, and typically reflects the market price.

However, sometimes anomalies are seen as big spikes or dips in this pattern. For example, consider Figure 5.8. This shows the variations of the shadow prices at a gas bus throughout a simulation, along with the per-unit flows through the city gate (link component) that supplies it. At the 354th time-step, the price shows a big spike up to nearly 800, compared to the range of 72–108 values of all the other hours.

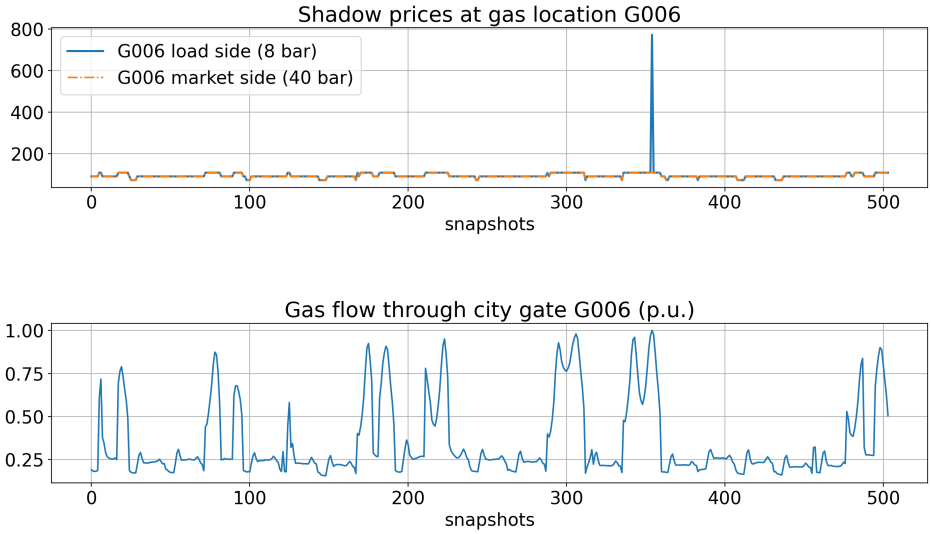

Figure 5.8: Shadow prices retrieved from a PyPSA optimisation, including a spike due to capacity.

This spike occurs due to congestion; at this hour, the flow through the link is 1 p.u. (as seen in the bottom part of Figure 5.8). The value arises from a combination of factors: the cost of expanding the link capacity, the cost of the additional gas and a factor of the snapshot weighting. This value is no longer representative of the market price. Therefore, when calculating energy import and export costs between the local and national grids, the shadow prices are first clipped to remove extremes like these. After doing this, the shadow prices can be interpreted as the hourly market prices at that bus, in €/MWh.

Figure 5.9 shows a revised version of Figure 5.8, with the extreme value clipped and different details visible. Here, the hourly gas prices can be seen to vary between the three levels of the market: 72, 90 and 108 €/MWh. Moreover, it can be seen that when the demand is low, the price too is low, and at times of peak demand, the price is driven up to the highest level. This effect is not one-to-one for one city gate and its price, since the other regions in the Sterrenburg sub-network also contribute to this effect.

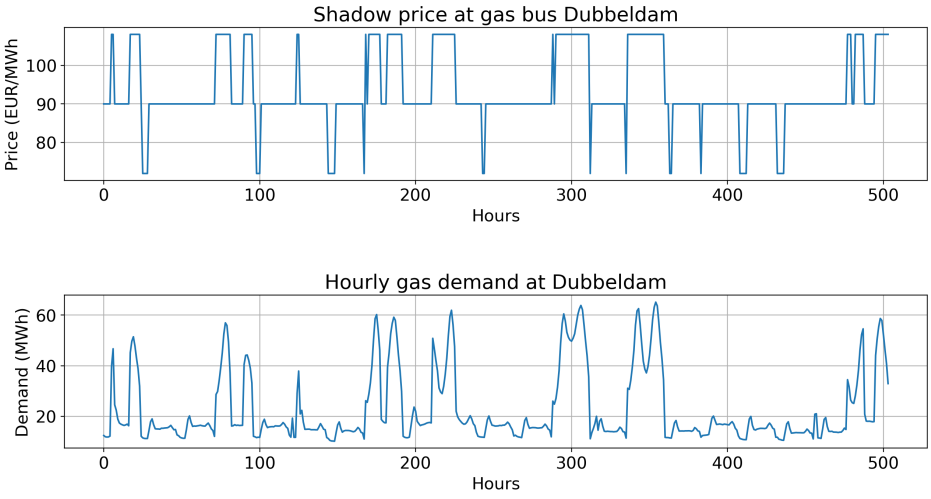

Figure 5.9: Hourly shadow prices and corresponding gas demand at the bus.

6 | Case study results and discussion

The case study analysis results are presented in this chapter, starting with the manual expert solution, and followed by analyses of power-gas integration, storage, spatial usage and sensitivity to changes in selected parameters. Throughout the chapter, discussions of specific analyses are presented together with the corresponding results. Figure 6.1 shows an overview of the main analyses carried out, for which the results are presented and compared in this chapter.

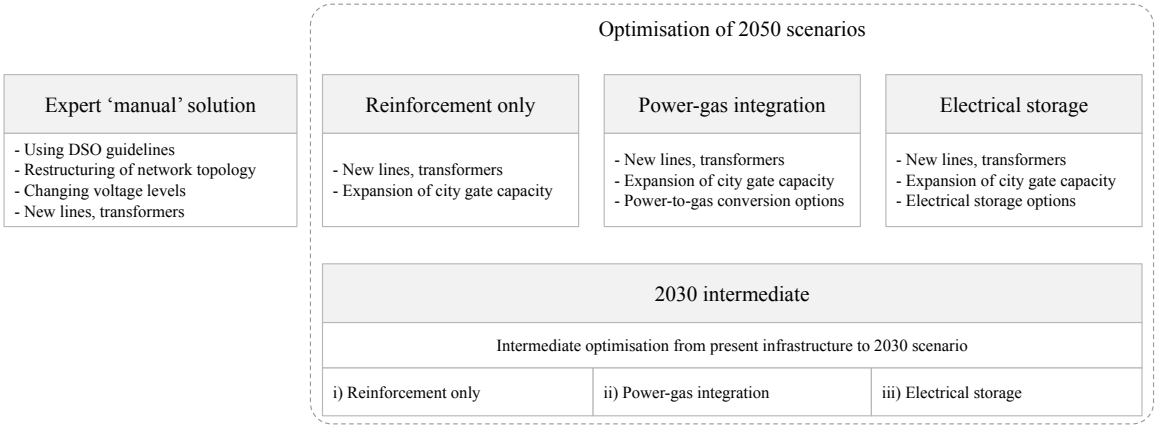

Figure 6.1: Overview of the different result analyses.

Section 6.1 sets a context for the optimisations: how would an expert grid operator adjust the topology and components of the network, given more freedom to make changes in the network? The results hereof are compared against the current network configuration. In the remaining parts, the present configuration is used as the starting point of the optimisation (allowing it to be expanded upon, but not removed or replaced with other components). In Section 6.2, the expansion planning results are compared for purely reinforcing the existing grid to meet 2050 requirements, compared to the option of also integrating the gas and electricity networks. Section 6.3 provides similar planning results for the option of electrical storage. In order to clearly observe the individual effects of storage and power-gas integration compared to reinforcement-only, and because different time-slicing inputs are used for these analyses (see Section 4.6), these are analysed separately.

The effect of input parameter uncertainty is investigated with the sensitivity analysis of Section 6.4. Another consideration is that 2050 is still decades away, and intermediate investments could be made which are not favourable for the 2050 situation. This is explored with the 2030 intermediate step in Section 6.5. Finally, spatial requirements might become bottlenecks in grid expansion projects in densely populated areas. The effect of sector coupling on spatial requirements is analysed in Section 6.6.

6.1. Manual expert solution

The manual expert solution type corresponds to how expert grid operators would restructure the grid based on the expected power flow levels in 2050. While the restructuring part is not an optimisation (hence "manual"), it is included to provide context for the optimisation-based solutions. The overall configuration is preserved (locations of substations and cables, and corresponding demand and supply profiles), but in this solution the freedom is taken to replace components with different types (voltage level, power rating), or even to remove components. In consultation with the grid operation experts from Stedin, the main changes chosen for this solution compared to the current infrastructure are as follows.

1. Removing the intermediate voltage level (50 kV) and removing the 150/50 kV transformer.
2. Replacing 52.5 kV cables with 150 kV cables, and 52.5/13 kV transformers with 150/21 kV transformers (along with suitable substation equipment).
3. Decoupling of Sterrenburg 150 kV area and Klaaswaal 150 kV area by removal of the cable from Klaaswaal to Sterrenburg.

A schematic showing the modified layout can be seen in Figure 6.2. One point to note here is that some of the infrastructure is at 150 kV, which as of current regulations falls under the responsibility of the transmission system operator TenneT. For consistent comparison, however, the costs and investments of these cables are still included in the analyses of this solution. The figure also shows that the intermediate 52.5 kV voltage level is eliminated altogether, and the 13 kV is replaced with 21 kV. Moreover, there are now additional locations with 150 kV, where connections to the national transmission grid are possible. In this case, Klaaswaal is also connected to the national grid near an industrial area, which allows the connection between Klaaswaal and Sterrenburg (the longest connection in this area at 15.7 km) to be removed, which saves space and money. The components also have higher capacities (compared to the existing configuration): the transformers have a capacity of 90 MVA each, and the 150 kV cables can transfer up to 100 MVA. Together, these changes simplify the network structure, and make it better suited for large power flows.

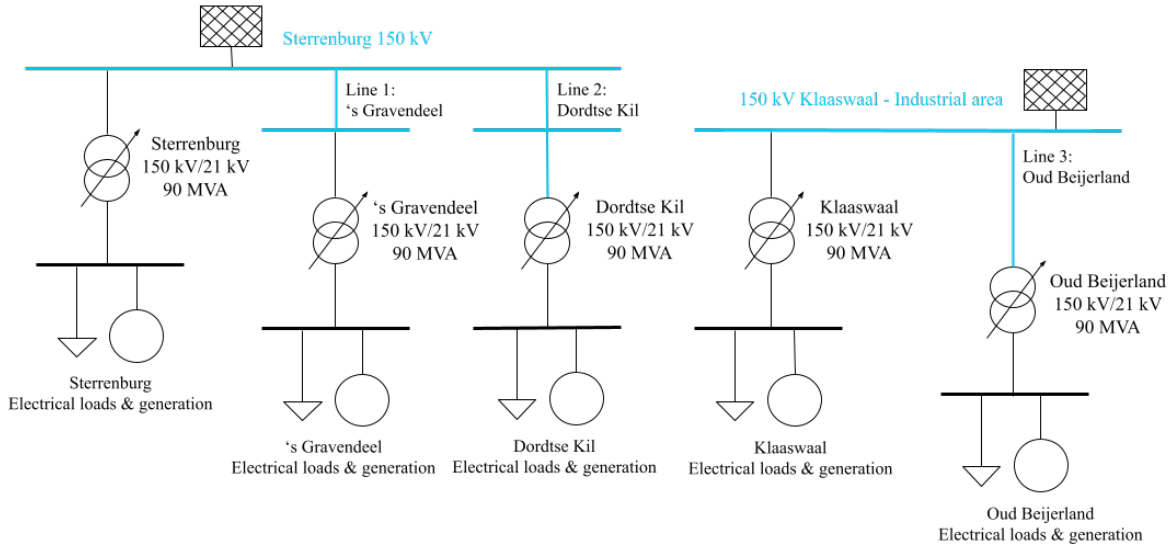

Figure 6.2: Single line diagram showing the network reconfigured by experts, for 2050.

Starting from the new configuration as visualised in Figure 6.2, the PyPSA model is still used to determine the number of components required at each location to accommodate the demand and supply profiles from the scenarios. It is again assumed that there are at least two of each electrical network component present at each location, to be able to satisfy the N-1 redundancy criterion. Furthermore, the gas network is still assumed to exist at the same capacities as today, but repurposed for hydrogen. For these "base" components, the fixed annualised costs are calculated and shown in Table 6.1. These costs add up to nearly €7 million per year, which arise predominantly from the 150 kV cable and the 150/21 kV substation costs. This is substantially higher than the annual cost of approximately €4 million for the base components of the existing configuration (see Table 5.4), but as mentioned, this new configuration is designed for higher flows, and makes more sense for the 2050 profiles as discussed next.

In addition to this minimal network, extra components are needed depending on the profiles of the 2050 scenarios. 21 representative days are chosen from the Regional and International scenarios, and based on these, the PyPSA model is used to calculate the necessary reinforcement investments for these scenarios (without gas-electricity coupling). The annualised costs of these additional investments are calculated and presented in Table 6.2.

More investments are required for the Regional scenario than in the International scenario. In fact, for the International scenario, no additional cables are necessary in this expert solution configuration.

Table 6.1: Annualised costs of basic existing infrastructure for the expert solution.

	Units	Price (€/unit)	Quantity	Total (€)
Base components, annualised costs				
Transformers 150/21 kV	Transformer	97,740	10	977,400
Substations 150/21 kV	Substation	411,390	5	2,056,950
Cables 150 kV 100 MVA	km	93,209	33	3,038,619
Gas city gate	MW	2,658	340	903,720
				6,976,689

Table 6.2: Overview of network reinforcement requirements and costs in the expert solution.

			Regional		**International**	
	Units	Price (€/unit)	Quantity	Total (€)	Quantity	Total (€)
Reinforcement, annualised costs						
Transformers 150/21 kV	Transformer	97,740	7	684,180	2	195,480
Substations 150/21 kV	Substation	411,390	5	2,056,950	2	822,780
Cables 150 kV 100 MVA	km	93,209	32.5	3,027,434	0	0
Gas city gate expansion	MW	2,658	0	0	7.3	19,445
				5,768,564		**1,037,705**

This is in part because the existing (base) cables have a higher capacity than in the current infrastructure, at 100 MVA. The Regional scenario still approximately requires cables to be doubled (in terms of length). The Regional scenario also requires much higher investments in transformers and substations than the International scenario, although the International scenario's high hydrogen demand requires a small increase in city gate capacity. Overall, the grid reinforcements in the International scenario cost just over €1 million per year, while for the Regional scenario, these costs are much higher, at nearly €5.8 million per year.

The costs of reinforcement and of the base network infrastructure are combined by adding the total costs from Tables 6.1 and 6.2, of which the results are shown in Table 6.3. Moreover, these costs are also compared to the annual costs of the reinforcement-only solutions for the current configuration, for the Regional and International scenarios. The table shows that for both (expert and current) configurations, the annual infrastructure costs are similar within a scenario, and that in both cases the Regional scenario costs more. This could be expected, since the Regional scenario aims to make regions more self-sufficient in energy, which translates to more infrastructure at the distribution level and less over the long distances at the transmission level.

Table 6.3: Comparison of total annual infrastructure costs of the manual expert solution and existing network, in the Regional 2050 scenario.

Total infrastructure, annualised costs	Units	**Regional**	**International**
Existing + reinforcement, expert solution	€/yr	12,745,252	8,014,394
Existing + reinforcement, current configuration	€/yr	12,533,212	7,544,483
Difference	€/yr	**212,041**	**469,910**

Interestingly, the annual infrastructure costs are higher in the expert solution for both scenarios. The difference, however, is not large (about 2% of the total costs in the Regional scenario and 6% in the International scenario). One factor contributing to the higher costs is the fact that the 150/21 kV substations are substantially more expensive than the 52.5/13 kV substations that they replace. However, the components in the expert configuration generally also have larger capacities than in the current configuration, which also means that the redundancy is higher. This can be beneficial in cases of outage or maintenance, or times of extreme flows like an unusually cold winter. Overall, the manual expert solution has some advantages like the higher voltages (losses are not modelled, but would be lower), fewer components and suitability for large flows. The current set-up has slightly lower costs, and is more efficient at locations where the flows are smaller (for example at Dordtse Kil, where much of the redundant 150/21 kV transformer capacity goes unused).

This solution shows that an optimisation produces a perfect answer only within the context of

optimisation; this solution depends greatly on which changes are allowed (optimisation variables) and what is being optimised (objective function). Additionally, cheaper infrastructure is not necessarily better, with other factors such as the spatial requirements (as analysed in Section 6.6), the efficiency of the layout, and robustness to contingencies also playing a role.

6.2. Power-gas integration versus only reinforcement

Having highlighted some of the limitations of optimisations, and explored the existing layout, this next section contains an investigation into the effect of introducing gas-electricity sector coupling. This, and all remaining analyses use the existing infrastructure as a starting point.

For the gas-electricity integration, each 13 kV and 52.5 kV is made into a potential location for a conversion device, with a connection to the nearest gas city gate. At each of these 10 locations, candidate electrolysers and gas turbines are placed, and the capacities (if any) are determined during the optimisation as any continuous value.

One immediate result to note is that the combined cycle hydrogen turbines are not chosen in any of the four 2050 scenarios with the standard input values. This would be because hydrogen prices are usually higher than electricity prices, and with an efficiency of 58%, the loss in value by converting hydrogen to electric energy is even greater. Moreover, at 59,718 €/MW-yr, the investment cost for hydrogen turbines is quite high, and the optimisations show that this investment does not lower the overall costs (objective function) in any of the scenarios.

Table 6.4: Overview of results for reinforcement only, and power-gas integration in the Regional scenario.

			Reinforcement only		**Power-gas integration**	
	Units	Price (€/unit)	Quantity	Total (€)	Quantity	Total (€)
Grid reinforcement, annualised costs						
Transformers 150/52.5 kV	Transformer	177,132	7	1,239,921	4	708,526
Substations 150/52.5 kV	Substation	94,813	3	284,440	2	189,627
Transformers 52.5/13 kV	Transformer	73,075	19	1,388,421	16	1,169,196
Substations 52.5/13 kV	Substation	78,072	11	858,796	9	702,651
Cables 52.5 kV 43.6 MVA	km	23,222	207	4,802,356	167	3,888,245
Gas city gate expansion	MW	2,658	0	0	0	0
				8,573,934		**6,658,246**
Power-gas, annualised costs						
Electrolysers	MW	37,982	0	0	226	8,592,896
Cables to electrolysers 13 kV	MW km	1,229	0	0	125	154,010
Cables to electrolysers 52.5 kV	MW km	799	0	0	142.7	114,032
Switchgear for electrolysers			0	0		62,407
Gas turbines	MW	55443	0	0	0	0
				0		**8,923,345**
Import from higher grids, annual costs						
Power from national grid	MWh	50	506,717	28,520,927	1,373,233	75,790,793
Gas from national grid	MWh	90	165,414	15,688,580	29,238	2,578,889
				44,209,507		**78,369,682**
Sale to higher grids, annual revenue						
Power to national grid	MWh	50	890,720	28,348,157	254,368	7,631,043
Gas to national grid	MWh	90	0	0	990,975	68,458,455
				28,348,157		**76,089,498**

That being said, electrolysis is chosen in all of the scenarios, and could add valuable benefits to the system. Table 6.4 shows a summary of the costs made in the Regional scenario for new infrastructure in 2050, comparing the solution of reinforcement only to the one when electrolysis is also possible. Note that here, the costs of local generation and existing infrastructure are not included since these are fixed, and they are not affected by the inclusion of electrolysis.

As can be seen in Table 6.4, fewer grid reinforcement investments need to be made due to the introduction of electrolysis in the Regional scenario. This applies to transformers (both 150/52.5 kV and 52.5/13 kV), substations and cables. Note that the numbers in the table are rounded off for better overview, but more precision is used in calculations. The unit prices listed are based on Section 5.3.

In this scenario, a total of 226 MW_e capacity of electrolysers is installed throughout the modelled

region. These electrolysers require some additional cables between the substation and the closest gas city gate, as well as additional switchgear at the substation for these new connections. In terms of the annualised costs, the total amount spent on network reinforcement without electrolysis is €8,573,934 per year, and with electrolysis (including the cables and switchgear for electrolysers), it costs €6,988,695 per year. This leads to savings of €1,585,238 per year for the grid operator in terms of electrical network infrastructure in the Sterrenburg sub-network. In fact, this is a reduction of about 18.5% of the annualised infrastructure costs.

There are, however, also costs (and revenue) related to electrolysers themselves. As electrolysers are not yet present in utility grids at any substantial scale and given the uncertainty surrounding the energy transition, it is not yet known whether grid operators would be allowed to own electrolysers (since this involves participating in the competitive market to buy power and sell hydrogen). If the electrolysers are to be owned privately, there must be a financial incentive to do so. The potential business case for ownership of the electrolysers is explored in Section 6.2.2, along with why only limited conclusions can be drawn from this model.

Looking at Table 6.4 again, it can be seen that as expected, introducing electrolysers causes more power to be imported from the external grid throughout the year (an increase of almost 900 GWh), and less to be fed back into the external grid (a decrease of about 636 GWh), as this is used for conversion to hydrogen. Because of this, less hydrogen is purchased from the external grid (a decrease of 136 GWh), and 990 GWh of hydrogen is instead sold back to the national grid. Hourly prices for the exchange with the external grid are determined from the shadow prices derived from the power balance constraint, with the mid-level price of €50/MWh for electric power and €90/MWh for hydrogen. Overall, the region spends about €34 million more per year on importing energy (hydrogen and electric power combined), and gains €47 million per year in selling energy back to the external grid.

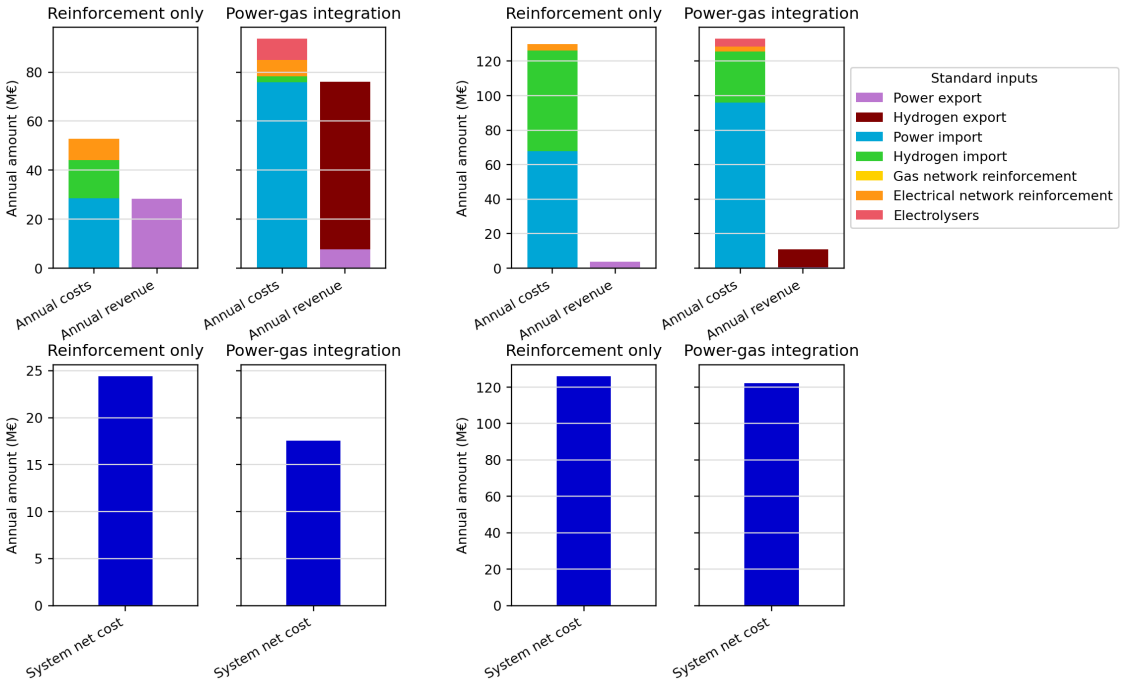

(a) Regional scenario

(b) International scenario

Figure 6.3: Comparison of total annualised costs and revenues for reinforcement and integration in the Sterrenburg sub-network area.

With reinforcement-only, the average electricity price per MWh in the Regional scenario is €45.57 and by including integration, the average electricity price rises to €50.29. The hydrogen price per MWh is observed to drop from €85.80 to €72.73. This shows the effect of electrolysers, which increase the electricity demand (and drive up the price) to subsequently provide hydrogen at a lower price than the external grid.

A visual summary of the annualised costs for network/conversion investments and energy trade with external grids is shown in Figure 6.3. The effect of introducing power-gas integration via electrolysers is compared to only reinforcing the energy networks for Regional and International scenarios. In brief, it can be seen that introducing power-gas integration decreases the network reinforcement costs and decreases the net system cost in both scenarios, which demonstrates that power-gas integration is financially beneficial. The system net costs, as plotted along the bottom of Figure 6.3, show the difference between the total annual investment and energy costs and the total annual revenue (from locally generated energy) for the Sterrenburg sub-network, i.e. a closer look at the difference between the costs and revenues plotted in the top half of the figure.

Note that within a scenario, the y-limits are shared for comparison, but they are different for the Regional and International figures. The overall system costs are higher for the International scenario because the emphasis in this scenario is on trade rather than regional self-sufficiency, such as through large offshore energy hubs. In this case, regions typically import energy from further away, and spend fewer resources on generating it themselves. Much more energy is imported into the region than exported. The net costs are lower in the Regional scenario since the region spends less on importing energy, and earns relatively more by selling back its surplus energy to the rest of the grid. In the Regional scenario, the introduction of electrolysis decreases the overall system cost by about €6.9 million; in the International scenario, this reduction is about €4 million.

Additionally, Figure 6.3 shows that in the International scenario, the role of hydrogen is bigger relative to electricity than in the Regional scenario, but hydrogen imports are substantially reduced in both scenarios by introducing electrolysers. Overall, the system net cost decreases for both scenarios by implementing power-gas integration.

For the International scenario, electrolysis has similar benefits of savings as in the Regional scenario. In this case, there is no difference in the 150/52.5 kV transformer and substation investments when electrolysis is introduced, but there are still savings in the 52.5/13 kV substations and electrolysers, and the 52.5 kV cables. When electrolysers are included, a total capacity of 122 MW_e is invested in. This leads to a cost reduction of €598,029 euros per year for the annualised cost of network reinforcements (including substation-city gate connections and switchgear for electrolysers). While these savings are smaller, the flows in the International scenario are also generally smaller and require fewer grid reinforcement investments than the Regional scenario. As a proportion, these grid investment savings arising from the inclusion of electrolysis are a 16.7% decrease compared to the reinforcement costs without electrolysis. The full table of the cost overview in the International scenario results is found in Table C.1 in the Appendix.

Next, in Section 6.2.1, a closer look is taken at the locations and capacities of electrolyser investments, and the hourly operation.

6.2.1. Electrolyser placement and operation

As mentioned, there are ten potential locations where electrolysers can be placed: five of which at 13 kV and the remaining five at 52.5 kV. Each of these locations has different characteristics such as electricity generation and demand profiles, distance to and capacity of the nearest city gate, and the hydrogen demand profile. Based on these and other factors (such as the remaining capacity for flows before new transformers and substations need to be invested in), the optimisation chooses:

(i) whether or not to invest in an electrolyser at a location,

(ii) how much capacity to invest in, and

(iii) how much power to convert to hydrogen at each hour.

13 kV buses are often preferred: this is where the cheap, local generation connects to first. Getting this energy to the 52.5 kV buses requires investing in the 52.5/13 kV transformers and substations. However, the investment costs of electrolysis are also offset by revenue from generating hydrogen, and it is preferable to operate at more hours (even when there is no surplus local generation). At times, the electrolyser also draws power from the external grid via the 150 kV connection. In this case, the 52.5 kV bus is preferred. Additionally, cables at 52.5 kV are cheaper (per MW) than at 13 kV, while

the switchgear at substations is more expensive at 52.5 kV. Some of these factors are explored by running the optimisation with different electrolysis costs, as shown in Table 6.5.

Table 6.5: Investigating the preferred locations in the Regional scenario for electrolyser investments in MW when modelling different electrolyser-related costs.

Location	**Voltage**	**Only identical electrolyser costs**	**Electrolysers and cable costs**	**Electrolysers, cables and switchgear**
Sterrenburg	13 kV	0.00	0.00	0.00
Oud-Beijerland	13 kV	57.08	24.84	24.84
Dordtse Kil	13 kV	20.79	20.79	20.79
's Gravendeel	13 kV	18.03	0.00	18.03
Klaaswaal	13 kV	34.54	32.68	34.46
Sterrenburg	52.5 kV	39.35	39.29	39.29
Oud-Beijerland	52.5 kV	0.00	32.21	32.21
Dordtse Kil	52.5 kV	56.63	56.63	56.63
's Gravendeel	52.5 kV	0.00	18.03	0.00
Klaaswaal	52.5 kV	0.00	1.81	0.00

In Table 6.5, the first column shows the locations and voltage levels where electrolysers can be placed. The next three columns show optimisation results for including electrolysers as options in the Regional scenario, but with different cost compositions. Larger values have a deeper yellow background to aid comparison.

First, the location preference is tested by setting the cost of electrolysers at each location to the same value (37,982 €/MW-yr), i.e., leaving out the location-specific cost of cables and switchgear. Here, the preference for 13 kV is clear, with all investments spread over the 13 kV investments except for 2.88 MW at the 52.5 kV Sterrenburg bus. In the next column, cable costs are included (as the distance from the substation to the nearest city gate times 533 €/MWkm-yr for 52.5 kV and 819 €/MWkm-yr for 13 kV, with a factor of 1.5 for redundancy). This makes it more expensive to place electrolysers at 13 kV than at 52.5 kV, and to place them at locations which are further from the closest gas city gate (this distance is greatest at Klaaswaal and Sterrenburg). The effect of this is that some of the electrolyser capacity is shifted to the 52.5 kV buses, for which the lines are cheaper (per MW). Finally, in the last column, some of this shift is reversed because of the inclusion of switchgear costs, which are higher at 52.5 kV (10,190 €/yr for a discrete investment of 50 MVA capacity) than at 13 kV (1,804 €/yr for a discrete investment of 10 MVA capacity).

Notably, the amount invested in electrolysers at each location varies slightly with these three cost compositions, but the total capacity of electrolysers (226 MW) remains the same for the scenario. At Dordtse Kil and Oud-Beijerland, the invested capacities of electrolysers are quite high at both 13 and 52.5 kV, which could be because the hydrogen demand is relatively high at these locations. Additionally, for all cost compositions, there is no electrolysis at Sterrenburg's 13 kV bus, and consistently about 39 MW at the 52.5 kV bus. This is probably because the electrical demand at Sterrenburg is quite high relative to the local generation, making it more attractive to place electrolysers closer to the external grid at this location.

This highlights how many factors are being traded off against each other in the placement and sizing of electrolysers: the proximity to cheap renewable energy sources, the capacity and demand for hydrogen, the cheaper cables but more expensive switchgear at 52.5 kV compared to 13 kV, the availability of power from the external grid when there is no local surplus production, distance to the nearest city gate, and the need for 52.5/13 kV transformers.

Next, the hourly operation of the electrolysers is looked into. The operation is determined by the optimisation, which means that the optimiser chooses how much power to convert to hydrogen at each location, and at each hour. It is observed that the electrolysers are typically off (no conversion) or near full capacity. The capacity factors of the electrolysers in the Regional scenario vary between 0.5 and 0.55 (the total production in the year divided by the production of running at full capacity the whole year). Figure 6.4 shows a period of 24 hours at the Oud-Beijerland area in the Regional scenario. The electrical and hydrogen demand, electrical generation and electrolyser operation are plotted in subplots with the same y-limits (which are different between the winter and summer figures). The electrolysers have a total electrical capacity of 57.05 MW_e, which at full capacity produces 42.8 MW

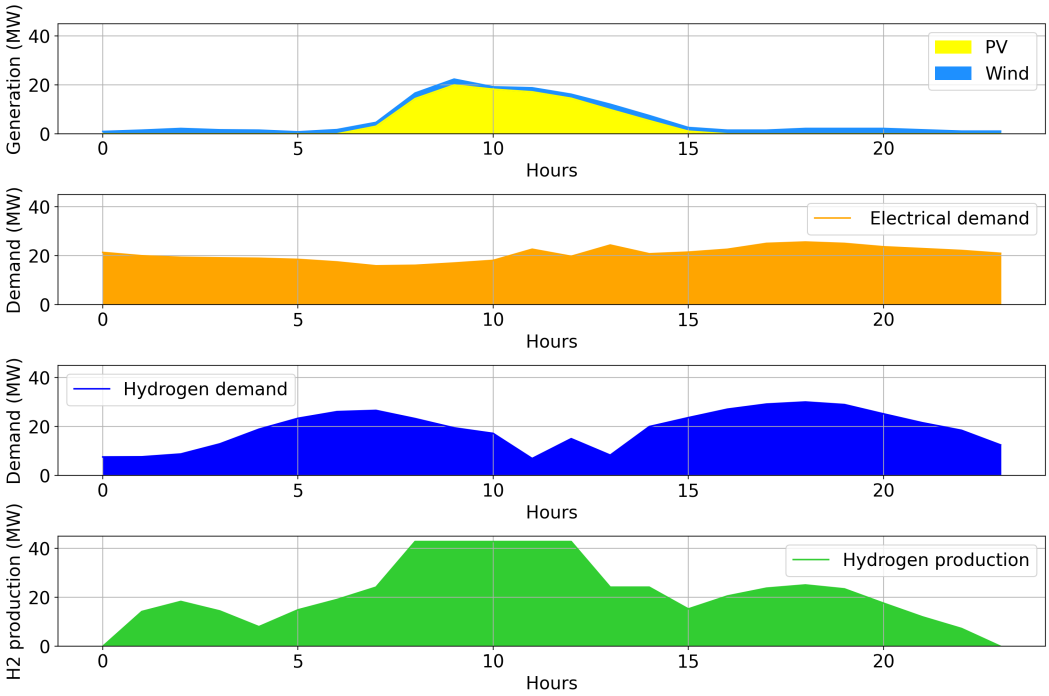

Figure 6.4: Hourly demand and supply values for a winter day in the Regional scenario at Oud-Beijerland showing electrolyser operation.

of hydrogen due to the 75% efficiency.

In Figure 6.4, the operation of the electrolyser (the green plot on the bottom of the figure) appears to be influenced by two main factors: the availability of cheap electrical energy, and the demand for hydrogen. From the two plots on top, it can be seen that the local renewable electricity generation exceeds the electrical demand around the middle of the day, and at this time the electrolysers also produce at full capacity. Towards the end of the day (between the 15th and 20th hour approximately), the hydrogen production instead follows the demand profile.

Introducing electrolysers in the Regional scenario decreases the necessary number of transformer reinforcements at Sterrenburg (150/52.5 kV), Dordtse Kil, Klaaswaal and Oud-Beijerland (52.5/13 kV each). This happens because the electrolyser can decrease the net amount of power flowing back into the grid, especially at peak times. This effect is illustrated for a 7-day period at the Oud-Beijerland location in Figure 6.5. As seen in the figure, without electrolysers, the net generation (total electrical generation minus electrical demand) without electrolysers peaks at almost 90 MW within the plotted hours. When electrolysers are included, their extra demand causes these peaks to be levelled off and not exceed 65 MW.

To take a broader look at the effect during the whole year, a load duration curve (LDC) is plotted at the 150 kV bus at Sterrenburg, by sorting the hourly values for the net flows modelled. Here, a positive value means there is net electrical demand in the Sterrenburg sub-network, and negative values indicate net electrical generation. The 504 hours are the 21 representative modelled days. The graph shows that without electrolysers, there is a peak for net demand at around 200 MW, and the peak net generation is nearly 800 MW (a remarkably large amount). With electrolysers in the system, this LDC is effectively shifted up (in the direction of net demand) such that the net demand peaks at 400 MW and the net generation also peaks slightly over 400 MW. This indicates a more efficient use of the infrastructure. That being said, electrolysers are limited in that they can only increase the demand for electricity at a given location, so in a case where net demand is the reason for extra reinforcement requirements, electrolysers cannot contribute to reducing the electrical infrastructure requirements.

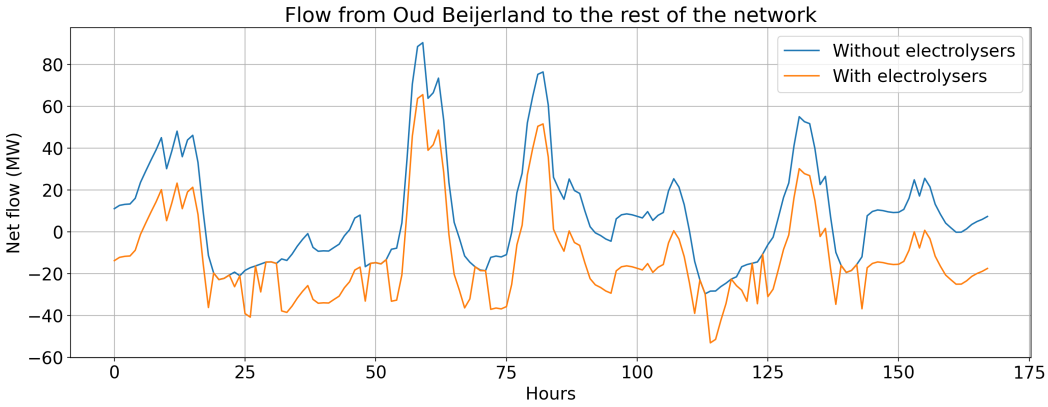

Figure 6.5: Hourly net generation at Oud-Beijerland for 7 days with and without the presence of electrolysers.

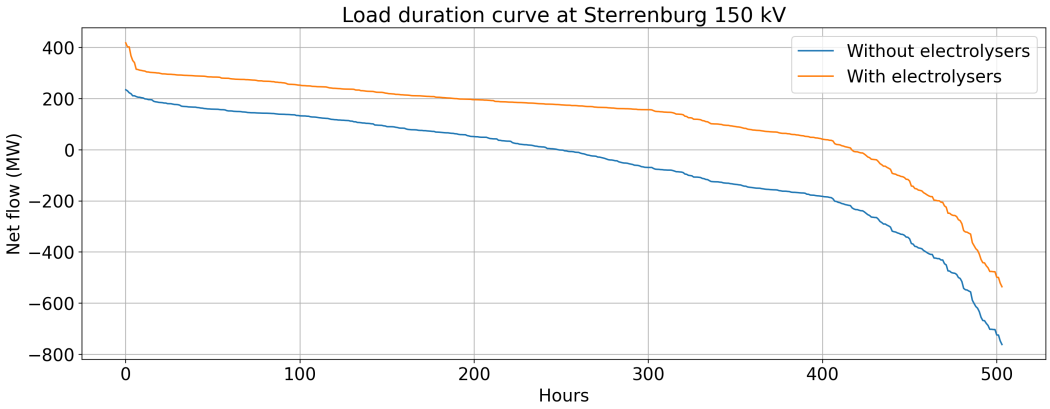

Figure 6.6: Load duration curve at the 150 kV bus in the Regional scenario, with and without electrolysis.

6.2.2. Business case electrolysis ownership

For estimating the viability of the business case for electrolysis ownership, the following costs are taken into account: fixed (OPEX + CAPEX) annualised electrolyser costs, land costs, electrical power input cost, fees for the electrical grid connection between the substation and gas city gate, and finally the revenue from selling hydrogen. Note that this evaluation is likely to give a more pessimistic outlook due to the likely over-estimations of the hourly electricity price and the annual grid connection payments, as will be discussed.

Firstly, there are several costs when requesting a new grid connection. These include a fixed one-time cost per connection (*eenmalige aansluitvergoeding*), an additional one-time fee per meter (*tarief meerlengte*), periodic costs (*periodieke aansluitvergoeding*), additional length-based periodic costs, and recurring transport costs (*transportvergoeding*) based on peak and actual usage. The one-time connection costs in this analysis are annualised for a period of 100 years. While the transport costs are normally dominant among the recurring costs, they are left out of this analysis – if the grid operator owned the electrolysers, it would not pay these costs to itself, and if the electrolysers were privately owned, the owners could possibly be exempted from paying these if their electrolysers contribute to a reduced need overall for infrastructure. The one-time and periodic costs are included, however, as they reflect actual costs made for the infrastructure of the connections.

The costs for the grid connections are based on the 2021 Stedin tariffs for large electricity connections [117]. This is, however, slightly complex. Typically, connections of more than 10 MVA are connected at 52.5 kV, while the smaller connections are placed at 13 kV. Yet, in the optimisation (and considering the resulting reduction in network reinforcement requirements), it is beneficial to have more than 10 MVA at 13 kV buses. Therefore, the connection costs for these are calculated as

multiple connections in one location if the capacity at 13 kV exceeds 10 MVA at 13 kV or 50 MVA at 52.5 kV.

The same costs are used at 13 kV and 52.5 kV, as the costs listed online are only for those up to 10 MVA. This is expected to be an overestimate (especially at 52.5 kV), since the prices listed are for connections up to 10 MVA, and for higher capacities the costs are "custom", i.e. lower (per MVA). At each of the 10 (two voltage levels, at five substations) locations, the cost for each $\leq$ 10 MVA connection is calculated based on the optimal electrolyser capacities chosen. This includes a one-time cost of €290,000 + €382 per meter, annualised for 100 years, and the annual fee of €8,360 + €6.35 per meter (with slightly different costs for connections less than 3 MVA). For more details, see [117]. The costs of these connections are added up and listed under "grid connections" in the business cases.

The other issue is determining the market price at each hour for hydrogen, and especially for electricity. The electrolyser operation is seen to coincide with the availability of (low-cost) locally generated power. However, calculating the cost of power for the electrolysers is not straightforward. As mentioned in Section 2.5, the short-run marginal cost price bids may not be a desirable auctioning structure in a market with a high penetration of near-zero marginal cost renewable generation. This is nevertheless used for the cost in this optimisation, leading the optimiser to understand that the energy of the local renewable generators is available at this price. In reality, at moments of excess renewable generation (for example, on a windy summer day), the merit order effect would cause the market price to equal the marginal cost of the last dispatched generator, which would likely be one of the cheap renewable generators. However, in this work, the local renewable generation is not dispatchable since the generation profiles are exogenous and must be dispatched. The market price (determined from the shadow price) is therefore equal to that of one of the dispatchable generators, i.e. one of the three external price level bids. This is not only a very limited range, but the lowest bid of €30/MWh is likely also an overestimate for times of abundant renewable energy generation, considering the marginal prices for PV and onshore wind generation are €1.28 and €2.22/MWh respectively. Even a different bidding mechanism, such as the levelised cost of energy (LCOE), would result in lower costs (€10.42 and €19.83/MWh) if these were the last dispatched resource as is expected at times of abundant renewable generation.

Table 6.6: Overview of annual costs and revenue for the electrolysis system.

(a) Regional scenario

Category	**€/year**	**€/year**
Power	70,029,113	
Electrolysis fixed	8,592,896	
Grid connections	1,203,742	
Land cost	34,008	
Total costs	**79,859,758**	
Hydrogen revenue		**79,215,474**
Net revenue		-644,284

(b) International scenario

Category	**€/year**	**€/year**
Power	30,625,932	
Electrolysis fixed	4,606,761	
Grid connections	785,652	
Land cost	18,232	
Total costs	**36,036,577**	
Hydrogen revenue		**34,372,552**
Net revenue		-1,664,025

Keeping these limitations in mind, the business case for electrolysis as determined from this model is presented in Table 6.6 for the Regional and International scenarios. In the Regional scenario, the costs and revenue are substantially higher than in the International scenario; this is because more electrolysis is chosen in this scenario (226 MW_e compared to 121 MW_e). For both scenarios, the business case as calculated comes out slightly negative, i.e., not enough (financial) incentive for private ownership of the electrolysers.

However, the outlook is better in the Regional scenario: the hydrogen revenue is enough to cover the electrolyser, land and power costs, and with a partial discount on the grid connection cost, (at least €644,284 per year out of the €1,203,742 per year), there could be sufficient incentive for financial ownership. Offering this discount would still be attractive for the grid operator, since in the Regional scenario, €1,585,238 is saved annually on grid infrastructure by including electrolysers. The same does not apply in the International scenario: even without the grid connection costs, the costs are greater than the revenue. Since the power costs are dominant among all the costs, it could still be that a more complex market model for calculating the hourly electricity price would result in a profitable

business case.

Some of the main limitations of the expansion planning model, especially in terms of evaluating operational profitability, are mentioned below:

(i) Since the local generation is fixed (not dispatchable), the calculated shadow electricity prices are only in the range of the external, dispatchable bids (which are substantially higher than the marginal renewable cost of generation).

(ii) Bidding in the competitive energy market with short-run marginal costs might not be an ideal approach in the future energy system, but even a different approach like LCOE would lead to lower electricity prices at times of abundant renewable generation than currently in the model.

(iii) Since the electrolysers are dispatchable, these are often the units which set the hydrogen prices (which might be realistic if the same effect is happening throughout the country, but contradicts the competitive market assumption of being price-takers).

(iv) The demand for both electricity and hydrogen is price-elastic (due to the three price levels), unlike the local (perfectly inelastic) demand.

(v) The expansion planning optimisation leads to a reduction of a combination of investment and operational costs, but does not promote profitability (or even explicitly model it).

This shows that for a quantitative analysis of the business case for electrolysers, it would be better to develop a separate operational model with more complex bidding and market mechanisms, and a profitability objective (based on the capacities from expansion planning models like this work's model). Nevertheless, the (limited) business cases are shown here as a tentative indication of financial viability.

To conclude, this analysis demonstrates that in the Regional scenario, electrolysis ownership by the grid operator is financially viable, and private ownership could still be beneficial for both the owner and the grid operator if there are certain exemptions on the grid connection payments. The International scenario does not have a positive business case outlook, but more realistic methods of calculating the electricity prices, and a different profit-oriented operational optimisation are likely to result in a more positive business case. In all cases, the infrastructure costs saved by introducing the electrolysers outweigh the costs of electrolyser connections, which means that including electrolysers is financially beneficial for the grid operator.

6.3. Electrical storage

The limitations of the selection of representative time slices for the energy system with storage units make quantitative comparisons with the optimisation results less insightful, as explained in Section 4.5.1. Nevertheless, using the 12 representative weeks instead of the 21 (more) representative days for the 2050 scenarios, the expansion planning optimisation is carried out for the Sterrenburg sub-network case with energy storage as an option in the formulation. The potential energy storage locations are at the same 52.5 and 13 kV electrical buses where electrolysis is investigated. At each of these locations, 4-hour electrical energy storage systems (based on lithium-ion battery projections at utility scale for 2050, see Table 5.7) are included in the optimisation formulation, and their size can be freely determined by the optimiser (as a continuous variable).

Table 6.7 shows the planning results for the Regional scenario, for both reinforcement-only and with storage. Note that the reinforcement-only results are different from when 21 representative days are used (see Table 6.4). The main difference is that one additional 52.5/13 kV transformer is placed at Klaaswaal in the 12-week input, and that the energy exchange (volumes and costs) with the external grids are slightly different. For this reason, the results of the storage optimisation are compared to the reinforcement-only formulation which uses the same scenario inputs (and these results are not directly compared to reinforcement-only from the 21 representative days).

From Table 6.7, it is evident that allowing the inclusion of energy storage as formulated in this model does not have a significant impact on the outcome. A total capacity of 2.66 MW of battery storage is chosen (located at the 13 kV bus at Klaaswaal), which leads to one fewer 52.5/13 kV

Table 6.7: Overview of results for reinforcement only, and electrical storage integration in the Regional scenario.

			Reinforcement only		**Storage integration**	
	Units	Price (€/unit)	Quantity	Total (€)	Quantity	Total (€)
Grid reinforcement, annualised costs						
Transformers 150/52.5 kV	Transformer	177,132	7	1,239,921	7	1,239,921
Substations 150/52.5 kV	Substation	94,813	3	284,440	3	284,440
Transformers 52.5/13 kV	Transformer	73,075	20	1,461,495	19	1,388,421
Substations 52.5/13 kV	Substation	78,072	11	858,796	11	858,796
Cables 52.5 kV 43.6 MVA	km	23,222	207	4,802,356	207	4,802,356
Gas city gate expansion	MW	2,658	0	0		0
				8,647,008		**8,573,934**
Storage, annualised costs						
Batteries	MW	57,690	0	0	2.66	153,455
				0		**153,455**
Import from higher grids, annual costs						
Power from national grid	MWh	50	526,413	29,830,705	524,789	29,690,726
Gas from national grid	MWh	90	165,414	15,987,027	165,414	15,987,027
				45,817,732		**45,677,753**
Sale to higher grids, annual revenue						
Power to national grid	MWh	50	910,417	28,831,521	908,141	28,783,360
Gas to national grid	MWh	90	0	0		0
				28,831,521		**28,783,360**

transformer being necessary (also at Klaaswaal) compared to reinforcement-only. In terms of infrastructure costs, the grid operator saves €73,075 per year, while the annual costs of the battery are in fact greater: €153,455. The costs of the battery are to some extent offset by its operation; the operation is explored in Figure 6.8 and its accompanying discussion. In terms of energy exchange with the external grid, there is a slight reduction in both power drawn from and supplied back to the external grid throughout the year. Compared to reinforcement-only, €139,979 is saved on importing power, and €48,161 of revenue from exporting power is lost on an annual basis. On the system scale of the whole case, all these differences are minor.

Looking at Figure 6.7, there is no noticeable visible difference between the outcomes of the reinforcement-only formulation and the inclusion of batteries. This is because the differences due to including batteries are present (see Table 6.7), but small compared to the total costs and revenues in the year. This applies to both the Regional and the International scenarios. Similar to the Regional scenario, in the International scenario only 2.25 MW of electrical storage is installed in the outcome which allows batteries, with minor effects at a system scale. For more detailed results, see Table C.2 in the Appendix.

Figure 6.8 shows hourly plots throughout a week (168 hours) of the Regional scenario to illustrate the hourly operation of the battery at the 13 kV bus at Klaaswaal. There are four plots: the topmost plot shows the hourly generation (PV and wind, with no CHP) and electrical demand from the scenario, aggregated at the 13 kV bus for Klaaswaal. The next plot shows the net electrical generation, which equals the sum of electrical generation minus the electrical demand. In the week plotted, there is (positive) net generation for most of the hours, with peaks of around 250 MW generation surplus, and a power deficit only for a few hours in the week. The third plot shows the hourly charging (positive) and discharging (negative) of the battery. The battery tends to charge or discharge briefly at full power (2.66 MW), and is inactive in the remaining hours. As a 4-hour battery, the energy capacity of the 2.66 MW battery is 10.64 MWh. The fourth plot of Figure 6.8 shows the state-of-charge (SoC) of the battery throughout the week. The plot shows that there is a tendency towards one charging/discharging cycle per day, and that there is a correlation between the net generation at the bus and the battery's state-of-charge. Additionally, the cyclic charge constraint (see Section 4.3.3) is seen to be satisfied, such that the last hour of the week has the same SoC which allows for the simulation of disconnected weeks as a single time series.

As might be expected, when there is a large electric energy generation surplus, the battery tends to charge, and conversely the battery discharges when there is less generation with respect to demand. This shows that despite the minor effect (of the 2.66 MW battery with a bus that has power flows in the order of hundreds of MW), having larger battery capacities present could help with peak shaving and load shifting, which would reduce the overall network infrastructure requirements. Different

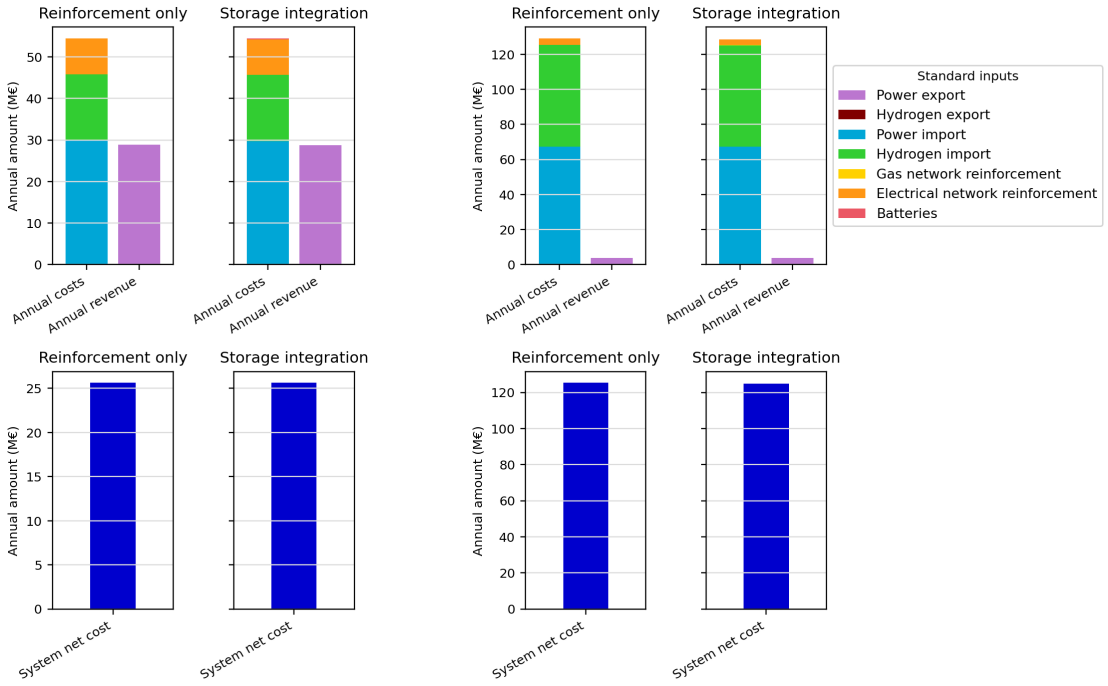

(a) Regional scenario

(b) International scenario

Figure 6.7: Comparison of total annualised costs and revenues for reinforcement and storage integration in the Sterrenburg sub-network area.

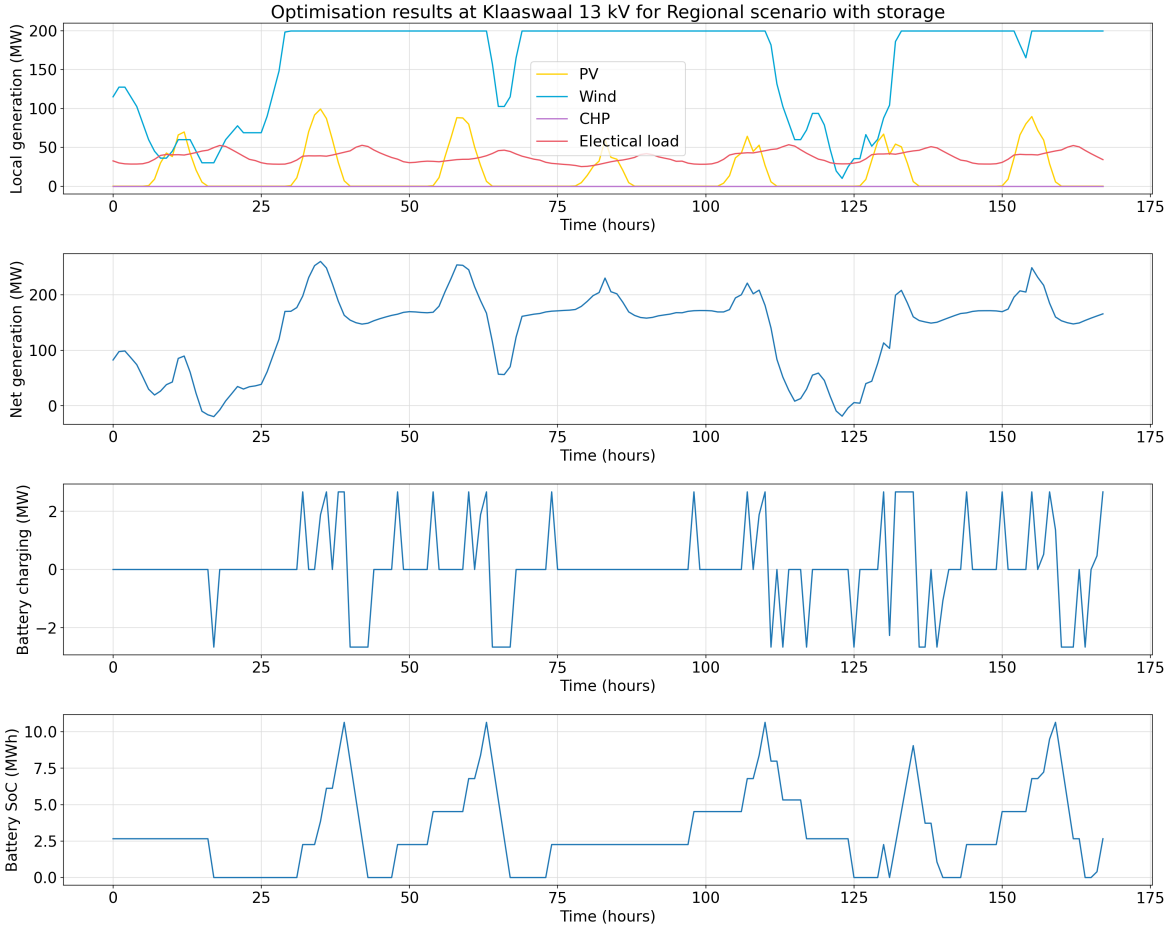

Figure 6.8: Illustration of the hourly operation of a battery for a week in the Regional scenario.

battery formulations (e.g., other technologies, power/energy ratios and long-term storage) could be explored in future work.

6.4. Sensitivity analysis

The sensitivity analysis is carried out to investigate the effect of changes in a selected number of important and uncertain parameters. All inputs remain at the standard values, except for one which is varied. The optimisation is then run, with the effects reflecting the sensitivity to the parameter which has been changed. These results are presented for changes in electricity price, hydrogen price, electrolyser cost, gas turbine cost and battery cost. Summaries of these results are provided in the following sections, and more detailed results are found in Appendix D. As discussed in Section 6.2.2, this model is not ideal for evaluating the operational business case of electrolysis ownership, but these analyses are still included as some indication of the financial aspects of the solutions.

6.4.1. Electricity price

First, changes in electricity prices are investigated by changing the prices which the external market dispatchable loads and generators bid at the 150 kV level. The standard central bid of 50 €/MWh is increased and decreased by 50%. When the price is decreased, the low/mid/high level bids are 15/25/35 €/MWh respectively, and for an increase in 50% these bids are 45/75/105 €/MWh. Changing the electricity price has an effect on the amount spent on trading with the external grid, and also affects the gas-electricity grid integration decisions. For this reason, both the reinforcement-only and the power-gas integration optimisations are run for the altered electricity price values and compared.

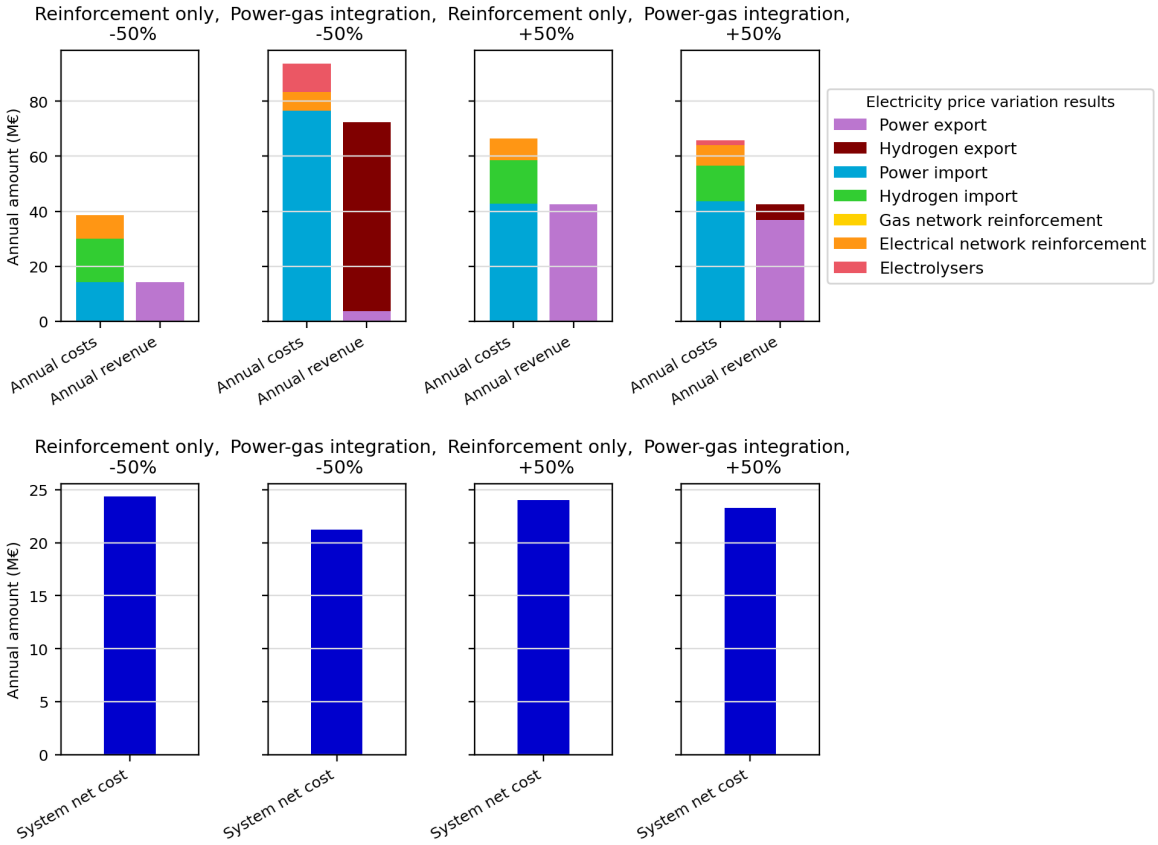

Figure 6.9: Sensitivity of annualised costs and revenues to electricity price in the Regional scenario.

Figure 6.9 shows a visual overview of the investment and external market trading costs and revenues for this sensitivity analysis. Looking at the reinforcement-only graphs, the effect of changing the

electricity price is straightforward: decreasing the price means that less money is spent on importing electric energy (light blue) and less money is earned by exporting it (purple). The effect on electrolysis qualitatively also aligns with what could be expected: cheaper electricity makes electrolysis more favourable, and leads to an increase in the capacity of installed electrolysers. This is confirmed by the power-gas integration graphs, where the red portion of the bars indicates the annualised cost of electrolysers in the system. Here, it is notable that electrolysers are still chosen when the market price is increased by 50%: a total of 49 MW_e. This is less than a fifth, however, of the amount chosen for cheaper electricity (275 MW_e). Hydrogen turbines are still not included in any of the optimal solutions. Furthermore, when the electricity price is decreased, the amount of electricity purchased from the external grid increases greatly (due to the electrolysers), and this also causes more hydrogen to be supplied back to the external grid. The detailed results are found in Table D.1 in the Appendix comparing the power-gas integration solutions for the changes in electricity price. For reinforcement-only, everything remains the same (investments and quantities traded) as the standard inputs for reinforcement-only. The changes in prices of trading with the external grid are shown for reference in Table D.3 of the Appendix.

Table 6.8: Overview of electrolyser-related costs when varying the electricity price by 50%.

(a) Electricity price -50%

Category	**€/year**	**€/year**
Power	68,786,034	
Electrolysis fixed	10,385,190	
Grid connections	1,488,847	
Land cost	41,102	
Total costs	**80,701,173**	
Hydrogen revenue		**79,829,222**
Net revenue		-871,951

(b) Electricity price +50%

Category	**€/year**	**€/year**
Power	6,994,198	
Electrolysis fixed	1,864,916	
Grid connections	318,986	
Land cost	7,381	
Total costs	**9,185,481**	
Hydrogen revenue		**8,236,640**
Net revenue		-948,841

For both an increase and decrease of electricity price, the inclusion of power-gas integration still leads to a (slight) decrease of net system cost compared to reinforcement-only. Moreover, even with the electricity price increased by 50%, the inclusion of electrolysers still decreases the overall grid infrastructure costs. When the electricity price is reduced, the large capacity of electrolysers causes the electricity grid to need slightly more infrastructure than the standard electricity price, but this still leads to an annual grid infrastructure cost reduction of €1,453,507 compared to the reinforcement-only solution. When the electricity price is higher, electrolysis is less favourable, but the savings are still €1,056,950 per year for electrical infrastructure. In both these cases, these savings are greater than the "loss" implied by the business case evaluations in Table 6.8. As mentioned, the electrolyser operation is likely to be more profitable than implied by this analysis, meaning that they are still financially beneficial for the grid operator and for private ownership (dependent on grid fee exemptions), regardless of a 50% deviation in electricity price.

6.4.2. Hydrogen price

The effect of a different hydrogen price is also investigated, by changing the bid levels of the external market buyers and sellers at each city gate. The original central bid of 90 €/MWh is varied by 50% resulting in decreased low/mid/high level bids of 36/45/54 €/MWh respectively, and increased bids of 108/135/162 €/MWh. A summary of the results for reinforcement-only compared to power-gas integration is shown in Figure 6.10. Again, hydrogen turbines are not chosen in any of the variations. Furthermore, when the hydrogen price is decreased by 50%, electrolysis is no longer favourable. In this case, the reinforcement-only and power-gas integration solutions are identical. It can be seen that less money is spent on importing hydrogen from the external grid (green) in these solutions. When the hydrogen price is increased, the reinforcement-only solution includes higher hydrogen import costs, which also drive up the system net cost. However, when electrolysis is allowed, a large capacity of electrolysers (303 MW_e) is chosen, as it is clearly favourable to produce and sell hydrogen. In fact, in this solution, no hydrogen is imported from the external grid throughout the year, with all the local consumption being supplied by local electrolysers, and the surplus of the electrolyser output sold back to the external grid.

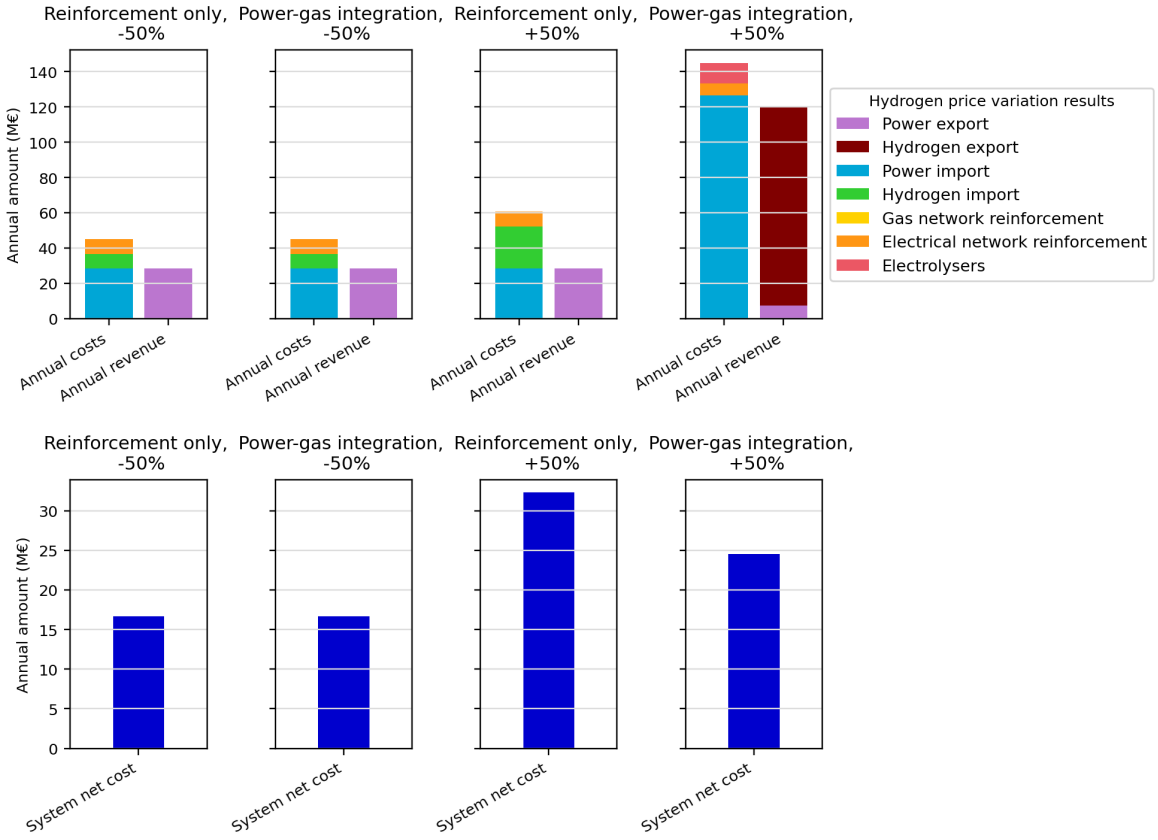

Figure 6.10: Sensitivity of annualised costs and revenues to hydrogen price in the Regional scenario.

When the price of hydrogen is lowered by 50%, there are clearly no infrastructure savings compared to reinforcement-only, since no sector coupling solutions are chosen in this case. However (see Table D.2 in the Appendix for details), including electrolysers once again leads to a reduction in the necessary grid infrastructure, and overall savings of €1,067,795 per year for the DSO. When evaluating the business case for this solution, however, the "loss" of electrolysis in Table 6.9 is greater than these savings. Nevertheless, it is expected that a profit-oriented operational optimisation would, in fact, show electrolyser ownership in this case to be profitable due to the high price of hydrogen.

Looking at the variations in net system cost and at the variations in installed electrolyser capacity, it can be concluded that the expansion planning algorithm is more sensitive to changes in hydrogen price than it is to changes in electricity price. Nevertheless, both of these can have a major impact on the investment decisions.

Table 6.9: Overview of electrolyser-related costs when increasing the hydrogen price by 50%.

Category	**€/year**	**€/year**
Power	117,544,928	
Electrolysis fixed	11,510,027	
Grid connections	1,633,001	
Land cost	45,553	
Total costs	**130,733,509**	
Hydrogen revenue		**129,352,425**
Net revenue		-1,381,084

6.4.3. Electrolyser cost

With the hydrogen and electricity price restored to their standard values, changes in the electrolyser prices are investigated. The costs of cables and switchgear for connecting electrolysers to the grid are assumed to remain the same; instead the annualised fixed cost of electrolysers (OPEX + CAPEX) is varied by 25%, with a reduced annualised cost of 28,486 €/MW_e and an increased cost of 47,477 €/MW_e. The optimisation results are relatively insensitive to changes in electrolysis price: for the reduced price, a total of 228.89 MW_e of electrolysers are invested in within the Sterrenburg sub-network, while for the higher price, the capacity of electrolysers falls to 224.93 MW_e. This means that the difference in the electrolyser capacity varies by less than 2% for a difference in fixed electrolyser costs of 50%. The results of the optimisations are summarised in Figure 6.11. For reinforcement-only, the costs are not affected by the electrolyser price, while in the following two plots, the red bar (electrolyser cost) is seen to be smaller for the lowered cost, and bigger for the increased electrolyser cost. More detailed results are found in Table D.4 in the Appendix.

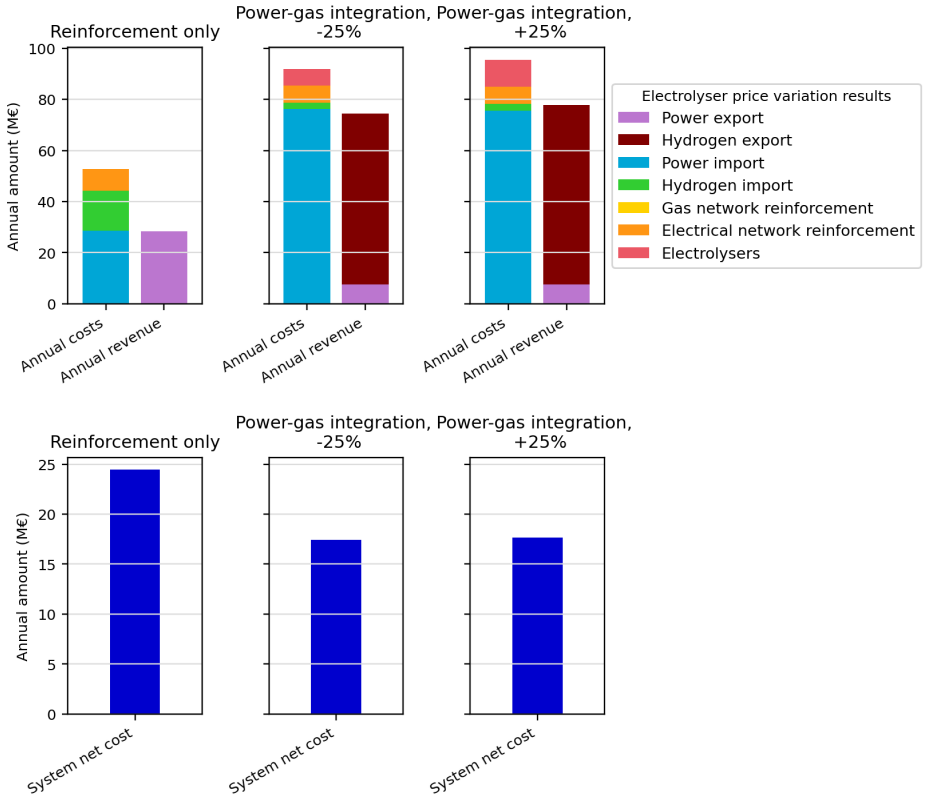

Figure 6.11: Sensitivity of annualised costs and revenues to electrolyser cost in the Regional scenario.

Remarkably, the system net cost is nearly the same for power-gas integration, regardless of the difference in electrolysis cost. The same is also reflected in the business cases shown in Table 6.10. Here, the input power cost is slightly less for the more expensive electrolysers (which also have

Table 6.10: Overview of electrolyser-related costs when varying the electrolyser cost by 25%.

(a) Electrolyser cost -25%

Category	**€/year**	**€/year**
Power	70,466,358	
Electrolysis fixed	6,517,597	
Grid connections	1,223,928	
Land cost	34,394	
Total costs	**78,242,277**	
Hydrogen revenue		**77,579,940**
Net revenue		-662,337

(b) Electrolyser cost +25%

Category	**€/year**	**€/year**
Power	69,786,300	
Electrolysis fixed	10,678,574	
Grid connections	1,174,518	
Land cost	33,810	
Total costs	**81,673,203**	
Hydrogen revenue		**81,074,762**
Net revenue		-598,441

a slightly smaller capacity). However, the revenue is substantially larger for the more expensive electrolysers, which balances out their higher investment costs. This could be traced back to the objective function and highlights why the model is suitable for expansion planning, but not ideal for planning or evaluating (profit-based) operation. Looking into the trading prices and capacity factors provides some more insight.

The goal of the optimisation is to minimise the objective function. Including electrolysers will increase the objective due to the investment costs for electrolysers, but it will decrease the objective function by i) avoiding grid-reinforcement investments and ii) decreasing the (generation) costs of drawing energy from the external grid and iii) increasing the sales to the external grid (this term is negative, so increased sales will achieve a decrease the objective function). The optimisation is a trade-off between all the terms in the objective; an investment will be made even if it increases a part of the objective function, if this leads to an overall reduction in the objective.

Looking broadly at the capacity factors of the electrolysers for the solutions with different prices, it is seen that the more expensive electrolysers have higher capacity factors (by a small amount, around 1%). Specifically, these electrolysers seem to be running even at some hours when electricity is expensive: the average hydrogen price per MWh throughout the year increases from €71.30 for the cheaper electrolysers to €74.19 with the more expensive electrolysers. This implies that the expensive electrolysers also run at some hours using the €70/MWh electricity bid (which with 75% efficiency results in a marginal hydrogen price of €93/MWh). The cheaper electrolysers tend to stop more often with the €50/MWh electricity bid, with a marginal hydrogen cost of €66.67/MWh, as demonstrated by the lower average hydrogen cost. The average electricity price between the two solutions is quite similar (50.30 €/MWh for the cheaper electrolysers and 50.29/MWh for the more expensive electrolysers). This demonstrates that the optimisation uses the electrolysis higher costs and (even higher) revenue to offset the higher investment costs for electrolysis, in a complex trade-off which also includes a slight reduction in total electrolysis capacity.

Nevertheless, this again highlights that profit is not an explicit objective (or even a variable) in the optimisation, and a profit-oriented optimisation with the same capacities as in this optimisation would likely result in a more positive business case (along with higher hydrogen prices), along with a different operational and bidding strategy. Power-gas integration by means of electrolysis clearly and consistently decreases the net system costs, but ownership, cost distribution and operational strategies need to be looked into further.

6.4.4. Gas turbine cost

When the costs of gas turbines were decreased and increased by 25% to 41,582 and 69,304 €/MW respectively, there were no changes in the results, i.e., no gas turbines were chosen. Even in the International scenario, the change in gas turbine cost is not enough incentive for it to be invested in. Since this has no effect on the outcome, no further results are presented from this analysis.

6.4.5. Battery cost

The sensitivity analysis for battery cost is carried out using the selection of 12 representative weeks as explained in Section 4.5.1. Using these inputs, the analysis is carried out for the Regional scenario while varying the cost of the batteries. Based on the low and high projections for utility-scale lithium-ion batteries in 2050 from [8], the annualised battery investment cost is decreased by 43.6% and increased by 40.4% while keeping the remaining parameters constant. Figure 6.12 shows a visual summary of the total costs and revenues for these different formulations, as well as for the reinforcement-only approach for the Regional scenario.

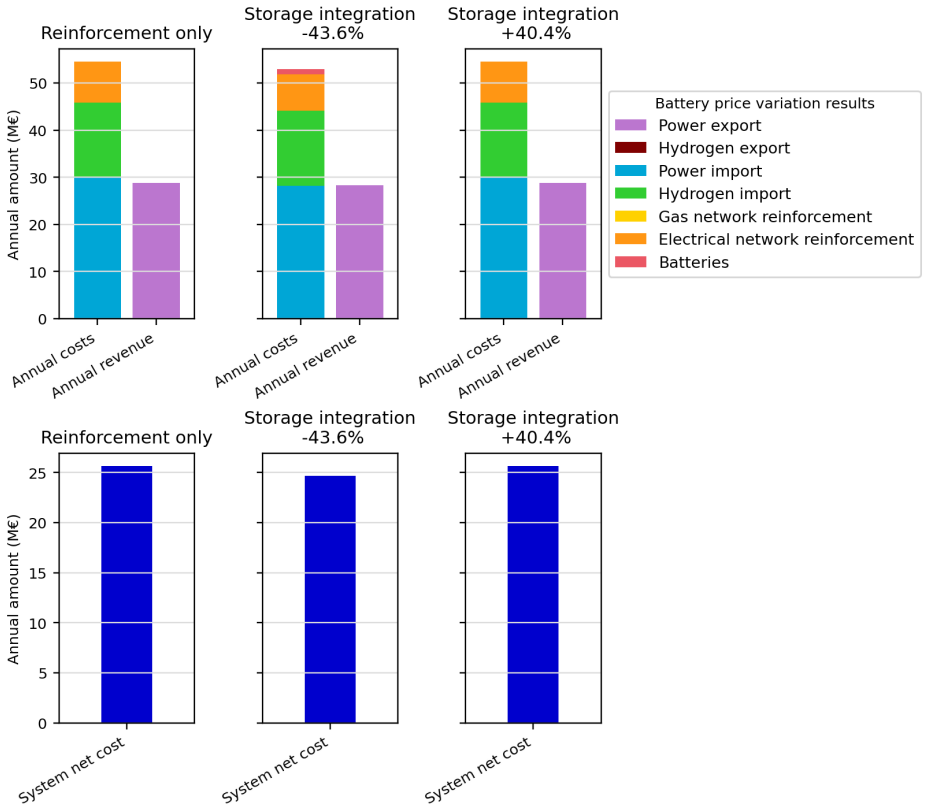

Figure 6.12: Sensitivity of annualised costs and revenues to battery cost in the Regional scenario.

While more detailed results are found in Table D.5 in the Appendix, Figure 6.12 shows that a decrease in battery price by 43.6% leads to the inclusion of batteries (red part of the bar plot), accompanied by lower grid reinforcement costs (orange). In fact, these results include a total installed battery capacity of 35.1 MW in the case region. This results in one fewer 150/52.5 transformer (and corresponding substation) being needed, and also one fewer 52.5/13 kV transformer. However, considering the sizeable decrease (43.6%) in price, the overall effect is modest as can be seen in Figure 6.12. The decrease in net system cost is about €0.95 million per year with the inclusion of storage, compared to reinforcement-only. The savings arise from lower grid reinforcement costs, but these are offset to some extent by the battery (CAPEX and OPEX) costs themselves, and the revenue lost due to selling less power back to the external grid. When the cost of storage is increased by 40.6%, no storage is chosen in the optimisation.

6.5. Intermediate investments 2030

When looking ahead to the 2050 scenarios, it is also relevant to consider an intermediate step such as the 2030 situation. This is because the electrical grid components typically have lifetimes around 40 years, which means that components placed for 2030 will still be functional in 2050. Any investments which were made for 2030 and turn out to be unnecessary in 2050 can be undesirable, because they

still incur operational and maintenance costs, or will have to be decommissioned before they reach the end of their lifetimes which is also costly. Another point to note is that in the best case, the 2030 investments change nothing for the 2050 investments, while in any other case, regrettable investments are made. That being said, the 2030 scenario is sooner and therefore more certain, while 2050 is much less predictable (and therefore has different scenarios). In this solution, the network requirements are first determined for 2030, and these are then used as a starting point for the 2050 scenarios to see if the solution changes.

For the 2030 intermediate step, only network reinforcement is considered. Electrolysers are left out as an option here because they are less feasible at utility scale at this point, including due to higher investment costs, lower efficiency and smaller stack lifetime, and less established hydrogen market. Additionally, it is unlikely that the current gas infrastructure is already repurposed for hydrogen by 2030.

As is evident from introducing the cases in Chapter 5 (see Figures 5.4 and 5.5), electrical demand and generation in the Sterrenburg sub-network are substantially less in 2030 than in all 2050 scenarios. This implies that while electrical power flows in 2050 will be far greater than today, much of the electrification (for example of heating and mobility) will take place between 2030 and 2050. Gas demand, on the other hand, is relatively high in 2030, especially the extremely high gas demand at Oud-Beijerland.

The expansion planning analysis is run for the full 8760 hours of the 2030 scenario since this only needs to be run once. This results in the following transformer investment requirements: Sterrenburg 150/52.5 kV (1), Sterrenburg 52.5/13 kV (2), 's Gravendeel 52.5/13 kV (1) and Klaaswaal (3). The 150/52.5 investment is only just required, with both the net generation and the net demand slightly exceeding 150 MW (which is the capacity of the existing transformer). This is plotted in the load duration curve of Figure 6.13. Comparing this to Figure 6.6 shows that the flows through the same bus are expected to get much larger in the 2050 Regional scenario, in which case there is no disadvantage in investing in this transformer in 2030 already.

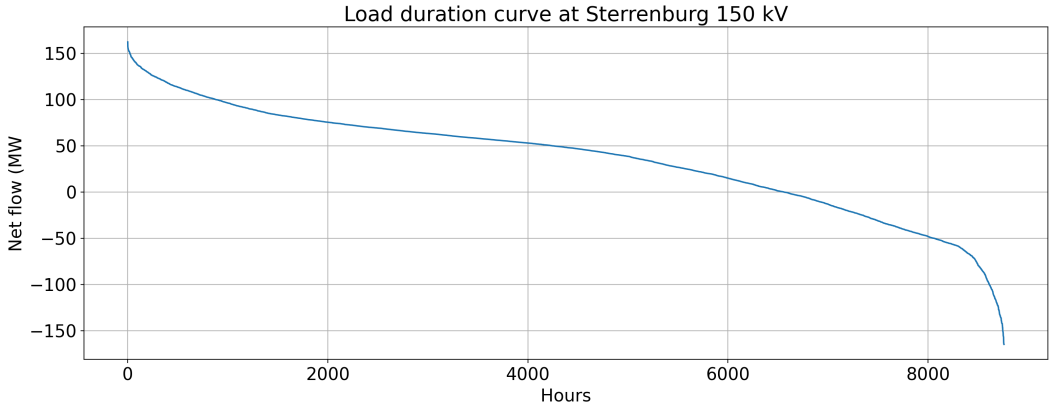

Figure 6.13: Load duration curve at the 150 kV bus in the 2030 scenario, with only grid reinforcement.

The 2030 investments in cables and transformers for the 2030 scenario are summarised in Table 6.11, along with the results from the Regional and International 2050 scenarios (with and without power-gas integration). As has been mentioned, including power-gas integration in the 2050 scenarios always leads to a reduced number of components compared to the solution with reinforcement only. The investment results for the formulation with electric storage are not included, because these are so similar to their reinforcement only counterparts, and none of the 2030 investments could lead to regret for a 2050 scenario in the case of storage integration.

There is only one occurrence where the 2030 investment exceeds the requirements in 2050 (in orange in the table): Cable 3 between Klaaswaal and Sterrenburg (see Figure 5.2) requires 4 cable reinforcements in 2030, but only 3 in the International scenario when electrolysers are included. When planning the 2030 investments in this sub-network, it is recommended to pay extra attention to the cable between Sterrenburg and Klaaswaal, to see what the expected future developments are. In fact, a more thorough investment planning at this location with cable options and better impedance matching

Table 6.11: Number of cable and transformer investments made at each location for different analyses.

	Scenario	2030	Regional	Regional	International	International
	Integration	No	No	Yes	No	Yes
Transformer						
Sterrenburg 150/52.5		1	7	4	2	2
Sterrenburg		2	2	2	3	3
S Gravendeel		1	5	5	2	1
Dordtse Kil		0	1	0	1	1
Klaaswaal		3	9	8	4	3
Oud Beijerland		0	2	1	0	0
Cable						
Cable 1		1	3	3	1	1
Cable 2		0	1	1	0	1
Cable 3		4	11	9	5	3
Cable 4		0	2	2	0	0

might already result in fewer investment requirements at this location. If all the 2030 investments are made according to the calculated requirements and subsequently the International scenario with the power-gas integration occurs as modelled here, then the "regret", i.e., the unnecessary investment will amount to €364,461 per year, which corresponds to one 43.6 MVA cable between Sterrenburg and Klaaswaal.

It is assumed that increasing the city gate capacity in 2030 does not increase the demand for hydrogen in 2050 (i.e., the external bid sizes for 2050 remain the same as in the original 2050 hydrogen bids, which are based on current city gate capacities). With the way that electrolysis is modelled in this work (40 bar output), only local demand and not electrolysers would cause the need to expand the city gate capacity. This is because city gates convert the 40 bar from gas transmission to 8 bar for distribution, and this conversion to 8 bar is only used to supply local demand. Additionally, electrolysis in this model should not cause the need for capacity expansion at higher pressures either, since the external demand is modelled such that it would be at most equal to the current city gate capacity (so that electrolysers would not feed back more than the city gate capacity back to the external grid).

As mentioned, the modelling of the gas network is greatly simplified firstly by modelling gas flows as energy flows through points rather than physical flows through pipes, and secondly by simplifying the gas network to the five most relevant city gates, which are in practice connected via pipelines, but disconnected in the model. Keeping these limitations in mind, the required capacities for the city gates in each scenario are summarised in Table 6.12. Since decreasing the capacities is not an option in the model, all the capacities are at least equal to their current capacity. In the 2030 scenario, there is a slight increase in capacity at 's Gravendeel (17.6 MW) and a very large increase at Oud-Beijerland (243 MW). Both of these would be regrettable investments within the scope of this model, since these two locations are sufficient with their current capacities for the 2050 Regional and International scenarios. In the (improbable) case that the 2030 city gate capacity expansions are carried out as listed in Table 6.12, this would cause an unnecessary extra expense of €692,777 per year for the extra capacities at Oud-Beijerland and 's Gravendeel.

Considering the oversimplification of the gas model and the uncertainty over whether the existing gas network will be repurposed for hydrogen, it is unlikely that these undesirable expansions will take place for 2030 only to be unnecessary in 2050. Instead, it is merely recommended to look closely at the expected gas demand at Oud-Beijerland in 2030 as this is an outlier, and to work with a more complex gas modelling tool to determine the actual required capacity expansion for 2030, keeping in mind the 2050 possibilities.

From this analysis, it can be concluded that reinforcing the electrical network for the 2030 requirements will probably cause few to no regrettable investments later on in 2050, regardless of which scenario develops. This is because most of the 2050 investment requirements are due to demand and

Table 6.12: Summary of city gate capacities (in MW) required in different scenarios.

City gate	Current capacities	2030	Regional	International
Dubbeldam	57.8	57.8	57.8	65.1
Oud-Beijerland	86.5	329.5	86.5	86.5
Dordrecht Wieldrecht	117.5	117.5	117.5	117.5
's Gravendeel	26.3	43.9	26.3	26.3
Numansdorp	51.9	51.9	51.9	51.9

generation increases which occur between 2030 and 2050. However, extra attention must be paid to the connection between Klaaswaal and Sterrenburg.

6.6. Spatial requirements

Considering the expected increase in need for electrical infrastructure between now and 2050, the spatial use is of practical concern. This is especially true for more urban areas, as cities are expanding and land is scarce. For this reason, an analysis of the spatial requirements of the different optimisation solutions is carried out. For this, the spatial requirements as listed in Table 5.9 are used. Note that spatial use is not explicitly included in the objective function, so it is not a direct outcome of the optimisation (if desired, this could be achieved, for example, by introducing weights for the investment terms in the objective function based on their spatial requirements).

One aspect to consider is whether infrastructure is above or below ground: substations (with transformers), electrolysers and gas city gates are above ground, while cables are below ground. In reality, one section of the cable between Klaaswaal and Sterrenburg is actually an overhead line, but for this work, the cables are considered to be underground. This is also supported by the fact that there is a preference to place any new cables at distribution and even 150 kV level only underground (in the area operated by Stedin). In the spatial analysis, the lateral (surface) area is considered rather than volume since this relates to the amount of land required and is of the most practical importance. For example, the 10 m width of the 52.5 kV cable describes the lateral length spanned by all three (-phase) conductors. This, multiplied by the length of the cable, results in the total area.

City gates are left out of this spatial analysis for a few reasons. Firstly, the gas network considered in this model gives an incomplete view of the Sterrenburg sub-network area; there are more than just the five gas city gates in this area, not to mention the pipelines. Secondly, even in this model there is very little expansion of the city gate capacity required in the 2050 scenarios (only 7.3 MW at the Dubbeldam city gate in the International scenario). The electrical network will have a dominant share of the need for acquiring new infrastructure space for 2050. Thirdly, sector coupling does not have an effect on the spatial requirements of the gas networks, since the output is already at 40 bar pressure (the transmission side of the city gate), and increasing the city gate capacity does not have an effect on the external network gas demand (which is limited at the current city gate capacity). Nevertheless, for context, a city gate can be approximated to have an area of 10,000 m^2 (source: Stedin). The five city gates considered in this thesis then have a combined area of 50,000 m^2.

For the electrical infrastructure, the existing components are considered first. In the current configuration, the substations and cables in the case region occupy a combined area of 734,640 m^2 (i.e., 73.464 ha). Of this, 29.5 ha is above-ground for the 150/52.5 and 52.5/13 kV substations, and the remaining 63.964 ha is underground for cables. Looking back at the manual expert solution (see Figure 6.2), this has a substantially smaller spatial footprint for the basic infrastructure (with the minimum number of components to achieve N-1 redundancy): 15 ha for the above-ground 150/21 kV substations and 32.6 ha for the underground 150 kV cables, totalling 47.6 ha. Details are shown in Table E.1 in the Appendix. However, more insight is gained by looking at how much additional space is needed for the 2050 scenarios, with the focus again on the Regional and International scenarios.

Table 6.13 shows the total spatial requirements of the Regional and International 2050 scenarios using the manual expert configuration. One spatial factor to point out here is that a substation has a fixed capacity for multiple transformers. It is built at full size, even if it houses only one transformer.

Table 6.13: Spatial requirements for the manual expert solution.

			Regional		**International**	
	Units	Area/width per unit	Quantity	Area (m^2)	Quantity	Area (m^2)
Type						
Substations 150/21 kV	Substation	30,000 m^2	5	150,000	2	60,000
Cables 150 kV 100 MVA	m	10 m	32,480	324,800	0	0
Existing infrastructure	-	-	-	476,000		476,000
				950,800		**536,000**
Of which partially empty						
Substation (half)	Substation	15,000 m^2	3	45,000	2	30,000

For that reason, the full size of the substation is counted in the spatial analysis, but the tables also highlight the areas of substations that are unused. If necessary, additional transformers can be placed in these substations without having to acquire more land. As seen in Table 6.13, there are five new substation investments required in the manual expert configuration for the Regional scenario. Each of these substations has a capacity of 180 MVA, which houses two 90 MVA transformers. Of the five substations, three of them have only one transformer, leaving 45.000 m^2 where new transformers can be added with relative ease. From the table, it can also be seen the 100 MVA cables from the "existing" (base) infrastructure are sufficient in the International scenario, and only two substation investments are required there. Overall, the spatial requirements of the manual solution are significantly less than for the same scenarios but using the current configuration, as documented in Table 6.14.

Table 6.14: Spatial requirements of current configuration with reinforcement-only in 2050.

			Regional		**International**	
	Units	Area/width per unit	Quantity	Area (m^2)	Quantity	Area (m^2)
Type						
Substations 150/52.5	Substation	45,000 m^2	3	135,000	1	45,000
Substations 52.5/13	Substation	10,000m^2	11	110,000	6	60,000
Cables 52.5 kV	m	10 m	206,802	2,068,020	83,410	834,100
Existing infrastructure	-	-	-	734,640	-	734,640
				3,047,660		**1,673,740**
Of which partially empty						
Substation (one-third) 150/52.5	Substation	15,000 m^2	2	30,000	1	15,000
Substation (half) 52.5/13	Substation	5,000 m^2	3	15,000	2	10,000
				45,000		**25,000**

Comparing Tables 6.13 and 6.14, a vast difference is seen between the spatial requirements of the manual and expert solutions: a little over three times as much area is needed in the current configuration for the 2050 requirements, in both the Regional and International scenarios. Looking a little more into this, the manual expert configuration eliminates components both above and below ground. Above ground, removing the intermediate voltage also removes the need to add infrastructure at two voltage conversion steps for increased flows. Underground, the longest cable (between Sterrenburg and Klaaswaal) is eliminated in the manual expert solution, since Klaaswaal directly connects to the transmission level. This connection takes up the most space among the cables because of its length, and is also the one that is most invested in (see Cable 3 in Table 6.11) because this is needed to connect Klaaswaal (with high renewable generation capacity) and Oud-Beijerland to the external via Sterrenburg. Of the infrastructure considered, the biggest part of it is underground in all cases, since the cables span several kilometres between the substations. In both the Regional and International scenarios, most of the space saved by changing from the current to the manual expert configuration results from fewer underground cables. The changes in spatial requirements are also compared in the current configuration, when power-gas integration is introduced by means of electrolysis. Table 6.15 contains an overview of the spatial requirements in the Regional and International scenarios of the electrical and electrolysis infrastructure.

As seen in Table 6.15, the International scenario requires less space for network infrastructure than the Regional scenario, and again most of this space is for underground cables. The spatial use of electrolysers is included in this analysis since it is being considered as an alternative to grid reinforcement, and regardless of who owns it, land will still have to be found to place the electrolysers. At 21,492 m^2 in the Regional scenario and 11,522 m^2 in the International scenario, the spatial use

Table 6.15: Spatial requirements with power-gas coupling for the Regional and International scenarios.

			Regional		**International**	
	Units	Area/width per unit	Quantity	Area (m^2)	Quantity	Area (m^2)
Type						
Substations 150/52.5	Substation	45,000	2	90,000	1	45,000
Substations 52.5/13	Substation	10,000	9	90,000	6	60,000
Cables 52.5 kV	m	10	167,438	1,674,380	55,346	553,460
Cables to electrolysers 13 kV		-	-	13,788	-	5,532
Cables to electrolysers 52.5 kV		-	-	37,890	-	61,380
Electrolysers	MW	95	226	21,492	121	11,522
Existing infrastructure	-	-	-	734,640	-	734,640
				2,712,906		**1,522,624**
Of which partially empty						
Substation (one-third) 150/52.5	Substation	15,000	2	30,000	1	15,000
Substation (half) 52.5/13	Substation	5,000	2	10,000	4	20,000
				40,000		**35,000**

of electrolysers is significant, but small compared to the total infrastructure. The space used by cables connecting the substations to gas city gates is relatively small compared to the cables between substations, since these distances are much smaller and at lower capacities.

Table 6.16: Comparing the relative change in spatial footprints of power-gas reinforcement and manual expert reconfiguration for the Regional and International scenarios.

	Current configuration Reinforcement-only	**Current configuration Power-gas integration**	**Expert configuration Reinforcement-only**
	Spatial use (m^2)	Change (%)	Change (%)
Regional scenario			
Above ground	340,000	-12.80%	-11.76%
Underground	2,707,660	-10.72%	-75.96%
International scenario			
Above ground	200,000	+5.76%	+5.00%
Underground	1,473,740	-9.96%	-77.88%

To compare the effect of either introducing power-gas integration in the existing configuration, or changing the configuration to that of the manual expert solution, an overview is made in Table 6.16. The column for reinforcement-only in the current configuration shows the spatial use above and below ground in m^2 for the Regional and International scenarios. The following two columns show the percentage increase (positive) or decrease (negative) in the corresponding spatial use when either power-gas integration or the expert configuration is implemented. The table shows that both these measures cause a reduction in spatial use for all variations, except above ground in the International scenario. In the power-gas integration, 5.76% more space is needed above ground because the number of substations is the same as with reinforcement-only (albeit with fewer transformers), while in the manual expert configuration, more space is needed above ground because the 150/21 kV substations are larger than the 52.5/13 kV ones.

Summarising the effect of power-gas integration and the expert configuration on the spatial use compared to reinforcement-only in the current configuration: both measures have similar effects above ground, which means a reduction in spatial use in the Regional scenario and a (slight) increase in spatial use in the International scenario. Both measures also decrease the underground spatial use in both scenarios, but the effect of the expert reconfiguration is bigger. This configuration, as mentioned in Section 6.1, does have higher costs than the current configuration. Moreover, these two measures are not mutually exclusive; if spatial use is a major bottleneck, both a reconfiguration of the network and implementation of power-gas reinforcement can be combined to save space, especially in the Regional scenario.

Figure 6.14 shows a summary of the above- and underground spatial usage in the Regional and International scenarios, comparing the reinforcement-only approach to power-gas integration. Note that the y-axis scale (area in ha) is the same between the Regional and International scenarios, but differs between the above- and below ground plots. The underground components, as mentioned,

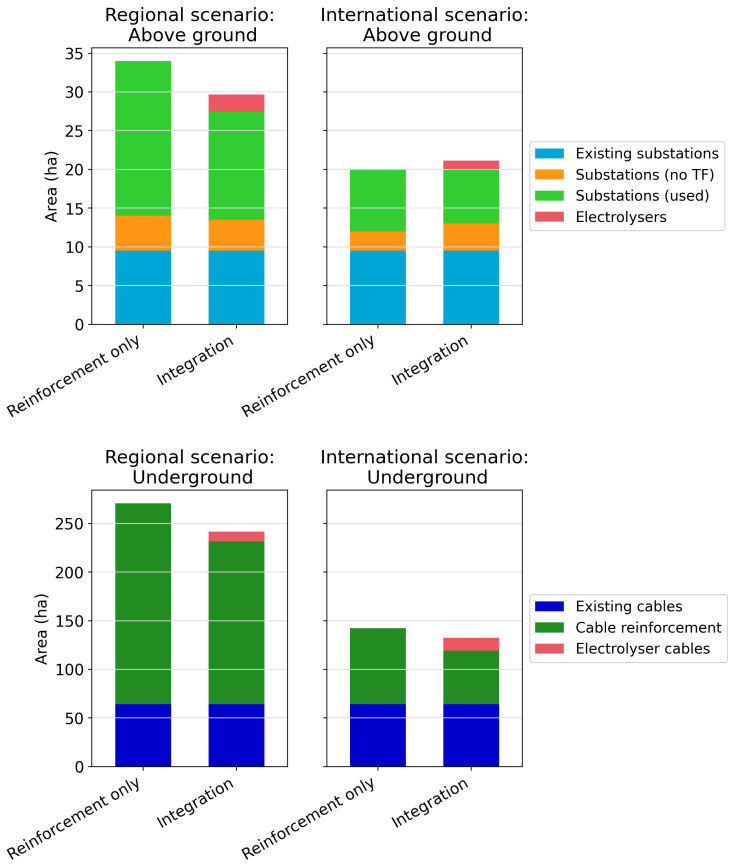

Figure 6.14: Comparison of existing and additional spatial requirements for the International and Regional scenarios, between reinforcement-only and power-gas integration approaches.

take up more space than the substations and electrolysers which are above the ground. The figure shows again that space can be saved by introducing power-gas integration, especially in the Regional scenario. In the International scenario, the above-ground spatial usage actually appears to increase due to electrolysers (red), but note that the amount of space in substations where there is no transformer (orange) also increases with power-gas integration. In both scenarios, space is saved underground by decreasing the need for longer cables between substations, and instead adding a few smaller cables between substations and their nearest city gate.

The storage formulation was seen to have little effect on the spatial requirements of infrastructure: at 71.4 m^2/MWh (i.e., 285.6 m^2/MW for 4-hour batteries) of space required for batteries, the Regional scenario results in 760 m^2 being used for 2.66 MW of batteries, while no space is saved on grid infrastructure above or below ground (there is one fewer transformer, but the same number of substations as with reinforcement-only). In the International scenario, the inclusion of 2.25 MW of batteries requires 643 m^2. This is accompanied by a decrease in spatial use above ground by 10,000 m^2 for one 52.5/13 kV substation compared to reinforcement-only. Note that this substation at Klaaswaal was only required for a small excess flow (since the investment was avoided by 2.25 MW battery capacity) and that this substation was not required in the 21-day time slice selection, i.e., it depends on the details of the scenario representation. Underground, one cable investment between Klaaswaal and Sterrenburg is avoided, which saves 156.820 m^2 of the total underground spatial use compared to reinforcement-only (about 10.6%). One advantage of batteries is that they could be placed right alongside (or even within) the substation, without the need for an additional connection (such as from the substation to the gas city gate for electrolysers). This could make batteries attractive for saving space underground, but their impact within the scope of this case is limited, especially on the spatial use in the Regional scenario.

7 | Conclusions and further work

In this chapter, conclusions are drawn from the case study results and are used to answer the research questions. Finally, the model is discussed in terms of how it can be extended and improved in future work.

7.1. Key findings

The results of the case analysis are presented and discussed at length in Chapter 6. In the following sections, the main results are summarised within the context of the research questions, focusing on the Regional and International scenarios. The research sub-questions and main question are repeated below for reference.

a. *To what extent do the economic costs and savings due to system integration vary between different 2050 scenarios?*

Introducing power-gas integration by means of electrolysis leads to savings for the DSO compared to a strategy of only reinforcing the network components. These savings are greater in the Regional scenario which has a higher capacity of distributed generation than in the International scenario: savings of €1.59 million per year in annualised infrastructure costs compared to about €598,000 per year in the International scenario. However, the benefits are more consistent as a proportion of the total network reinforcement costs, because the International scenario also requires fewer reinforcement investments overall: 18.5% savings in the Regional scenario, and 16.7% in the International scenario compared to their respective network investment costs using reinforcement-only.

Electrolysis also contributes to lowering the net costs of the case region that is spent on importing (gas and electric) energy. Additionally, the electrolyser-related costs could be recovered by hydrogen revenue depending on some exemption from grid connection fees, and the profitability of electrolysis ownership could better be investigated in an operational optimisation with a focus on market and bidding mechanisms. Hydrogen-to-power conversion is not chosen within the scope of the case, and electric storage by means of 4-hour lithium-ion batteries leads to limited impact (with 2.66 and 2.25 MW capacity of li-ion batteries chosen in the Regional and International scenarios, respectively).

b. *What effect does integrated planning in the Sterrenburg case have on the spatial use of the energy infrastructure?*

Power-gas integration reduces the overall spatial requirements for energy infrastructure in both the Regional and International scenarios. Electrolysers require new connections to be placed between substations and city gates, but their presence decreases the number of cable reinforcements required between the substations which are further apart. In both the Regional and International scenarios, power-gas integration by means of electrolysis could lead to about a 10% reduction in the total underground spatial requirements for cables. However, more space could be saved on underground cables by restructuring the network, which does come at a higher cost. Above ground, power-gas integration saves about 12.8% space compared to reinforcement-only in the Regional scenario. In the International scenario, slightly more space is needed above ground for electrolysers because the space used by substations remains the same (despite a decrease in the number of transformers) compared to reinforcement-only. The effect of batteries is again smaller than electrolysis, but one advantage is that no additional connections need to be placed underground for batteries.

c. *Are there intermediate investments made for the 2030 scenario which become unnecessary in any of the 2050 solutions?*

Based on the scenarios used, a lot of electrification in the Sterrenburg sub-network takes place between

2030 and 2050. Therefore, regretting network-reinforcement investments made for 2030 is not a major concern. That being said, the natural gas demand at Oud Beijerland is remarkably high in 2030 and could require reexamination. Additionally, one of the four cable reinforcement investments between Sterrenburg and Klaaswaal of 2030 could become unnecessary in the International scenario with the use of power-gas integration. In that case, it could be beneficial to explore alternatives for this cable in 2030.

d. *How robust is the optimisation result in terms of sensitivity to model parameter values?*

The power-gas integration solutions are highly sensitive to 50% variations in the electricity and hydrogen trading prices, with the effect of the hydrogen price variations being slightly greater on the amount of electrolysis capacity chosen (between 0 and 303 MW_e total electrolysis capacity for an increase and decrease in hydrogen price respectively) than the electricity price. Regardless of price variations, the net system cost decreases whenever electrolysis is chosen. The optimisation results are less sensitive to 25% variations in the cost of electrolysers and gas turbines. The total electrolysis capacity varies by less than 1% for the electrolysis price variations, and gas turbines are not chosen in any of the scenarios regardless of price variations. When the battery price is decreased by 43.6%, the installed capacity goes up to 35.1 MW, and no batteries are chosen when the battery price is increased by 40.4%.

How can the flexibility provided by energy system integration in network planning lead to benefits compared to only electric infrastructure reinforcements for the 2050 generation and demand scenarios for the Sterrenburg sub-network?

This thesis has demonstrated that power-gas integration with electrolysers can be valuable at the distribution grid level in 2050, although hydrogen turbines were not chosen within the scope of the model. The benefits provided by the flexibility include avoiding some grid-reinforcement investments, lowering the system costs and decreasing the spatial footprint of energy infrastructure. These benefits are greater in the scenario with more distributed generation. Because of the low complexity of the gas network in the model, any conclusions related to the gas network are limited and could use further investigation. Within the case scope, electrical storage at the distribution grid level has a limited impact. Some reinforcement investments can be avoided by introducing 4-hour lithium-ion batteries, but the effect of electrolysers is greater.

7.2. Future work

Considering this work is a broad, early-stage investigation in a high-stakes, societally relevant and developing topic, there are many directions in which future research can build on this work. These can be categorised under the scope of the analysis, the model complexity and the optimisation structure. Some ideas for future work are discussed below. Future work could explore a single idea from among these, or also the interactions of different combinations (such as long-term gas energy storage in combination with a model that includes physical gas flows through pipelines).

Analysis scope

Broadening the electrical system scope: in this thesis, distributed generation was treated as exogenous (based on the scenarios), and the transmission network was not included in the scope of the network. When exploring the effects of system integration on the distribution network, it might also be interesting to see how this affects the transmission network. Alternatively, by including generation capacity investments as investment options, the suitable generation locations can also be used to advise energy generation projects.

Energy storage: in this thesis, a limited analysis of 4-hour electrical storage is included. Considering the diversity of storage technologies and their corresponding applications, it could be interesting to carry out a study focused on different types of energy storage coupled to different energy carriers in an integrated energy system, especially by focusing on the potential benefits at the distribution level. Aside from different storage technologies, a follow-up study could also focus on different storage capacities, including seasonal storage. Storage could also better be investigated in a formulation that

avoids the selection of time slices, and rather uses continuous time data (e.g. hourly values for a full year). Another potentially interesting investigation could be made for a combination of the distribution and (gas) transmission networks: with a large amount of distributed electricity generation, there might be benefits in distributed electrolysis along with centralised, large-scale gas storage.

Gas network investigation and elaboration: the model of this thesis included the electrical network and a simplified gas network, along with their respective loads, generation and conversion. The gas network was modelled in conceptual energy flows through city gates of limited capacity, and there was no interconnection among the city gates. Extending the gas network model to include the meshed network of pipelines and a physical model of gas flows would give a more realistic view of the available gas network capacity and any necessary reinforcement investment. Additionally, it was assumed that the existing gas network would be repurposed for hydrogen by 2050, and all the gas demand from the scenarios was treated to be for hydrogen. In reality, it is unclear whether (or to what extent) the existing natural gas network will be repurposed for hydrogen. It could also be, for example, that parts of the existing gas network are removed altogether and that an entirely new hydrogen infrastructure is developed. This could also be explored in a model with natural gas alongside a Greenfield approach to hydrogen.

Gas pipelines from substation to electrolyser: placing electrolysers in the network requires a connection between the gas and electricity networks. In this thesis, it was modelled as electrical cables placed between a substation and the nearest city gate. Alternatively, a gas pipeline that is suitable for the output pressure of the electrolyser (modelled at 40 bar) could be placed. In this case, the electrolyser would be near the substation, and the gas pipeline would transport the hydrogen to the nearest city gate. The effect of this option on costs and spatial requirements would be different compared to the option of cables as used in this thesis.

Heat network: aside from electricity and gas networks, integration with heat networks could also be beneficial. While their current presence in the Netherlands is limited, heat networks are also being explored as an option to decarbonise urban heating infrastructure, and there are opportunities for interconnection with both electric and gas networks.

Replacement and decommissioning of components: the focus of this work was expansion planning based on an existing network. However, as briefly explored in the manual expert solution, there can be benefits in replacing some components with a different type of component or removing some components altogether. This could be modelled using a similar optimisation algorithm as in this work, and it would require assigning the appropriate costs for decommissioning and replacing any components to gain insights into these options.

Model complexity

Market model: the region modelled in the case study of this thesis is far from self-sufficient in energy at any hour. The energy surplus and deficits are modelled as exchange with an external grid via the 150 kV electric and city gate gas connections. However, when exploring system integration, it was found to be realistic to include some market signals. Specifically, a simple market was modelled by including supply and demand bids from the external grid at three price levels, of which the bid size varies with local demand and generation to approximate the effect of weather and time. When looking at operational aspects such as profitability, it could be interesting to develop a more complex market. Other works have, for example, fitted to historical data or used game theory/agent-based modelling to develop more realistic market bids. Moreover, a profit-seeking strategy could also be explored for electrolysis ownership in a model with a more elaborate market. In a sense, some demand response from the external grid was implicitly included in this model by the demand bids at different price levels from the external market. Considering the limitations of PyPSA, other modelling tools could be good alternatives for a more elaborate bidding and market model. Demand response could also be explored more explicitly, in how it interacts with system integration.

Physical infrastructure realism: several simplifications were made in modelling costs and operation of the energy infrastructure components. Future works focusing on a specific aspect could model some components in more detail. For example, in linearising the power flows, cable losses were neglected. Additionally, electrolysers were assumed to perform at a constant efficiency, regardless of output level, age or other conditions. Modelling aspects like this could be elaborated on to better reflect real

behaviour.

Reliability: this thesis results in infrastructure with N - 1 reliability under all conditions. In the future, the requirements might be different, such as requiring N - 1 only for net demand from end-users, and only N reliability for distribution network infrastructure at times of net generation. In the Regional scenario, it was indeed net generation which outweighed net demand and was the cause for many of the investment, so it could be insightful to develop a model which is able to apply these conditional reliability requirements. Additionally, probabilistic reliability criteria could be explored.

Candidate investment selection: this thesis included a standard type of investment candidate at each of the possible locations in the case. A more elaborate selection, either by automatic or manual means, could help in determining a more optimal solution. For example, this could involve looking into the size of the excess power flows, the number of hours at which capacity is exceeded, the capacities of adjacent components (for example, the cables connected to a transformer) and at matching impedance for electrical components.

Optimisation structure

Solving time: rather than optimising over all 8760 hours of a year for the scenarios in this thesis, a representative selection was made to reduce the solving time. Alternatives for keeping the solving time manageable while using more time-steps could be looked into. The computational complexity of optimising power systems is addressed in various ways in literature. For example, alternative methods for managing the power flow, or different methods for solving the optimisation problem might be more efficient in finding solutions. It would be especially valuable to be able to bypass the selection of representative time slices (and use a full year) when investigating systems with energy storage. This would also facilitate the analysis of long-term storage.

Solving methods: mathematical optimisation methods were used in the mixed-integer linear programming problem formulation. However, the use of heuristic methods could also be explored, especially if non-linear aspects are introduced to the model (such as non-linear costs and power flows). Heuristic methods might lead to faster solving times, and their speed and optimality could be compared to mathematical optimisation.

Ownership structures: in this thesis, a system approach was taken to the optimisation, which aims to minimise investment and operational cost without regard for who owns what, and for minimising the overall costs rather than maximising any profit. Different ownership structures could have different outcomes, which could also be interesting to explore.

Weighted multi-objective function: the annualised investment cost and total annual hourly operational costs were included in the objective function of the optimisation in this work. Depending on the desired outcome, the objective function could be modified. For example, if a reduction in spatial use of the infrastructure is desired, the investment candidates could be weighted in the objective function according to their relative spatial use. Alternatively, if the goal is to reduce investments despite a potential increase in energy costs, then the investment terms can be given a bigger weight in the objective function than the operational terms.

8 | Bibliography

[1] P. Murray, K. Orehounig, D. Grosspietsch, and J. Carmeliet, "A comparison of storage systems in neighbourhood decentralized energy system applications from 2015 to 2050," *Applied Energy*, vol. 231, pp. 1285–1306, 12 2018.

[2] J. Marco, "Connecting the dots: Distribution grid investment to power the energy transition," E.DSO, Eurelectric, Monitor Deloitte, Tech. Rep., 2021. [Online]. Available: https://www.eurelectric.org/connecting-the-dots/

[3] T. Stetz, M. Kraiczy, K. Diwold, M. Braun, B. Bletterie, C. Mayr, R. Bründlinger, B. Noone, A. Bruce, I. MacGill, and others, "High Penetration PV in Local Distribution Grids-Outcomes of the IEA PVPS Task 14 Subtask 2," in *29th European Photovoltaic Solar Energy Conference and Exhibition*, vol. 15, no. 1, 2014, pp. 3994–3999.

[4] International Renewable Energy Agency, "Power system flexibility for the energy transition, Part 1: Overview for policy makers," IRENA, Tech. Rep., 2018.

[5] M. W. Melaina, O. Antonia, and M. Penev, "Blending Hydrogen into Natural Gas Pipeline Networks: A Review of Key Issues," NREL, Tech. Rep., 2013.

[6] D. Peters, K. van der Leun, W. Terlouw, J. van Tilburg, T. Berg, M. Schimmel, I. van der Hoorn, M. Buseman, M. Staats, M. Schenkel, and others, "Gas Decarbonisation Pathways 2020–2050: Gas for Climate," 2020.

[7] K. T. Møller, T. R. Jensen, E. Akiba, and H. w. Li, "Hydrogen - A sustainable energy carrier," *Progress in Natural Science: Materials International*, vol. 27, no. 1, pp. 34–40, 2 2017.

[8] W. Cole and A. W. Frazier, "Cost Projections for Utility-Scale Battery Storage: 2020 Update," NREL, Tech. Rep., 2020.

[9] M. Abeysekera, J. Wu, and N. Jenkins, "Integrated energy systems: An overview of benefits, analysis methods, research gaps and opportunities," Hubnet Position Paper Series, Tech. Rep., 2016.

[10] A. Zauner, H. Böhm, D. C. Rosenfeld, and R. Tichler, "Innovative large-scale energy storage technologies and Power-to-Gas concepts after optimization Analysis on future technology options and on techno-economic optimization," European Commission, Tech. Rep., 2019.

[11] M. Ruska and L. Similä, "Electricity markets in Europe: Business environment for Smart Grids," *VTT Tiedotteita - Valtion Teknillinen Tutkimuskeskus*, pp. 1–70, 2011.

[12] P. Schavemaker and L. der Sluis, *Electrical power system essentials*. John Wiley & Sons, 2017.

[13] PBL, "Klimaat- en Energieverkenning 2020," Planbureau voor de Leefomgeving, Tech. Rep., 2020.

[14] T. Brown, J. Hörsch, and D. Schlachtberger, "PyPSA: Python for power system analysis," *Journal of Open Research Software*, vol. 6, no. 1, 2018.

[15] P. Mancarella, "MES (multi-energy systems): An overview of concepts and evaluation models," pp. 1–17, 2 2014.

[16] "The Paris Agreement | UNFCCC," 2021. [Online]. Available: https://unfccc.int/process-and-meetings/the-paris-agreement/the-paris-agreement

[17] European Commission, "A Clean Planet for all: A European strategic long-term vision for a prosperous, modern, competitive and climate neutral economy," COM, Brussels, Tech. Rep., 2018.

[18] M. Child, C. Kemfert, D. Bogdanov, and C. Breyer, "Flexible electricity generation, grid exchange and storage for the transition to a 100% renewable energy system in Europe," *Renewable Energy*, vol. 139, pp. 80–101, 8 2019.

[19] E. Guelpa, A. Bischi, V. Verda, M. Chertkov, and H. Lund, "Towards future infrastructures for sustainable multi-energy systems: A review," pp. 2–21, 10 2019.

[20] H. Lund, "Renewable heating strategies and their consequences for storage and grid infrastructures comparing a smart grid to a smart energy systems approach," *Energy*, vol. 151, pp. 94–102, 5 2018.

[21] M. O'malley, B. Kroposki, B. Hannegan, H. Madsen, M. Andersson, W. D'haeseleer, M. F. Mcgranaghan, C. Dent, G. Strbac, S. Baskaran, and M. Rinker, "International Institute for Strategic Energy Systems Integration: Defining and Describing the Value Proposition," NREL, Tech. Rep., 6 2016.

[22] COM, "Powering a climate-neutral economy: An EU Strategy for Energy System Integration," European Commission, Brussels, Tech. Rep., 7 2020.

[23] Werkgroep integraal netwerk en energiesysteem van de toekomst, "Ontwikkelingen op het netwerk en energiesysteem," Netbeheer Nederland, Tech. Rep., 10 2019.

[24] M. A. Mahmud, M. J. Hossain, and H. R. Pota, "Analysis of voltage rise effect on distribution network with distributed generation," in *IFAC Proceedings Volumes (IFAC-PapersOnline)*, vol. 44, no. 1 PART 1. IFAC Secretariat, 1 2011, pp. 14 796–14 801.

[25] C. Koronen, M. Åhman, and L. J. Nilsson, "Data centres in future European energy systems—energy efficiency, integration and policy," *Energy Efficiency*, vol. 13, no. 1, pp. 129–144, 1 2020.

[26] P. Sterchele, K. Kersten, A. Palzer, J. Hentschel, and H. M. Henning, "Assessment of flexible electric vehicle charging in a sector coupling energy system model – Modelling approach and case study," *Applied Energy*, vol. 258, p. 114101, 1 2020.

[27] A. Chakrabarti, R. Proeglhoef, G. B. Turu, R. Lambert, A. Mariaud, S. Acha, C. N. Markides, and N. Shah, "Optimisation and analysis of system integration between electric vehicles and UK decentralised energy schemes," *Energy*, vol. 176, pp. 805–815, 6 2019.

[28] P. Murray, J. Carmeliet, and K. Orehounig, "Multi-Objective Optimisation of Power-to-Mobility in Decentralised Multi-Energy Systems," *Energy*, vol. 205, 8 2020.

[29] Z. Huang, B. Fang, and J. Deng, "Multi-objective optimization strategy for distribution network considering V2G-enabled electric vehicles in building integrated energy system," *Protection and Control of Modern Power Systems*, vol. 5, no. 1, pp. 1–8, 12 2020.

[30] J. B. Nunes, N. Mahmoudi, T. K. Saha, and D. Chattopadhyay, "A stochastic integrated planning of electricity and natural gas networks for Queensland, Australia considering high renewable penetration," *Energy*, vol. 153, pp. 539–553, 6 2018.

[31] A. Turk, Q. Wu, M. Zhang, and J. Østergaard, "Day-ahead stochastic scheduling of integrated multi-energy system for flexibility synergy and uncertainty balancing," *Energy*, vol. 196, 4 2020.

[32] J. Wang, Z. Hu, and S. Xie, "Expansion planning model of multi-energy system with the integration of active distribution network," *Applied Energy*, vol. 253, 11 2019.

[33] I. Petkov and P. Gabrielli, "Power-to-hydrogen as seasonal energy storage: an uncertainty analysis for optimal design of low-carbon multi-energy systems," *Applied Energy*, vol. 274, p. 115197, 9 2020.

[34] L. F. Grisales-Noreña, O. D. Montoya, and W. Gil-González, "Integration of energy storage systems in AC distribution networks: Optimal location, selecting, and operation approach based on genetic algorithms," *Journal of Energy Storage*, vol. 25, 10 2019.

[35] C. Müller, A. Hoffrichter, L. Wyrwoll, C. Schmitt, M. Trageser, T. Kulms, D. Beulertz, M. Metzger, M. Duckheim, M. Huber, M. Küppers, D. Most, S. Paulus, H. J. Heger, and A. Schnettler, "Modeling framework for planning and operation of multi-modal energy systems in the case of Germany," *Applied Energy*, vol. 250, pp. 1132–1146, 9 2019.

[36] D. Meha, A. Pfeifer, N. Duić, and H. Lund, "Increasing the integration of variable renewable energy in coal-based energy system using power to heat technologies: The case of Kosovo," *Energy*, vol. 212, 12 2020.

[37] W. Huang, N. Zhang, J. Yang, Y. Wang, and C. Kang, "Optimal configuration planning of multi-energy systems considering distributed renewable energy," *IEEE Transactions on Smart Grid*, vol. 10, no. 2, pp. 1452–1464, 3 2019.

[38] M. Pavičević, A. Mangipinto, W. Nijs, F. Lombardi, K. Kavvadias, J. P. Jiménez Navarro, E. Colombo, and S. Quoilin, "The potential of sector coupling in future European energy systems: Soft linking between the Dispa-SET and JRC-EU-TIMES models," *Applied Energy*, vol. 267, p. 115100, 6 2020.

[39] T. Brown, D. Schlachtberger, A. Kies, S. Schramm, and M. Greiner, "Synergies of sector coupling and transmission reinforcement in a cost-optimised, highly renewable European energy system," *Energy*, vol. 160, pp. 720–739, 10 2018.

[40] E. Panos, T. Kober, and A. Wokaun, "Long term evaluation of electric storage technologies vs alternative flexibility options for the Swiss energy system," *Applied Energy*, vol. 252, p. 113470, 10 2019.

[41] M. F. Tahir, C. Haoyong, K. Mehmood, N. Ali, and J. A. Bhutto, "Integrated energy system modeling of China for 2020 by incorporating demand response, heat pump and thermal storage," *IEEE Access*, vol. 7, pp. 40 095–40 108, 2019.

[42] E. A. M. Cesena, E. Loukarakis, N. Good, and P. Mancarella, "Integrated Electricity-Heat-Gas Systems: Techno-Economic Modeling, Optimization, and Application to Multienergy Districts," *Proceedings of the IEEE*, 9 2020.

[43] L. Yu, Y. P. Li, and G. H. Huang, "Planning municipal-scale mixed energy system for stimulating renewable energy under multiple uncertainties - The City of Qingdao in Shandong Province, China," *Energy*, vol. 166, pp. 1120–1133, 1 2019.

[44] N. Mohajeri, A. T. Perera, S. Coccolo, L. Mosca, M. Le Guen, and J. L. Scartezzini, "Integrating urban form and distributed energy systems: Assessment of sustainable development scenarios for a Swiss village to 2050," *Renewable Energy*, vol. 143, pp. 810–826, 12 2019.

[45] H. L. Willis, *Power distribution planning reference book*. CRC press, 2004.

[46] Gasunie, Tennet, Liander, Enexis, Stedin, Enduris, Coteq, Rendo Netwerken, Westland Infra, and Elaadnl, "Basisinformatie over energie-infrastructuur," Netbeheer Nederland, Tech. Rep., 5 2019. [Online]. Available: www.netbeheernederland.nl/_upload/Files/Basisdocument_over_energie-infrastructuur_149.pdf

[47] H. Seifi and M. S. Sepasian, *Electric power system planning: issues, algorithms and solutions*. Springer Science & Business Media, 2011.

[48] G. Muñoz-Delgado, J. Contreras, and J. M. Arroyo, "Distribution System Expansion Planning," in *Electric Distribution Network Planning*, F. Shahnia, A. Arefi, and G. Ledwich, Eds. Singapore: Springer Singapore, 2018, pp. 1–39.

[49] A. Ulbig and G. Andersson, "Analyzing operational flexibility of electric power systems," *International Journal of Electrical Power and Energy Systems*, vol. 72, pp. 155–164, 3 2015.

[50] J. J. Grainger and W. D. Stevenson, *Power System Analysis*, ser. Electrical engineering series. McGraw-Hill, 1994.

[51] P. S. R. Murty, *Power systems analysis*. Butterworth-Heinemann, 2017.

[52] International Energy Agency, "The Netherlands 2020 - Energy Policy Review," IEA, Tech. Rep., 2020.

[53] D. ENER Energy, "A hydrogen strategy for a climate-neutral Europe," European Commission, Tech. Rep., 2020. [Online]. Available: https://www.eu2018.at/calendar-events/political-events/BMNT-

[54] IEA, "The Future of Hydrogen - Seizing today's opportunities," IEA, Tech. Rep., 6 2019.

[55] F. v. Alphen, M. v. Dan, H. Engberts, N. v. d. Hout, J. Jonkman, J. Lieffering, P. t. Morsche, and C. Lauwerijs, "Toekomstbestendige gasdistributienetten," Kiwa, Tech. Rep., 2018. [Online]. Available: www.kiwatechnology.nl

[56] E. W. Gaykema, I. Skryabin, J. Prest, and B. Hansen, "Assessing the viability of the ACT natural gas distribution network for reuse as a hydrogen distribution network," *International Journal of Hydrogen Energy*, vol. 46, no. 23, pp. 12 280–12 289, 3 2021.

[57] J. Qiu, Z. Y. Dong, J. H. Zhao, K. Meng, Y. Zheng, and D. J. Hill, "Low carbon oriented expansion planning of integrated gas and power systems," *IEEE Transactions on Power Systems*, vol. 30, no. 2, pp. 1035–1046, 3 2015.

[58] M. Chaudry, N. Jenkins, and G. Strbac, "Multi-time period combined gas and electricity network optimisation," *Electric Power Systems Research*, vol. 78, no. 7, pp. 1265–1279, 7 2008.

[59] J. Qiu, Z. Y. Dong, J. H. Zhao, Y. Xu, Y. Zheng, C. Li, and K. P. Wong, "Multi-Stage Flexible Expansion Co-Planning Under Uncertainties in a Combined Electricity and Gas Market," *IEEE Transactions on Power Systems*, vol. 30, no. 4, pp. 2119–2129, 7 2015.

[60] R. Bent, S. Blumsack, P. Van Hentenryck, C. Borraz-Sanchez, and M. Shahriari, "Joint Electricity and Natural Gas Transmission Planning with Endogenous Market Feedbacks," *IEEE Transactions on Power Systems*, vol. 33, no. 6, pp. 6397–6409, 11 2018.

[61] C. Bell, "fluids: Fluid dynamics component of Chemical Engineering Design Library (ChEDL)," 2021. [Online]. Available: https://github.com/CalebBell/fluids.

[62] H. Lund, S. Werner, R. Wiltshire, S. Svendsen, J. E. Thorsen, F. Hvelplund, and B. V. Mathiesen, "4th Generation District Heating (4GDH). Integrating smart thermal grids into future sustainable energy systems." pp. 1–11, 4 2014.

[63] S. Werner, "International review of district heating and cooling," pp. 617–631, 10 2017.

[64] X. Xu, M. Bishop, O. Donna G, and H. Chen, "Application and modeling of battery energy storage in power systems," *CSEE Journal of Power and Energy Systems*, vol. 2, no. 3, pp. 82–90, 9 2016.

[65] T. Kousksou, P. Bruel, A. Jamil, T. El Rhafiki, and Y. Zeraouli, "Energy storage: Applications and challenges," pp. 59–80, 1 2014.

[66] P. Denholm, J. Nunemaker, P. Gagnon, and W. Cole, "The potential for battery energy storage to provide peaking capacity in the United States," *Renewable Energy*, vol. 151, pp. 1269–1277, 5 2020.

[67] O. Schmidt, S. Melchior, A. Hawkes, and I. Staffell, "Projecting the Future Levelized Cost of Electricity Storage Technologies," *Joule*, vol. 3, no. 1, pp. 81–100, 1 2019.

[68] F. Mwasilu, J. J. Justo, E. K. Kim, T. D. Do, and J. W. Jung, "Electric vehicles and smart grid interaction: A review on vehicle to grid and renewable energy sources integration," pp. 501–516, 6 2014.

[69] X. Zhang, L. Che, M. Shahidehpour, A. S. Alabdulwahab, and A. Abusorrah, "Reliability-Based Optimal Planning of Electricity and Natural Gas Interconnections for Multiple Energy Hubs," *IEEE Transactions on Smart Grid*, vol. 8, no. 4, pp. 1658–1667, 7 2017.

[70] S. A. Grigoriev, V. N. Fateev, D. G. Bessarabov, and P. Millet, "Current status, research trends, and challenges in water electrolysis science and technology," *International Journal of Hydrogen Energy*, vol. 45, no. 49, pp. 26 036–26 058, 10 2020.

[71] European Commission, "Progress towards completing the Internal Energy Market," COM, Brussels, Tech. Rep., 2014.

[72] S. Stoft, "Power system economics," *Journal of Energy Literature*, vol. 8, pp. 94–99, 2002.

[73] M. J. Morey, *Power Market Auction Design: Rules and Lessons in Market-Based Control for the New Electricity Industry.* Edison Electric Institute, 2001. [Online]. Available: www.eei.org.

[74] R. Madlener and M. Kaufmann, "Power exchange spot market trading in Europe: theoretical considerations and empirical evidence ," OSCOGEN, Tech. Rep., 2002.

[75] A. Moser, A. Maaz, and N. v. Bracht, "Simulating electricity market bidding and price caps in the European power markets S18 Report," METIS Studies European Commission, Tech. Rep., 2017. [Online]. Available: http://europa.eu

[76] L. Hirth, "The market value of variable renewables. The effect of solar wind power variability on their relative price," *Energy Economics*, vol. 38, pp. 218–236, 7 2013.

[77] J. Blazquez, R. Fuentes-Bracamontes, C. A. Bollino, and N. Nezamuddin, "The renewable energy policy Paradox," pp. 1–5, 2 2018.

[78] S. Djørup, J. Z. Thellufsen, and P. Sorknæs, "The electricity market in a renewable energy system," *Energy*, vol. 162, pp. 148–157, 11 2018.

[79] G. W. Leslie, D. I. Stern, A. Shanker, and M. T. Hogan, "Designing electricity markets for high penetrations of zero or low marginal cost intermittent energy sources," *Electricity Journal*, vol. 33, no. 9, p. 106847, 11 2020.

[80] S. Haffner, L. F. A. Pereira, L. A. Pereira, and L. S. Barreto, "Multistage model for distribution expansion planning with distributed generation - Part I: Problem formulation," *IEEE Transactions on Power Delivery*, vol. 23, no. 2, pp. 915–923, 4 2008.

[81] S. Lumbreras, A. Ramos, and P. Sánchez, "Automatic selection of candidate investments for Transmission Expansion Planning," *International Journal of Electrical Power and Energy Systems*, vol. 59, pp. 130–140, 7 2014.

[82] A. M. Rei, M. Armando, L. D. Suva, J. L. Jardim, and J. C. O. De Mello, "Static and dynamic aspects in bulk power system reliability evaluations," *IEEE Transactions on Power Systems*, vol. 15, no. 1, pp. 189–195, 2 2000.

[83] P. Kundur, J. Paserba, V. Ajjarapu, G. Andersson, A. Bose, C. Canizares, N. Hatziargyriou, D. Hill, A. Stankovic, C. Taylor, T. Van Cursem, and V. Vittal, "Definition and classification of power system stability," *IEEE Transactions on Power Systems*, vol. 19, no. 3, pp. 1387–1401, 8 2004.

[84] M. de Nooij, B. Baarsma, G. Bloemhof, H. Slootweg, and H. Dijk, "Development and application of a cost-benefit framework for energy reliability. Using probabilistic methods in network planning and regulation to enhance social welfare: The N-1 rule," *Energy Economics*, vol. 32, no. 6, pp. 1277–1282, 11 2010.

[85] G. T. Heydt and T. J. Graf, "Distribution system reliability evaluation using enhanced samples in a Monte Carlo approach," *IEEE Transactions on Power Systems*, vol. 25, no. 4, pp. 2006–2008, 11 2010.

[86] G. Mavromatidis, K. Orehounig, and J. Carmeliet, "A review of uncertainty characterisation approaches for the optimal design of distributed energy systems," pp. 258–277, 5 2018.

[87] H. Zhang, "Introduction to Transmission Expansion Planning in Power Systems," in *Electric Power Engineering Research and Education*, E. Kyriakides, S. Suryanarayanan, and V. Vittal, Eds. Cham: Springer International Publishing, 2015, pp. 155–183.

[88] T. Akbari, A. Rahimi-Kian, and M. Tavakoli Bina, "Security-constrained transmission expansion planning: A stochastic multi-objective approach," *International Journal of Electrical Power and Energy Systems*, vol. 43, no. 1, pp. 444–453, 12 2012.

[89] J. A. Aguado, S. De La Torre, J. Contreras, A. J. Conejo, and A. Martínez, "Market-driven dynamic transmission expansion planning," *Electric Power Systems Research*, vol. 82, no. 1, pp. 88–94, 1 2012.

[90] R. Hemmati, R. A. Hooshmand, and A. Khodabakhshian, "State-of-the-art of transmission expansion planning: Comprehensive review," pp. 312–319, 7 2013.

[91] Y. Hu, Z. Bie, T. Ding, and Y. Lin, "An NSGA-II based multi-objective optimization for combined gas and electricity network expansion planning," *Applied Energy*, vol. 167, pp. 280–293, 4 2016.

[92] M. Cortés-Carmona, R. Palma-Behnke, and O. Moya, "Transmission network expansion planning by a hybrid simulated annealing algorithm," in *2009 15th International Conference on Intelligent System Applications to Power Systems, ISAP '09*, 12 2009.

[93] J. Aghaei, K. M. Muttaqi, A. Azizivahed, and M. Gitizadeh, "Distribution expansion planning considering reliability and security of energy using modified PSO (Particle Swarm Optimization) algorithm," *Energy*, vol. 65, pp. 398–411, 2 2014.

[94] H. Mori and Y. Iimura, "Application of parallel tabu search to distribution network expansion planning with distributed generation," in *2003 IEEE Bologna PowerTech - Conference Proceedings*, vol. 1, 2003, pp. 61–66.

[95] A. M. Leite Da Silva, L. S. Rezende, L. A. Da Fonseca Manso, and L. C. De Resende, "Reliability worth applied to transmission expansion planning based on ant colony system," *International Journal of Electrical Power and Energy Systems*, vol. 32, no. 10, pp. 1077–1084, 12 2010.

[96] J. Zhu, *Optimization of power system operation.* John Wiley & Sons, 2015.

[97] "Mixed-Integer Programming (MIP) - A Primer on the Basics - Gurobi." [Online]. Available: https://www.gurobi.com/resource/mip-basics/

[98] S. Binato, M. V. F. Pereira, and S. Granville, "A new Benders decomposition approach to solve power transmission network design problems," *IEEE Transactions on Power Systems*, vol. 16, no. 2, pp. 235–240, 5 2001.

[99] I. Van Beuzekom, M. Gibescu, and J. G. Slootweg, "A review of multi-energy system planning and optimization tools for sustainable urban development," in *2015 IEEE Eindhoven PowerTech, PowerTech 2015.* Institute of Electrical and Electronics Engineers Inc., 8 2015.

[100] H. K. Ringkjøb, P. M. Haugan, and I. M. Solbrekke, "A review of modelling tools for energy and electricity systems with large shares of variable renewables," pp. 440–459, 11 2018.

[101] M. G. Prina, G. Manzolini, D. Moser, B. Nastasi, and W. Sparber, "Classification and challenges of bottom-up energy system models - A review," p. 109917, 9 2020.

[102] B. Den Ouden, J. Kerkhoven, J. Warnaars, R. Terwel, M. Coenen, and T. Verboon, "Klimaatneutrale energiescenario's 2050," Berenschot, Kalavasta, Tech. Rep., 3 2020.

[103] N. A. J. Hastings, "Financial Methods," in *Physical Asset Management: With an Introduction to ISO55000.* Cham: Springer International Publishing, 2015, pp. 93–111.

[104] R. A. Brealey, S. C. Myers, and A. J. Marcus, "Net Present Value and Other Investment Criteria," in *Fundamentals of Corporate Finance*, ser. McGraw-Hill/Irwin series in finance, insurance, and real estate. McGraw-Hill Education, 2015, ch. 8.

[105] M. Bray, "Rational Expectations, Information and Asset Markets: An Introduction," *Oxford Economic Papers*, vol. 37, no. 2, pp. 161–195, 1985.

[106] L. Bahiense, G. C. Oliveira, M. Pereira, and S. Granville, "A mixed integer disjunctive model for transmission network expansion," *IEEE Transactions on Power Systems*, vol. 16, no. 3, pp. 560–565, 8 2001.

[107] W. E. Hart, J.-P. Watson, and D. L. Woodruff, "Pyomo: modeling and solving mathematical programs in Python," *Mathematical Programming Computation*, vol. 3, no. 3, pp. 219–260, 2011.

[108] Gurobi Optimization LLC, "Gurobi Optimizer Reference Manual," 2021. [Online]. Available: http://www.gurobi.com

[109] P. Nahmmacher, E. Schmid, L. Hirth, and B. Knopf, "Carpe diem: A novel approach to select representative days for long-term power system modeling," *Energy*, vol. 112, pp. 430–442, 10 2016.

[110] J. H. Ward, "Hierarchical Grouping to Optimize an Objective Function," *Journal of the American Statistical Association*, vol. 58, no. 301, pp. 236–244, 1963.

[111] Netbeheer Nederland, GTS, Enexis, Stedin, Coteq Netbeheer, Alliander, Enduris, TenneT, and Rendo, "Net voor de Toekomst," CE Delft, Tech. Rep., 9 2017.

[112] CBS, "Wijk- en buurtkaart 2017." [Online]. Available: https://www.cbs.nl/nl-nl/dossier/nederland-regionaal/geografische-data/wijk-en-buurtkaart-2017

[113] "Klimaatakkoord | Klimaatakkoord." [Online]. Available: https://www.klimaatakkoord.nl/

[114] B. Elzen, F. W. Geels, and P. S. Hofman, "Sociotechnical Scenarios (STSc) Development and evaluation of a new methodology to explore transitions towards a sustainable energy supply Report for NWO/NOVEM," University of Twente, Tech. Rep., 2002.

[115] M. Fasihi and C. Breyer, "Baseload electricity and hydrogen supply based on hybrid PV-wind power plants," *Journal of Cleaner Production*, vol. 243, p. 118466, 1 2020.

[116] Generation Energy, "Ruimtelijke uitwerking Energiescenario's | Rapport," 2020. [Online]. Available: https://www.rijksoverheid.nl/documenten/rapporten/2020/03/31/ruimtelijke-uitwerking-energiescenarios

[117] "Tarieven Grootzakelijk | Stedin." [Online]. Available: https://www.stedin.net/zakelijk/betalingen-en-facturen/tarieven

[118] Ioannis Tsiropoulos, Dalius Tarvydas, and Andreas Zucker, "Cost development of low carbon energy technologies - Scenario-based cost trajectories to 2050," *JRC Science and Policy Reports*, 2018.

[119] IEA ETSAP, "Biomass for heat and power," *Energy technology systems analysis programme*, 2010.

[120] M. Thema, F. Bauer, and M. Sterner, "Power-to-Gas: Electrolysis and methanation status review," pp. 775–787, 9 2019.

[121] E. Taibi, R. Miranda, W. Vanhoudt, T. Winkel, J.-C. Lanoix, and F. Barth, *Hydrogen from renewable power: Technology outlook for the energy transition.* IRENA, 2018.

[122] W. Kuckshinrichs and J. C. Koj, "Levelized cost of energy from private and social perspectives: The case of improved alkaline water electrolysis," *Journal of Cleaner Production*, vol. 203, pp. 619–632, 12 2018.

[123] B. Lux and B. Pfluger, "A supply curve of electricity-based hydrogen in a decarbonized European energy system in 2050," *Applied Energy*, vol. 269, p. 115011, 7 2020.

[124] A. De Vita, I. Kielichowska, P. Mandatowa, P. Capros, E. Dimopoulou, S. Evangelopoulou, T. Fotiou, M. Kannavou, P. Siskos, and G. Zazias, "Technology pathways in decarbonisation scenarios," *Tractebel, Ecofys, E3-Modelling: Brussels, Belgium*, 2018.

Appendix A
Technical and Economic Parameters

This appendix contains the technical and economic parameters and corresponding sources used in inputs for the model. From these parameters, it is possible to determine annual equivalent costs for investment candidates, and marginal generation costs. All annualised costs are determined using a discount factor of 3% and annuity factor calculated according to Equation 4.2.

A.1. Electricity network components

Table A.1 shows the parameters associated with the costs of transformers and substations. These costs are based on present-day figures at Stedin, and it is assumed that these remain the same in 2030 and 2050. Additionally, the capacities of the substations are assumed to be 300 MVA, 180 MVA and 80 MVA for the 150/52.5 kV, 150/21 kV and 52.5/13 kV levels respectively, i.e. capacities for three, two and two transformers respectively. The substation costs which are in principle one-time, are assumed to have a lifetime of 100 years for the purpose of annualising the cost. OPEX here is the yearly recurring operational and maintenance cost, as a percentage of one-time CAPEX.

Table A.1: Transformer parameters used to calculate the annual equivalent costs (source: Stedin).

(a) Transformer cost parameters

Transformer	**CAPEX (€)**	**OPEX (% of CAPEX)**	**Lifetime (yr)**	**Annual Cost (€/MW·yr)**
150/52.5 kV, 100 MVA	1,876,000	2%	40	1,187
150/21 kV, 90 MVA	1,545,000	2%	40	1,086
52.5/13 kV, 40 MVA	938,000	2%	40	1,484

(b) Substation cost parameters

Component	**150/50 kV costs (€)**	**50/13 kV costs (€)**
Building	1,651,000	1,651,000
Land acquisition	1,000,000	500,000
Other one-time costs	345,000	316,000
Transformer switchgear bay primary side	1,500,000	347,000
Transformer switchgear bay secondary side	347,000	87,000
Switchgear bay primary side	-	322,000
Switchgear bay secondary side	322,000	57,000

Transformers are connected to the substation on both ends via switchgear bays, which allow them to be disconnected if necessary. Each additional transformer therefore requires two switchgear bays to be installed. Similarly if connection is made to the substation for another component (like a connection to an electrolyser), these are also connected via a switchgear bay, but only one of these is needed for such a connection, and this type is cheaper than for a transformer (as shown in the last rows of Table A.1b.

The 150/21 kV substation costs are less detailed than those in Table A.1b. The total one-time cost is taken to be €13 million (including the buildings, land, switchgear bays and other costs), with a depreciation period of 100 years. At a capacity of 180 MVA (two transformers), this results in 4,571 €/MW·yr.

Table A.2 shows the cost parameters associated with electrical cables, where annual OPEX costs are assumed to be 1% of the initial CAPEX. For the 150 kV line, the cost is €3.5 million for a double circuit with a total capacity of 200 MVA. It would cost more than half this amount (namely around €2.5 million to place a single circuit by itself) but the cost of 17,500€/MWkm is derived from the €3.5 million amount because at any location there will be at least a double circuit (due to the N-1 redundancy rule).

Table A.2: Electric cable cost parameters. (source: Stedin)

Component	**CAPEX (€/MWkm)**	**OPEX (% of CAPEX)**	**Lifetime (yr)**	**Annual Equivalent (€/MWkm·yr)**
150 kV 100 MVA line	17,500	1%	40	1,332
50 kV 50 MVA cable	10,000	1%	40	533
13 kV 13 MVA cable	15,385	1%	40	819

A.2. Generation, conversion and storage component parameters

For generation, it is assumed that the local renewable energy generation is already invested in and in place, therefore their investment costs are left out of consideration of the optimisation. Instead, only their marginal cost is considered which is also used in trade-offs for example of converting, using locally or selling back to the external grid. Table A.3 summarises the marginal costs of PV, onshore wind and biomass CHP based on the estimated OPEX: the OPEX costs are spread evenly over the active hours to arrive at a marginal cost per MWh. The number of active hours are based on the load duration curves of the respective technologies.

Table A.3: Parameters used to calculate the 2050 marginal cost of renewable generation.

Generation source	**Investment cost (€/MWe)**	**OPEX (€/MW·yr)**	**Active hours (h/yr)**	**Marginal cost (€/MWh)**	**Source**
Solar PV	280,000	5,600	4,380	1.28	[102]
Onshore wind	710,000	17,750	8,000	2.22	[102]
Biomass CHP	3,000,000	60,000	2,000	55.0	[118, 119]

Solar PV and onshore wind have no fuel costs, but for biomass CHP these are taken to be 25 €/MWh [119]. This is added to the fixed OPEX of 30 €/MWh to obtain 55 €/MWh as marginal cost.

For electrolysers, there are one-time stack replacement costs in addition to initial CAPEX investment and the annual fixed OPEX costs. This introduces some additional parameters which are summarised along with their sources in Table A.4. Where possible, preference was given to sources estimating parameters specifically for 2050, and otherwise any available future or long-term projection was used.

Table A.4: Electrolyser techno-economic parameters used for 2050.

Parameter/cost	**2050 Value**	**Source(s)**
Initial CAPEX	450/kWe	[54, 120]
OPEX	2% of CAPEX	[70, 121]
Stack replacement cost	40% of CAPEX	[121, 122]
Stack lifetime (operating hours)	125000 h	[54, 70]
System lifetime	30 years	[115, 123]
Electrical efficiency	75% LHV	[54, 123]

For hydrogen-to-power conversion, parameters of the hydrogen turbine were based on the 2050 combined cycle gas turbine values in [115], which are close to those listed in [124], and somewhat higher in cost but comparable to the combined cycle hydrogen gas turbine parameters of [123]. An overview is presented in Table A.5.

Table A.5: Techno-economic parameters used for modelling hydrogen turbines in 2050.

Parameter/cost	**2050 Value**
Initial CAPEX	775 €/kWe
OPEX	2.5% of CAPEX
System lifetime	35 years
Net efficiency	58% LHV
Marginal cost	2 €/MWh

Table A.6 shows a summary of the parameters used for modelling the 4-hour lithium ion batteries for electrical energy storage. This is based on [8], which in turn draws from a number of sources in literature. However, as with other technologies such as electrolysis, there is much uncertainty in the costs, accompanied by large variations in the values used in literature. For example, [115] projects substantially lower battery costs for 2050. Note also that the battery degradation related to charging and discharging is lumped under fixed OPEX in this model, and for that reason the marginal cost is zero. Additionally, the energy CAPEX (per kWh) is multiplied by 4 to arrive at the 4-hour capital cost for power (per kW). A conversion rate of $ 1.00 = € 0.85 is used to calculate the battery costs, since the study uses US dollars.

Table A.6: Techno-economic parameters used for modelling lithium-ion batteries in 2050 [8].

Parameter/cost	**2050 Value**
Battery CAPEX	156 $/kWh
OPEX	2.5% of CAPEX
System lifetime	15 years
Round-trip efficiency	85%
Marginal cost	0 $/MWh

Appendix B

Demand and generation profiles: International scenario

Figure B.1 contains plots of the total monthly electrical demand, electrical generation and gas demand, throughout 2050 for the International scenario. Some biomass-based CHP can be seen especially in January, February and October, but overall this contributes very little to the generation in the sub-network, with PV and wind generation being predominant. Among electrical demand, the build environment contributes most through the year, followed by industry.

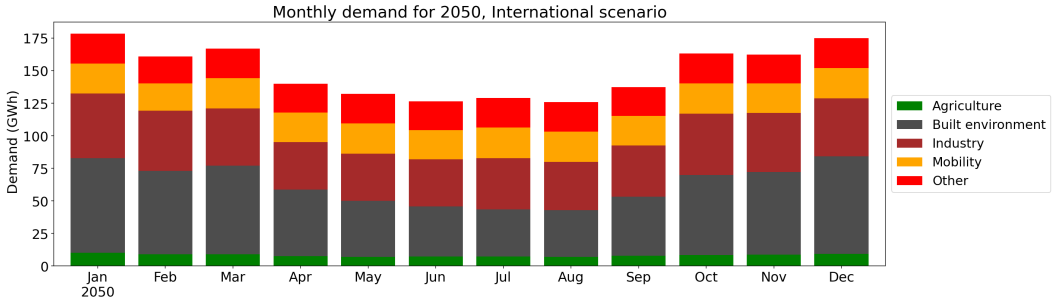

(a) Total monthly electrical demand.

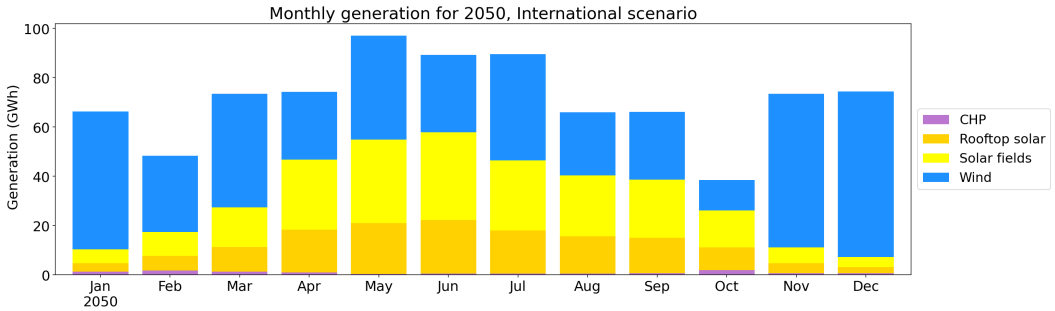

(b) Total monthly generation.

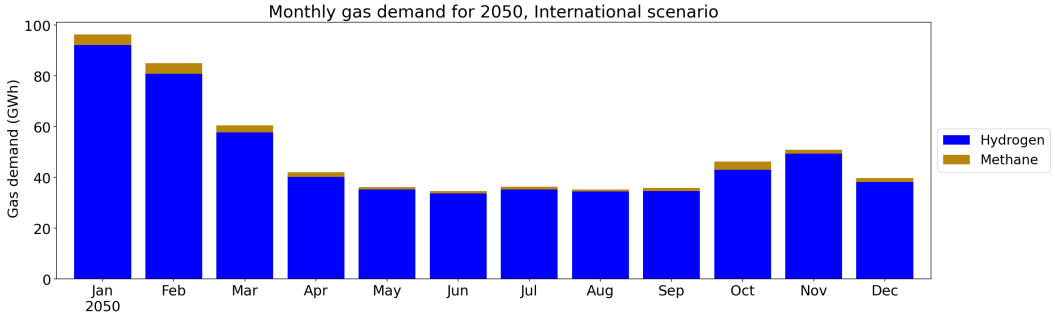

(c) Total monthly gas demand.

Figure B.1: Monthly profiles for in the Sterrenburg sub-network from the 2050 International scenario.

Figure B.2 shows hourly plots of the demand and generation profiles in the Sterrenburg sub-network for a week. PV generation shows a clear day/night cycle, while wind generation is more sporadic. Daily cycles can also be observed in the demand profiles for electricity and gas.

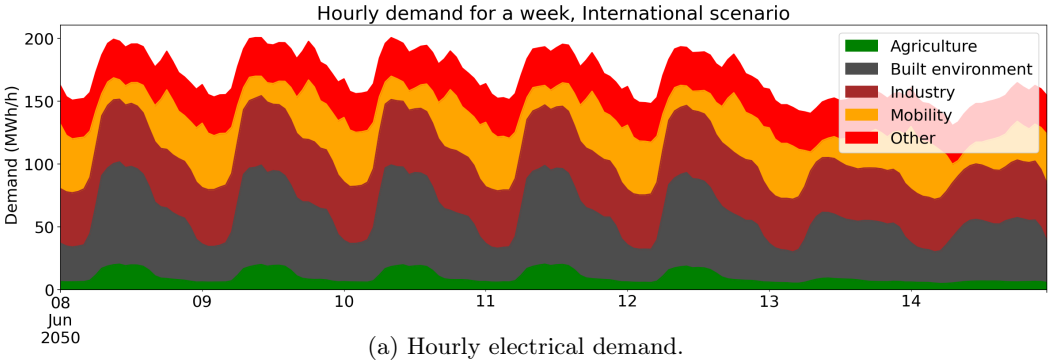

(a) Hourly electrical demand.

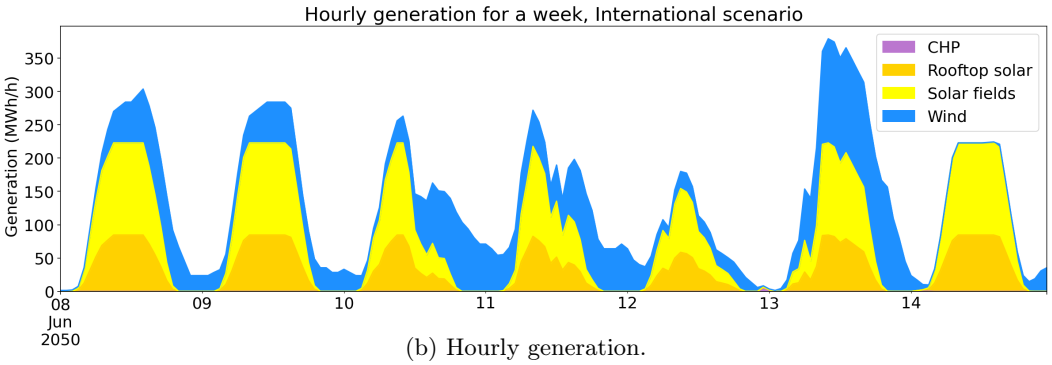

(b) Hourly generation.

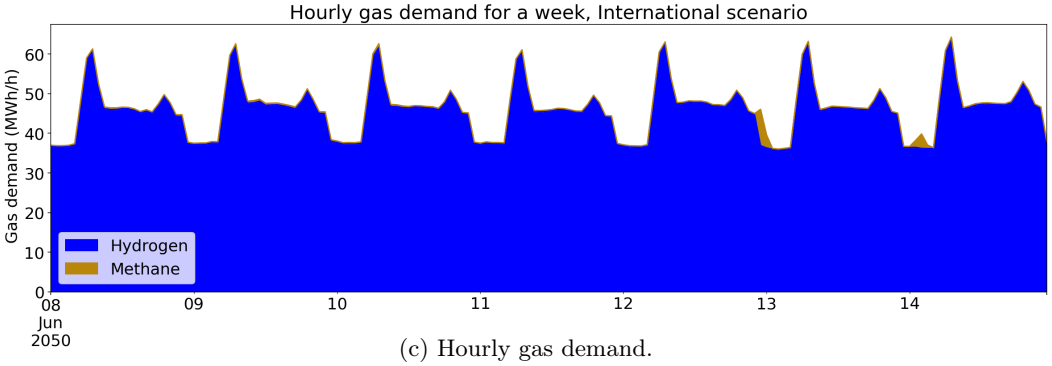

(c) Hourly gas demand.

Figure B.2: Total hourly profiles for a week in the Sterrenburg sub-network for the International scenario.

Appendix C

Reinforcement versus integration: International scenario

C.1. Power-gas integration

The expansion planning optimisation is carried out for the International scenario, with only reinforcement of grid infrastructure, and again with the option for power-gas integration. Table C.1 shows the results for the new investments required in both variants. Gas-to-power conversion via gas turbines is not chosen, but with 121 MW_e of electrolysis capacity, the overall need for grid reinforcement investments decreases, and surplus hydrogen production can be fed back to the national gas grid.

Table C.1: Overview of results for reinforcement only, and power-gas integration in the International scenario.

			Reinforcement only		**Power-gas integration**	
	Units	Price (€/unit)	Quantity	Total (€)	Quantity	Total (€)
Grid reinforcement, annualised costs						
Transformers 150/52.5 kV	Transformer	177,132	2	354,263	2	354,263
Substations 150/52.5 kV	Substation	94,813	1	94,813	1	94,813
Transformers 52.5/13 kV	Transformer	73,075	10	730,748	8	584,598
Substations 52.5/13 kV	Substation	78,072	6	468,434	6	468,434
Cables 52.5 kV 43.6 MVA	km	23,222	83	1,936,947	55	1,285,245
Gas city gate expansion	MW	2,658	7.3	19,445	7.3	19,445
				3,585,205		**2,787,354**
Power-gas, annualised costs						
Electrolysers	MW	37,982	0	0	121	4,606,761
Cables to electrolysers 13 kV	MW km	1,229	0	0	47	57,199
Cables to electrolysers 52.5 kV	MW km	799	0	0	122	97,623
Switchgear for electrolysers			0	0		45,002
Gas turbines	MW	55443	0	0	0	0
				0		**4,806,584**
Import from higher grids, annual costs						
Power from national grid	MWh	50	1,030,847	67,912,214	1,529,935	96,016,214
Gas from national grid	MWh	90	598,601	58,319,320	310,276	29,567,224
				126,231,534		**125,583,438**
Sale to higher grids, annual revenue						
Power to national grid	MWh	50	89,519	3,709,943	19,050	747,875
Gas to national grid	MWh	90	0	0	138,842	10,062,587
				3,709,943		**10,810,462**

C.2. Electrical storage

Table 6.7 shows the costs for energy infrastructure and energy exchange with the external grid, in case of reinforcement-only and with electrical energy storage for the International scenario. Instead of 21 representative days, 12 representative weeks are used from the scenario as explained in Section 4.7. Due to the difference in the selection of representative hours, the reinforcement-only solution in Table C.2 is slightly different compared to that of Table C.1 (as explained in Section 6.3 for the Regional scenario).

Table C.2: Overview of results for reinforcement only, and electrical storage integration in the International scenario.

			Reinforcement only		**Storage integration**	
	Units	Price (€/unit)	Quantity	Total (€)	Quantity	Total (€)
Grid reinforcement, annualised costs						
Transformers 150/52.5 kV	Transformer	177,132	2	354,263	2	354,263
Substations 150/52.5 kV	Substation	94,813	1	94,813	1	94,813
Transformers 52.5/13 kV	Transformer	73,075	12	876,897	11	803,822
Substations 52.5/13 kV	Substation	78,072	7	546,506	6	468,434
Cables 52.5 kV 43.6 MVA	km	23,222	83	1,936,947	68	1,572,780
Gas city gate expansion	MW	2,658	30.7	81,569	30.7	81,569
				3,809,427		**3,294,113**
Storage, annualised costs						
Batteries	MW	57,690	0	0	2.25	129,803
				0		**129,803**
Import from higher grids, annual costs						
Power from national grid	MWh	50	1,021,163	67,392,635	1,020,993	67,335,035
Gas from national grid	MWh	90	598,601	57,844,714	598,601	57,844,714
				125,237,349		**125,179,749**
Sale to higher grids, annual revenue						
Power to national grid	MWh	50	79,834	3,726,388	79,166	3,695,988
Gas to national grid	MWh	90	0	0	0	0
				3,726,388		**3,695,988**

Appendix D

Sensitivity analysis: supplementary results

Table D.1 shows an overview of the new investments and trade with the external grids selected by the the expansion planning analysis when the electricity price is changed by a decrease and increase of 50% respectively. In both these analyses, power-gas integration is allowed as an option and chosen for (but no gas turbines for gas-to-power are chosen). The cheaper electricity price is shown to encourage more electrolysis in the system.

Table D.1: Results of sensitivity analysis for changing the electricity price by 50% in the Regional scenario, with electrolysis.

		Electricity price	**-50%**		**+50%**	
	Units	Price (€/unit)	Quantity	Total (€)	Quantity	Total (€)
Grid reinforcement, annualised costs						
Transformers 150/52.5 kV	Transformer	177,132	4	708,526	6	1,062,790
Substations 150/52.5 kV	Substation	94,813	2	189,627	2	189,627
Transformers 52.5/13 kV	Transformer	73,075	16	1,169,196	17	1,242,271
Substations 52.5/13 kV	Substation	78,072	9	702,651	10	780,723
Cables 52.5 kV 43.6 MVA	km	23,222	171	3,964,878	180	4,175,780
Gas city gate expansion	MW	2,658	0	0	0	0
				6,734,878		**7,451,191**
Power-gas, annualised costs						
Electrolysers	MW	37,982	273	10,385,190	49	1,864,916
Cables to electrolysers 13 kV	MW km	1,229	123	150,771	40	49,559
Cables to electrolysers 52.5 kV	MW km	799	201	160,375	0.0	0
Switchgear for electrolysers				74,401		16,235
Gas turbines	MW	55,443	0	0	0	0
				10,770,738		**1,930,710**
Import from higher grids, annual costs						
Power from national grid	MWh	50± **50%**	1,955,558	76,606,414	517,264	43,642,822
Gas from national grid	MWh	90	22	2,048	135,654	12,888,611
				76,608,462		**56,531,433**
Sale to higher grids, annual revenue						
Power to national grid	MWh	50± **50%**	244,435	3,666,527	756,350	36,871,162
Gas to national grid	MWh	90	1,405,953	68,799,279	78,928	5,713,050
				72,465,806		**42,584,212**

Similarly, Table D.2 contains an overview of the investment decisions and trade with the external grids when the hydrogen price is varied. Decreasing the hydrogen price by 50% makes electrolysis unattractive, and no power-gas integration is chosen in that case. On the other hand, increasing the hydrogen price causes a large amount of electrolysis capacity to be chosen in the Sterrenburg sub-network, for the Regional 2050 scenario.

Table D.2: Results of sensitivity analysis for changing the hydrogen price by 50% in the Regional scenario, with electrolysis.

		Hydrogen price	**-50%**		**+50%**	
	Units	Price (€/unit)	Quantity	Total (€)	Quantity	Total (€)
Grid reinforcement, annualised costs						
Transformers 150/52.5 kV	Transformer	177,132	7	1,239,921	4	708,526
Substations 150/52.5 kV	Substation	94,813	3	284,440	2	189,627
Transformers 52.5/13 kV	Transformer	73,075	19	1,388,421	17	1,242,271
Substations 52.5/13 kV	Substation	78,072	11	858,796	10	780,723
Cables 52.5 kV 43.6 MVA	km	23,222	207	4,802,356	179	4,150,654
Gas city gate expansion	MW	2,658	0	0		0
				8,573,934		**7,071,801**
Power-gas, annualised costs						
Electrolysers	MW	37,982	0	0	303	11,510,027
Cables to electrolysers 13 kV	MW km	1,229	0	0	113	138,712
Cables to electrolysers 52.5 kV	MW km	799	0	0	252.2	201,476
Switchgear for electrolysers				0		94,149
Gas turbines	MW	55,443	0	0	0	0
				0		**11,944,364**
Import from higher grids, annual costs						
Power from national grid	MWh	50	506,716	28,520,927	2,024,552	126,392,058
Gas from national grid	MWh	90± **50%**	165,414	7,925,886	0	0
				36,446,813		**126,392,058**
Sale to higher grids, annual revenue						
Power to national grid	MWh	50	890,720	28,348,157	243,861	7,315,846
Gas to national grid	MWh	90± **50%**		0	1,458,106	113,116,163
				28,348,157		**120,432,009**

When the hydrogen or electricity price is changed for the sensitivity analysis without allowing power-gas integration, this does not affect the grid reinforcement decisions (since any surplus or deficit of energy in one form must be exchanged with the external grid, and cannot be converted to another form of energy, there is little freedom to affect the energy flows). The amounts of energy exchanged are also not affected. However, the total price of buying energy from and selling energy to the grid does change. The total annual values of energy trade with the external grid the Regional scenario are summarised in Table D.3 for changes in the electricity and hydrogen prices.

Table D.3: Costs of trade with external grid without for reinforcement-only in the Regional scenario, when analysing changes in hydrogen and electricity prices.

		Electricity	**price**	**Hydrogen**	**price**
		-50%	+50%	-50%	+50%
	MWh	**€/year**	**€/year**	**€/year**	**€/year**
Import from higher grids, annual costs					
Power from national grid	506,717	14,260,463	42,781,390	28,520,927	28,520,927
Gas from national grid	165,414	15,688,580	15,688,580	7,925,886	23,532,870
		29,949,043	**58,469,970**	**36,446,813**	**52,053,797**
Sale to higher grids, annual revenue					
Power to national grid	890,720	14,174,078	42,522,236	28,348,157	28,348,157
Gas to national grid	0	0	0	0	0
		14,174,078	**42,522,236**	**28,348,157**	**28,348,157**

Table D.4 shows a summary of the investment decisions with power-gas integration when fixed annualised cost of electrolysis is varied by 25%. Looking at the capacities of electrolysers installed, the planning algorithm is not very sensitive to changes in electrolyser prices.

Table D.4: Results of sensitivity analysis for changing the electrolyser price by 25% in the Regional scenario, with electrolysis.

		Electrolyser price	**-25%**		**+25%**	
	Units	Price (€/unit)	Quantity	Total (€)	Quantity	Total (€)
Grid reinforcement, annualised costs						
Transformers 150/52.5 kV	Transformer	177,132	4	708,526	4	708,526
Substations 150/52.5 kV	Substation	94,813	2	189,627	2	189,627
Transformers 52.5/13 kV	Transformer	73,075	16	1,169,196	16	1,169,196
Substations 52.5/13 kV	Substation	78,072	9	702,651	9	702,651
Cables 52.5 kV 43.6 MVA	km	23,222	167	3,888,245	167	3,888,245
Gas city gate expansion	MW	2,658		0	0	0
				6,658,246		**6,658,246**
Power-gas, annualised costs						
Electrolysers	MW	**28,486/47,477**	229	6,517,597	225	10,678,574
Cables to electrolysers 13 kV	MW km	1,229	127	156,149	160	196,573
Cables to electrolysers 52.5 kV	MW km	799	145	115,622	106.7	85,210
Switchgear for electrolysers				62,407		64,211
Gas turbines	MW	55,443	0	0	0	0
				6,851,775		**11,024,568**
Import from higher grids, annual costs						
Power from national grid	MWh	50	1,380,172	76,167,180	1,369,361	75,597,637
Gas from national grid	MWh	90	29,441	2,596,022	29,810	2,631,393
				78,763,202		**78,229,030**
Sale to higher grids, annual revenue						
Power to national grid	MWh	50	252,056	7,561,684	256,023	7,680,700
Gas to national grid	MWh	90	998,117	66,947,087	987,402	70,273,569
				74,508,771		**77,954,269**

Table D.5: Results of the sensitivity analysis for the Regional scenario when changing the battery price for the storage formulation.

		Battery price	**-43.6%**		**+40.4%**	
	Units	Price (€/unit)	Quantity	Total (€)	Quantity	Total (€)
Grid reinforcement, annualised costs						
Transformers 150/52.5 kV	Transformer	177,132	6	1,062,790	7	1,239,921
Substations 150/52.5 kV	Substation	94,813	2	189,627	3	284,440
Transformers 52.5/13 kV	Transformer	73,075	18	1,315,346	19	1,388,421
Substations 52.5/13 kV	Substation	78,072	11	858,796	11	858,796
Cables 52.5 kV 43.6 MVA	km	23,222	183	4,252,413	207	4,802,356
Gas city gate expansion	MW	2,658	0	0		0
				7,678,970		**8,573,934**
Storage, annualised costs						
Batteries	MW	**32,543/80,988**	35.10	1,142,357	0	0
				1,142,357		**0**
Import from higher grids, annual costs						
Power from national grid	MWh	50	505,080	28,151,913	524,789	29,690,726
Gas from national grid	MWh	90	165,414	15,987,027	165,414	15,987,027
				44,138,940		**45,677,753**
Sale to higher grids, annual revenue						
Power to national grid	MWh	50	880,758	28,282,965	908,141	28,783,360
Gas to national grid	MWh	90	0	0		0
				28,282,965		**28,783,360**

Appendix E

Spatial analysis: supplementary results

Using the component lengths, existing amounts and spatial footprints introduced in Chapter 5, the spatial footprints are calculated and presented. Table E.1 shows the areas of the existing, or base spatial footprints. Substations and city gates are above ground, and cables are under ground. In both cases, only the lateral area is considered (and not height/depth in the ground), since this is the metric with practical value.

Table E.1: Summary of the spatial footprint of existing/base network infrastructure in the Sterrenburg sub-network.

(a) Current configuration, existing infrastructure.

	Units	Area/width per unit	Quantity	Area (m^2)
Existing infrastructure, area				
Substations 150/52.5	Substation	45,000 m^2	1	45,000
Substations 52.5/13	Substation	10,000 m^2	5	50,000
Cables 52.5 kV	m	10 m	63,964	639,640
				734,640

(b) Manual expert configuration, base infrastructure.

	Units	Area/width per unit	Quantity	Area (m^2)
Existing infrastructure, area				
Substations 150/21 kV	Substation	30,000 m^2	5	150,000
Lines 150 kV 100 MVA	m	10 m	32,600	326,000
				476,000